UCLA School of Engineering and Applied Science

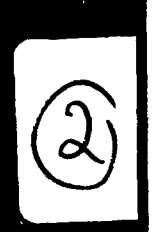

REPORT UCLA-ENG-92-28 April 1992

FINAL TECHNICAL REPORT FOR AFOSR GRANT 89-0421

ADAPTIVE AND NONADAPTIVE CONTROL OF GLOBAL INSTABILITIES WITH APPLICATION TO A HEATED TWO-DIMENSIONAL JET

Peter A. Monkewitz (P.I.) & Tino D.L. Mingori (co-P.I.)
Department of Mechanical, Aerospace and Nuclear Engineering

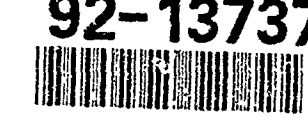

REPORT DOCUMENTATION PAGE

Form Approved
OMB No. 0704-0188

1. AGENCY USE ONLY (Leave blank)	2. REPORT DATE	3. REPORT TYPE AND DATES COVERED
	April , 1992	Final Technical Report 6/15/89-12/31/91

4. TITLE AND SUBTITLE

(U) Adaptive and Nonadaptive Feedback Control of Global Instabilities with Application to a Heated 2-D Jet

5. FUNDING NUMBERS

PE - 61102F
PR - 2307
SA - BS
G - 89 - 0421
AFOSR

6. AUTHOR(S)

Peter A. Monkewitz and D.L. (Tino) Mingori

7. PERFORMING ORGANIZATION NAME(S) AND ADDRESS(ES)

University of California, Los Angeles
School of Engineering and Applied Science
405 Hilgard Avenue
Los Angeles, CA 90024

8. PERFORMING ORGANIZATION REPORT NUMBER

UCLA-ENG-92-28

AFOSR-TR- 92 0427

9. SPONSORING/MONITORING AGENCY NAME(S) AND ADDRESS(ES)

AFOSR/NA
Building 410
Bolling AFB DC 20332-6448

NA

10. SPONSORING/MONITORING AGENCY REPORT NUMBER

AFOSR - 89-0421

11. SUPPLEMENTARY NOTES

12a. DISTRIBUTION/AVAILABILITY STATEMENT

Approved for public release; distribution is unlimited

12b. DISTRIBUTION CODE

13. ABSTRACT (Maximum 200 words)

Close to the onset of self-excited fluid oscillations the generic complex Ginzburg-Landau is proposed as the lowest order model for the "plant". Its linear part which provides the stability boundaries is derived from first principles for both doubly-infinite and semi-infinite flow domains. Concentrating on a single global mode, the model is further simplified to the Stuart-Landau equation. For this latter model a methodology is developed for the design of single-input single-output controllers. The so designed controllers have been implemented on a self-excited, heated two-dimensional jet with one hot wire as sensor and an acoustic speaker as actuator, and are shown to be effective within their limitations in suppressing or enhancing limit-cycle oscillations. Finally, the effect of of a controller designed to suppress the most unstable global mode on other modes is investigated experimentally in the wake of a cylinder at low Reynolds number, where an encouraging semi-quantitative correspondence to the Ginzburg-Landau model is found.

14. SUBJECT TERMS

Feedback Control, Self-excited fluid oscillations, Heated jets, Bluff-body wakes

15. NUMBER OF PAGES

62

16. PRICE CODE

17. SECURITY CLASSIFICATION OF REPORT	18. SECURITY CLASSIFICATION OF THIS PAGE	19. SECURITY CLASSIFICATION OF ABSTRACT	20. LIMITATION OF ABSTRACT
Unclassified	Unclassified	Unclassified	UL

TABLE OF CONTENT

1. THE DERIVATION OF THE LINEARIZED GINZBURG-LANDAU (GL) EQUATION FROM FIRST PRINCIPLES

1.1. Related Publications and Presentations

MONKEWITZ, PETER A., HUERRE, PATRICK & CHOMAZ, JEAN-MARC, Global linear stability analysis of weakly nonparallel shear flows. Submitted to J. Fluid Mech.

1.2. Introduction and Basic Equations

This part of the report addresses the extension of the concept of absolute instability to nonparallel flows. As in the case of parallel flows, in which an initial impulsive excitation leads to the ultimate dominance of the most amplified Fourier or normal mode with zero group velocity (Briggs, 1964, Bers, 1983, ecc.), we attempt to answer the question of the asymptotic (in time) impulse response of a nonparallel flow and we will call the equivalent of the "absolute" normal mode a linear "global" mode. The latter is simply a time-harmonic solution of the homogeneous linearized disturbance equations with homogeneous boundary conditions in space. Such solutions can in general be obtained only numerically, especially if the basic flow is strongly nonparallel. Examples of such computations in shear flows have been published by Zebib (1987), Hannemann & Oertel (1989) and many others.

If the the mean flow is weakly nonparallel, i.e. evolves slowly on the scale of a typical instability wave length, global modes become accessible to WKBJ-type analyses. This involves the step from the "slowly diverging" approach of Bouthier (1972) and Crighton & Gaster (1976), who treat the spatial evolution of a <u>forced</u> wave in an inhomogeneous medium (the signaling problem), to the problem of finding the <u>unforced global modes</u> where the <u>streamwise direction</u> also becomes an "<u>eigenvalue direction</u>".

In the following we treat the case of <u>infinte or semi-infinite shear flows</u> that contain regions of both absolute and convective instability by a WKBJ analysis. In particular, the cross-stream structure of the global modes is taken into account and an explicit discussion of the connection between the properties of global modes and local absolute and convective instability is given. This connection, which is supported by several examples (Monkewitz 1990), is put on firmer ground. We note, however, that the analysis admits only "local feedback" by vorticity waves to drive global modes. It is therefore <u>restricted to cases where long-range feedback is negligible</u> and important problems such as edge tones are not addressed, for which the primary driver of the instability is the acoustic feedback from a downstream point of intense fluid-surface interaction to a trailing edge.

To study two-dimensional instability waves in a spatially inhomogeneous, incompressible medium, we start from the equation for the z-vorticity $-\nabla^2\Psi$, where Ψ is the total stream function.

$$[\partial_t + (\partial_y\Psi)\partial_x - (\partial_x\Psi)\partial_y]\,\nabla^2\Psi = R^{-1}\,\nabla^2\nabla^2\Psi \qquad (2.1)$$

Next, Ψ is decomposed into time-independent mean flow ψ and a small disturbance ψ'

$$\Psi = \psi(X,y) + \psi' \; ; \quad X = \epsilon x \; . \tag{2.2}$$

At this point we assume that, in the terminology of the method of multiple scales (see e.g. Bender & Orszag, 1978), the mean flow ψ depends only on the "slow" coordinate $X=\epsilon x$. The parameter

$$\epsilon = \lambda_{typ}\{\delta^{-1}(x)[d\delta/dx]\}_{typ} \ll 1 \tag{2.3}$$

characterizes the degree of spatial inhomogeneity of the basic flow by providing a measure of the small change of the typical cross-stream length scale $\delta(x)$ over one typical instability wavelength λ_{typ}. In the absence of body forces, the assumption of a slow evolution of the mean flow immediately restricts viscous effects to $O(\epsilon)$, or in terms of the Reynolds number $\Re$

$$\Re = \epsilon^{-1}R \; ; \quad R=O(1) \; . \tag{2.4}$$

Introduction of the decomposition (2.2) and of (2.4) into the governing equation (2.1) first leads to the boundary layer equation for the basic flow

$$(\partial_y\psi)(\partial_x\partial_y^2\psi) - (\partial_x\psi)(\partial_y^3\psi) = R^{-1}\,(\partial_y^4\psi) \tag{2.5a}$$

$$U(X,y) = \partial_y\psi \; ; \quad V(X,y) = -\partial_x\psi = -\epsilon^{-1}\,\partial_x\psi \tag{2.5b}$$

Linearizing around the basic flow and keeping only terms up to $O(\epsilon)$ then yields the following equation for the small disturbance ψ'

$$\begin{aligned}&\left[(\partial_t + U\,\partial_x)\nabla^2 - (\partial_y^2 U)\partial_x\right]\psi' + \\ &\epsilon\left[V\,\partial_y\nabla^2 + (\partial_x\partial_y U)\partial_y - R^{-1}\,\nabla^2\nabla^2\right]\psi' + O(\epsilon^2|\psi'|,|\psi'|^2) = S(x,y,t) \; ,\end{aligned} \tag{2.6}$$

where ∂_x and the Laplacian ∇^2 have not yet been split into fast and slow parts. The source S has been added for the study of the impulse response in the next section, but the ultimate aim of the paper is the search for global modes, i.e. homogeneous solutions of (2.6) with homogeneous boundary conditions in space.

1.3. The WKBJ Approximation for the Green Function and its Breakdown

Following Bouthier (1972), Crighton and Gaster (1976) and others, we use the WKBJ approximation up to the level of "physical optics" (see e.g. Bender & Orszag, 1978) to describe the evolution of a pulse on the weakly nonparallel basic flow and identify the locations of its breakdown which are "turning points" of the problem (see section 10 of Bender & Orszag, 1978).

To obtain the Green function G of (2.6), the source at $x=x^s$ and $y=y^s$ is specified as

$$S(x,y,t) = \{\delta(x-x^s) + i[\pi(x-x^s)]^{-1}\}\delta(y-y^s)\delta(t) \; . \tag{3.1}$$

This form explicitly accounts for the non-analyticity of G on the imaginary axis of the wavenumber plane when the lateral extent of the flow domain is

infinite, as discussed in detail by Huerre & Monkewitz (1985). Next, we take the Fourier transform of (2.6) in time according to

$$G(x,y,t) = (2\pi)^{-1} \int_L \hat{G}(x,y,\omega) \exp(-i\omega t)\, d\omega \quad , \tag{3.2}$$

where the contour L is taken parallel to the real ω-axis and above all singularities in order to obtain a causal solution (Briggs, 1964). Finally, all x-derivatives in the disturbance equation (2.6) are transformed according to the chain rule

$$\partial_x \rightarrow \partial_x + \epsilon \partial_X \quad , \tag{3.3}$$

keeping in mind that ∂_x and ∂_X do not commute. Concentrating on a flow domain of doubly-infinite streamwise extent, G is required to vanish at up- and downstream infinity as well as on the lateral boundaries $|y| \rightarrow \infty$. Hence, following section 10.3 of Bender & Orszag (1978), the WKBJ approximation for G can be written in the standard form away from the source at $x=x^s$

$$\hat{G}^{\pm} \sim \{\hat{G}_0^{\pm}(X,y) + \epsilon \hat{G}_1^{\pm}(X,y) + O(\epsilon^2)\} \exp[i\epsilon^{-1} \int_{X^s}^{X} k^{\pm}(X';\omega)\, dX'] \quad , \tag{3.4}$$

where ϵ plays the role of the WKBJ-parameter. The superscripts "+" and "−" denote the approximation downstream and upstream of the source, respectively. The $k^{\pm}(X';\omega)$ are the corresponding local wavenumbers in the upper and lower half k-plane, respectively, as shown on figure 2b of Huerre & Monkewitz (1985). For simplicity we assume here that there is only a single pair of eigenvalues $k^{\pm}$.

Introducing the WKBJ-Ansatz (3.4) into the Fourier-transformed equation (2.6) the stability problem reduces, at leading order in ϵ, to a streamwise succession of locally <u>parallel</u> problems which are governed by the homogeneous Rayleigh equation. Its solution depends only parametrically on X through the shape of the local mean velocity profile U(X,y) and yields $k^{\pm}(X;\omega)$ as well as the local transverse structure of G_0 up to an unknown amplitude $A_0(X)$. The latter describes in essence the "transmission" of the instability wave from one locally parallel region to the next and will be determined at the next order.

$$O(\epsilon^0): \quad \mathcal{L}(\phi_0^{\pm};k^{\pm},\omega,X) = 0 \; ; \quad |\phi_0^{\pm}(|y|\rightarrow\infty;X)| = 0 \quad , \tag{3.5a}$$

$$\text{with} \quad \hat{G}_0^{\pm}(X,y) = A_0^{\pm}(X)\, \phi_0^{\pm}(y;X) \quad . \tag{3.5b}$$

The Rayleigh operator $\mathcal{L}$, which includes a list of all relevant parameters in the argument, is defined as (see also appendix A)

$$\mathcal{L}(\bullet;k,\omega,X) = [kU(y;X) - \omega][\partial_y^2 - k^2]\bullet - k[\partial_y^2 U(y;X)]\bullet \quad . \tag{3.6}$$

At linear order in ϵ, the following inhomogeneous Rayleigh equation for $\hat{G}_1^{\pm}$ is obtained, where the derivatives of the operator $\mathcal{L}$ are defined in appendix A

$$O(\epsilon^1): \quad \mathcal{L}(\hat{G}_1^{\pm};k^{\pm},\omega,X) = i\,\partial_X A_0^{\pm}\,\mathcal{L}_k(\phi_0^{\pm};k^{\pm},\omega,X) + \\ + i\,A_o^{\pm}\Big\{\mathcal{L}_k(\partial_X\phi_0^{\pm};k^{\pm},\omega,X) + \\ + \frac{1}{2}\,\partial_X k\,\mathcal{L}_{kk}(\phi_0^{\pm};k^{\pm},\omega,X) + \mathcal{L}_\epsilon(\phi_0^{\pm};k^{\pm},\omega,X)\Big\} \quad . \tag{3.7}$$

It will prove useful to replace $\partial_X\phi_0^{\pm}$ by the expression (C.4) of appendix C where the functions $\phi_{1k}^{\pm}$ etc. are defined by (C.5). In order to avoid secular terms in the solution of (3.7), the solvability condition (3.8) has to be satisfied. After dividing by $L_\omega(\phi_0^{\pm};k^{\pm},\omega,X)$ and using (B.4) for $\partial_k\omega^{\pm}$, the condition reads

$$\partial_k\omega^{\pm}\,\partial_X A_0^{\pm} = -A_0^{\pm}\,[\,i\delta\omega^{\pm} + (^1/_2)\omega_{kk}^{\pm}\,\partial_X k^{\pm} + \omega_{k\omega}^{\pm}\,\partial_X\omega^{\pm}] \quad . \tag{3.8}$$

$$\delta\omega^{\pm}(\omega,X) = i\,[L_\epsilon(\phi_0^{\pm};k^{\pm},\omega,X) - L_k(\phi_{1X}^{\pm};k^{\pm},\omega,X)]\,[L_\omega(\phi_0^{\pm};k^{\pm},\omega,X)]^{-1} \quad , \tag{3.9a}$$

$$\omega_{kk}^{\pm}(\omega,X) = [2L_k(\phi_{1k}^{\pm};k^{\pm},\omega,X) - L_{kk}(\phi_0^{\pm};k^{\pm},\omega,X)]\,[L_\omega(\phi_0^{\pm};k^{\pm},\omega,X)]^{-1} \quad , \tag{3.9b}$$

$$\omega_{k\omega}^{\pm}(\omega,X) = L_k(\phi_{1\omega}^{\pm};k^{\pm},\omega,X)\,[L_\omega(\phi_0^{\pm};k^{\pm},\omega,X)]^{-1} \quad . \tag{3.9c}$$

The L's above are defined by (B.3) in appendix B and represent inner products of the corresponding $\mathcal{L}$'s with the solution of the adjoint Rayleigh equation. Equation (3.8) is now readily integrated to yield $A_0(X)$

$$A_0^{\pm}(X) = A_0^{s\pm}\,\exp\left[\,i\int_{X^s}^{X}\frac{[-\delta\omega^{\pm} + (^1/_2)\,\omega_{kk}^{\pm}\,\partial_X k^{\pm} + i\,\omega_{k\omega}^{\pm}\,\partial_X\omega^{\pm}](X';\omega)}{\partial_k\omega^{\pm}(X';\omega)}\,dX'\right] \tag{3.10}$$

This brings the approximate description of the Green function away from the source to the level of "physical optics". What remains to be done is the connection of G_0^- and G_0^+ across the source. For this the analysis of Bender & Orszag (1978) has to be generalized: instead of patching the two solutions G_0^- and G_0^+, which is only possible for ODE's, we use in essence the approach of Burridge and Weinberg (1977) in which the connection is achieved by matching G_0^- and G_0^+ to the local parallel Green function at X^s. The latter is obtained from the double Fourier transform $\hat{G}$ in time t and space x at $X=X^s$ which is given as equation (8) in Huerre & Monkewitz (1985). Integration of $\hat{G}$ with respect to k along the contours shown on figure 2b of Huerre & Monkewitz (1985) yields, upon evaluating the residues at k^+ and k^- respectively for any frequency on the contour L of (3.2),

$$\hat{G}(x,y,\omega;X^s) = -\frac{2H(x-x^s)\,\phi_0^+(y;X^s)\,\phi_0^+(y^s;X^s)\,\exp[ik^+(\omega;X^s)x]}{[k^+(\omega;X^s)U(X^s,y^s) - \omega]\,\partial_k D[\omega,k^+(\omega;X^s)]} + \\ + \frac{2H(x^s-x)\,\phi_0^-(y;X^s)\,\phi_0^-(y^s;X^s)\,\exp[ik^-(\omega;X^s)x]}{[k^-(\omega;X^s)U(X^s,y^s) - \omega]\,\partial_k D[\omega,k^-(\omega;X^s)]} \quad . \tag{3.11}$$

In this expression H is the Heaviside function and D the dispersion relation associated with the local Rayleigh equation at X^s. We note that in (3.11) the contribution from the integration along the imaginary k-axis, which is a branch cut of the dispersion relation, has been omitted under the assumption

that the long-time behavior is dominated by the discrete spectrum. Comparison of (3.4), (3.5) and (3.10) with (3.11) finally yields

$$A_0^{s\pm} = \mp \frac{2\,\phi_0^{\pm}(y^s;X^s)}{[k^{\pm}(\omega;X^s)U(X^s,y^s) - \omega]\;\partial_k D[\omega,k^{\pm}(\omega;X^s)]} \quad . \tag{3.12}$$

We now turn to the discussion of the long-time behavior of G which runs analogous to the discussion of absolute and convective instability in the parallel case. The basic idea is that the leading-order time-asymptotic behavior of G is determined by the uppermost singularity of G in the ω-plane, i.e. the singularity with the largest temporal growth rate, which becomes "pinned" as the ω-contour is lowered . In the parallel case, the singularities in the ω-plane, which correspond to zeroes $\omega(k)$ of the dispersion relation D, can be moved by deforming the Fourier-inversion contour in the k-plane until the latter is pinched between two branches $k^+(\omega)$ and $k^-(\omega)$ (see Briggs, 1964, Bers, 1983, etc.). When this happens, the singularity $\omega_o=\omega(k_o)$ becomes "pinned" at the absolute frequency ω_o which corresponds to the saddle point k_o where the complex group velocity $\partial_k\omega$ is zero and the k-contour is pinched.

In the weakly nonparallel case we can argue in a completely analogous manner: If $G(X,\omega)$ becomes singular at a location X^t from which the X-integration contour cannot be moved, the corresponding pole $\omega(X^t)$ becomes "pinned". Again, the "pinned" pole with the largest temporal growth rate determines the time-asymptotic behavior of G. From (3.10) it is seen that $\hat{G}$, in particular $A_0(X)$, becomes singular at the zeroes of $\partial_k\omega(X,\omega)$. Such points are in fact turning points X^t where the WKBJ-approximation breaks down, which is easily seen by noting the correspondence between $A_0(X)$ and $[Q(X)]^{-1/4}$ in standard textbook notation (see chapter 10 of Bender & Orszag, 1978). In the following, we have to distinguish between two types of pole "pinning":

The first is the exact analogue of the parallel case where the X-integration contour is pinched between two branches $X^{\pm}(\omega|\partial_k\omega=0)$ on which the group velocity is zero. The pinching occurs at the saddle point, or second order turning point X^t where

$$\partial_X\omega_o(X^t)=0 \quad , \tag{3.13}$$

as shown on figure 1b. This is the case discussed in detail by Chomaz, Huerre & Redekopp (1991), which arises when the absolute growth rate $\omega_{oi}(X)$ has a maximum within the flow domain, and represents a generalization of Pierrehumbert's (1984) frequency selection criterion to the complex X-plane. The assumption that a maximum of $\omega_{oi}(X)$ exists within the flow domain is in fact rather weak and corresponds to the existence of a maximum of the temporal amplification rate and an associated saddle point of $\omega(k)$ in parallel flows (see Gaster,1968). In the following we make the same assumption and consider, for simplicity, only one saddle (3.13) between regions of stable flow far upstream and downstream.

The second possibility of pole "pinning" arises when the complex group velocity first becomes zero at, say, the flow boundary X=0. In this case the pole $\omega_o(X^t)$ is "pinned" because the X-integration contour has to start or end at the boundary, as shown on figure 1c. Hence we have

$$X^t = 0 \qquad (3.14)$$

and in this case X^t corresponds to a first order turning point. This is the situation we will consider for the semi-infinite domain where the upstream boundary at X=0 dominates the evolution of the disturbance while we assume that the flow is stable far downstream. The same situation has already been considered in a model by Chomaz, Huerre & Redekopp (1988).

In both cases the global mode frequency is given, to leading order, by $\omega_0(X^t)$ and global instability is determined by the sign of the leading order global growth rate $\omega_{0i}(X^t)$. Hence it appears that the mean flow must contain a region of absolute instability for a global mode to become temporally amplified. This is confirmed by the detailed analysis, which also yields the next approximation of the global mode frequency beyond $\omega_0(X^t)$. The latter is obtained as eigenvalues of the streamwise two-point boundary value problem and are determined either by the connection of the upstream and downstream solutions through the second order turning point (3.13), or by the connection of the downstream solution through the first order turning point (3.14) to the boundary.

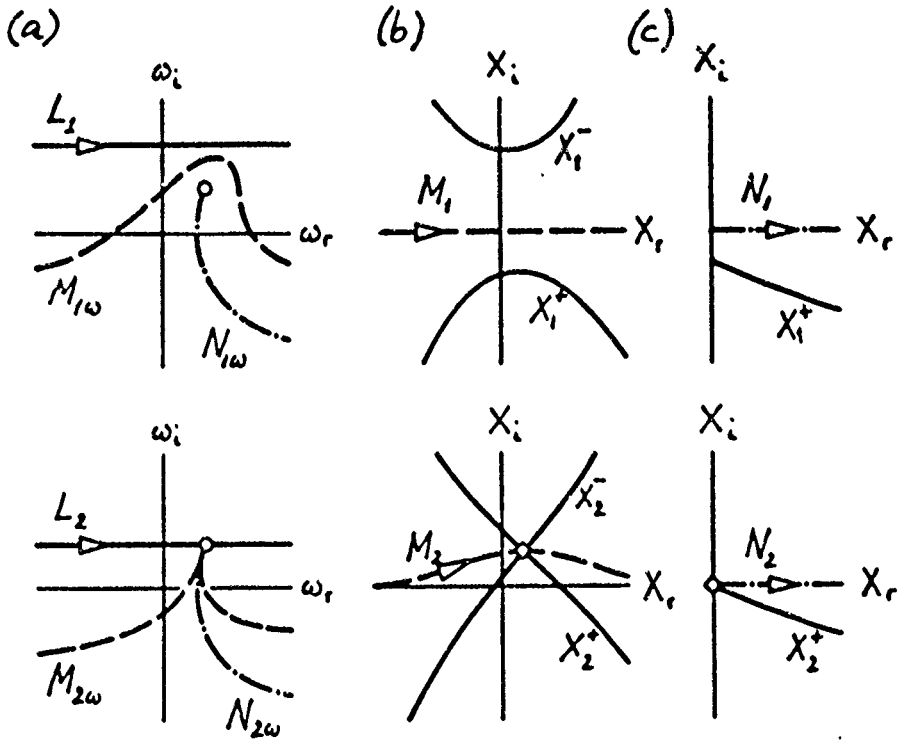

Figure 1. (a) Sketch of the Fourier inversion contour L in the complex ω-plane. (b) The WKBJ integration path M in the complex X-plane for the doubly-infinite flow domain with images X^+ and X^- of L on which the group velocity is zero. (c) Corresponding path N and X^+ for the semi-infinite case. The top row (subscripts 1) shows the situation where L is above all singularities (O), while the bottom row (subscripts 2) shows the points (◊) of the X-contour where the breakdown of the WKBJ-approximation can no longer be avoided as L is lowered.

1.4. The Turning Point Region for the Doubly-Infinite Domain

In this section the ideas of Soward & Jones (1983), Huerre & Monkewitz (1990) & Chomaz, Huerre and Redekopp (1991) on global modes in a doubly infinite flow domain are applied to shear flows. In terms of application the following analysis may not only be useful in truly infinite domains, typically found in geophysical shear flows, but also in finite flow domains, as long as the boundaries do not significantly influence the flow instability. The two-dimensional bluff-body wake appears to be a case in point as suggested by Monkewitz (1988) and the numerical experiment of Triantafyllou & Karniadakis (1990) who obtained essentially the same Kármán vortex street after replacing the cylinder by an inflow boundary condition downstream of the cylinder.

At the turning point defined by (3.13) the first-order equation (3.8) for $A_0^{\pm}$ becomes singular and one has to bring in the second derivative $\epsilon^2 \partial_X^2 A_0^{\pm}$. Since X^t is also a saddle point of the absolute growth rate $\omega_o(X)$, $(\omega_o-\omega_o^t)$ behaves like $(X-X^t)^2$. Hence X^t is a second order turning point where the second derivative of $A_0^{\pm}$ must be of the same order as $(X-X^t)^2 A_0^{\pm}$ (see Bender & Orszag, 1978). This leads immediately to the rescaling

$$\bar{X} = \epsilon^{-1/2}(X-X^t) \quad . \tag{4.1}$$

In the inner turning point region, characterized by $|\bar{X}| \le O(1)$, the disturbance streamfunction is expanded accordingly:

$$\bar{\psi}' = [\bar{\Phi}_0 + \epsilon^{1/2}\bar{\Phi}_1 + \epsilon\bar{\Phi}_2 + O(\epsilon^{3/2})](\bar{X},y) \times \exp[i\epsilon^{-1}k_o^t(X-X^t) - i\omega_G t] \quad , \tag{4.2}$$

where $k_o^t = k_o(X^t)$. By the same token the global frequency ω_G is expanded around $\omega_o(X^t)=\omega_o^t$

$$\omega_G = \omega_o^t + \epsilon^{1/2}\bar{\omega}_1 + \epsilon\bar{\omega}_2 + O(\epsilon^{3/2}) \quad , \tag{4.3}$$

and the mean flow components are expanded in Taylor series around X^t. In terms of the inner variable (4.1) they are given by

$$\begin{aligned} U(X,y) &\sim U(X^t,y) + \epsilon^{1/2}\bar{X}[\partial_X U(X^t,y)] + \epsilon(\bar{X}^2/2)[\partial_X^2 U(X^t,y)] + O(\epsilon^{3/2}) \quad , \\ V(X,y) &\sim V(X^t,y) + O(\epsilon^{1/2}) \quad . \end{aligned} \tag{4.4}$$

Introducing the expansions (4.2) and (4.4) as well as the "slow" variable (4.1) (using the chain rule $\partial_x \to \partial_x + \epsilon^{1/2}\partial_{\bar{X}}$) into the governing equation (2.6) yields, at leading order in ϵ, the local Rayleigh equation at X^t

$$O(\epsilon^0): \quad \mathcal{L}^t(\phi_0^t) = 0 \; ; \quad |\phi_0^t(|y|\to\infty;X)| = 0 \quad , \tag{4.5}$$

where $\phi_0^t(y)$ is the local eigenfunction and the short-hand notation $\mathcal{L}^t$ (see A.1), together with the corresponding integral L^t (see B.3), is defined by

$$\mathcal{L}^t(\cdot) \equiv \mathcal{L}(\cdot;k_o^t,\omega_o^t,X^t) \quad , \tag{4.6a}$$

$$L^t(\cdot) \equiv L(\cdot;k_o^t,\omega_o^t,X^t) \quad . \tag{4.6b}$$

Hence the leading order solution $\bar{\Phi}_0$ in (4.2) is given by

$$\bar{\Phi}_0(\bar{X},y) = \bar{A}_0(\bar{X})\ \phi_0^t(y) \quad , \tag{4.7}$$

with the "free" amplitude $\bar{A}_0(\bar{X})$ to be determined at higher order. At the next order $O(\epsilon^{1/2})$ a solvability condition yields only

$$\bar{\omega}_1 = 0 \quad . \tag{4.8}$$

Hence we have to proceed to $O(\epsilon)$ to determine $\bar{A}_o$ and obtain the solvability condition

$$\partial_{\bar{X}}^2\bar{A}_0\ (\omega_{kk}^t/2) + i\bar{X}\ \partial_{\bar{X}}\bar{A}_0\ \omega_{kX}^t + \bar{A}_o[\bar{\omega}_2 - \delta\omega^t - \bar{X}^2(\omega_{XX}^t/2)] = 0 \ , \tag{4.9}$$

with the abbreviations

$$\omega_{kk}^t = [2L_k^t(\phi_{1k}^t) - L_{kk}^t(\phi_0^t)][L_\omega^t(\phi_0^t)]^{-1} \quad , \tag{4.10a}$$

$$\omega_{kX}^t = [L_k^t(\phi_{1X}^t) + L_X^t(\phi_{1k}^t) - L_{kX}^t(\phi_0^t)][L_\omega^t(\phi_0^t)]^{-1} \quad , \tag{4.10b}$$

$$\delta\omega^t = i[L_\epsilon^t(\phi_0^t) - L_k^t(\phi_{1X}^t)][L_\omega^t(\phi_0^t)]^{-1} \quad , \tag{4.10c}$$

$$\omega_{XX}^t = [2L_X^t(\phi_{1X}^t) - L_{XX}^t(\phi_0^t)][L_\omega^t(\phi_0^t)]^{-1} \quad , \tag{4.10d}$$

where the L_γ^t, etc. are defined analogous to (4.6b). The resulting amplitude equation (4.9) is a linearized Ginzburg-Landau equation with variable coefficients. The nomenclature (4.10) becomes immediately transparent when equation (4.9) is tranformed to the spectral domain by

$$\partial_{\bar{X}} \to i\epsilon^{-1/2}(k-k_o^t) \quad . \tag{4.11}$$

Using (4.3) and (4.8) this yields the Taylor series representation of the dispersion relation in the neighborhood of the turning point X^t

$$\epsilon\ \bar{\omega}_2 = \omega-\omega_o^t = \epsilon\ \delta\omega^t + (\omega_{kk}^t/2)(k-k_o^t)^2 + \omega_{kX}^t(k-k_o^t)(X-X^t) + (\omega_{XX}^t/2)(X-X^t)^2 \quad . \tag{4.12}$$

Hence we have shown that the dispersion relation (4.12) which had been postulated by Huerre & Monkewitz (1990) and Chomaz et al. (1991) is generic to the turning point region of the WKBJ approximation and can be derived in a rational fashion from the governing equations under rather weak assumptions. The solution of (4.9) is now easily found by transforming it into the standard Hermite equation. Setting

$$\bar{A}_0(\bar{X}) = \exp[(i/2)k_{oX}^t\ \bar{X}^2]\ \alpha(\xi) \quad \text{with} \quad \xi = (4\omega_{oXX}^t/\omega_{kk}^t)^{1/4}\ \bar{X} \ , \tag{4.13}$$

(4.9) becomes

$$\partial_\xi^2\alpha + \alpha\{[\bar{\omega}_2-\delta\omega^t+(i/2)\omega_{kk}^t k_{oX}^t][\omega_{kk}^t\omega_{oXX}^t]^{-1/2} - \xi^2/4\} = 0 \quad ,$$
$$|\alpha|(\xi\to\infty) = 0 \quad . \tag{4.14}$$

The boundary conditions are chosen such as to ensure the matching to the subdominant WKBJ solutions both upstream and downstream of X^t and restrict the frequency correction $\bar{\omega}_2$ to a set of discrete eigenvalues given by (4.15a) with the corresponding global eigenfunctions given by (4.15b)

$$\bar{\omega}_{2n} = \delta\omega^t - (i/2)\omega^t_{kk}k^t_{oX} + (n+\tfrac{1}{2})(\omega^t_{kk}\omega^t_{oXX})^{1/2} \quad , \qquad (4.15a)$$

$$\alpha_n(\xi) = \exp[-\xi^2/4]\, He_n(\xi) \quad , \qquad (4.15b)$$

where the $He_n(\xi)$ are Hermite polynomials as defined by Abramowitz and Stegun (1965). We reiterate here that, according to the discussion leading to the frequency selection criterion (3.13), the global mode (4.15) represents the asymptotic solution for long times. The recent feat of Hunt & Crighton (1991) who determined the exact Green function of (4.9) puts us into the unique position of verifying this statement explicitly. If the limit $t\to\infty$ is taken in their expression (36)and (44) for the Green function, one indeed recovers the most unstable global mode (4.15) with n=0. The higher modes are more stable since the imaginary parts of ω^t_{kk} and ω^t_{oXX} are negative, corresponding to a high wave number "cutoff" and to stability at $|\bar{X}|\to\infty$ respectively. At this point the solution of (2.6) in the inner or turning point region is complete. Its matching to the WKBJ-"tails" presents no further problems and is described in the preprint listed in section 1.1. To avoid misunderstandings it is worth pointing out here that the notion of WKBJ-"tails" does not in any way imply that the amplitude of the global mode should peak near the turning point which acts as the "wave-maker" for the entire flow. Depending on the imaginary part of k^t_o and the downstream evolution of $Im[k^t]$ the wave "leaking" from the "wave-maker" region can experience substantial spatial amplification.

1.5. The Turning Point Region for the Semi-Infinite Flow Domain

In this section the model investigated by Chomaz et al. (1988) is reexamined in the context of the present rational asymptotic analysis starting from the governing equation (2.6). The main assumption, besides the exclusion of long-range feedback, is that the flow is most (absolutely) unstable at the boundary, i.e. that the location of the "wave maker" is given by (3.14). Furthermore we will assume that $\partial_X\omega_o(X^t)\neq 0$, i.e. that $\omega_o(X)$ has no saddle point at the boundary $X^t=0$, and that the global mode amplitude is zero at the boundary.

The analysis is very similar to the one of section 1.4. and will be kept as brief as possible. In the present case the absolute growth rate $\omega_o(X)$ is assumed to be a linear function of $(X-X^t)$ and X^t is a first order turning point. Hence, the balance between $\epsilon^2\,\partial^2_X A^{\pm}_0$ and $(X-X^t)A^{\pm}_0$ near X^t leads to the scaling

$$\bar{X} = \epsilon^{-2/3}(X-X^t) \quad . \qquad (5.1)$$

The disturbance stream function is expanded accordingly

$$\tilde{\psi}' = [\Phi_0 + \epsilon^{1/3}\Phi_1 + \epsilon^{2/3}\Phi_2 + \epsilon\Phi_3 + O(\epsilon^{4/3})](\bar{X},y) \times \exp[i\epsilon^{-1}k^t_o(X-X^t) - i\omega_G t] \quad , \qquad (5.2)$$

where $k_o^t=k_o(X^t)$ and the global frequency is represented by

$$\omega_G = \omega_o^t + \epsilon^{1/3}\,\tilde{\omega}_1 + \epsilon^{2/3}\,\tilde{\omega}_2 + \epsilon\tilde{\omega}_3 + O(\epsilon^{4/3}) \quad . \tag{5.3}$$

Analogous to (4.4), the mean flow is expanded around X^t

$$\begin{aligned} U(X,y) &\sim U(X^t,y) + \epsilon^{2/3}\,\bar{X}[\partial_X U(X^t,y)] + O(\epsilon^{4/3}) \quad , \\ V(X,y) &\sim V(X^t,y) + O(\epsilon^{2/3}) \quad . \end{aligned} \tag{5.4}$$

This, together with the transformation of x-derivatives according to $\partial_x \to \partial_x + \epsilon^{1/3}\partial_{\bar{X}}$ yields, at leading order, the same Rayleigh problem (4.5) at X^t and the leading order inner solution is thus determined up to a free amplitude $\bar{A}_0(\bar{X})$

$$\phi_0(\bar{X},y) = \bar{A}_0(\bar{X})\;\phi_0^t(y) \quad . \tag{5.5}$$

At the next order $O(\epsilon^{1/3})$ one again obtains

$$\tilde{\omega}_1 = 0 \quad . \tag{5.6}$$

At order $O(\epsilon^{2/3})$ one finds the solvability condition

$$\begin{aligned} &\partial_{\bar{X}}^2\bar{A}_0\;(\omega_{kk}^t/2) + \bar{A}_0(\tilde{\omega}_2 - \bar{X}\,\omega_X^t) = 0 \\ &\bar{A}_i(\bar{X}\!=\!-\epsilon^{-2/3}X^t) = \bar{A}_i(\bar{X}\!\to\!\infty) = 0 \quad . \end{aligned} \tag{5.7}$$

The coefficient ω_{kk}^t is thereby given by (4.10a) and

$$\omega_X^t = -\,L_X^t(\phi_0^t)\,[L_\omega^t(\phi_0^t)]^{-1} \quad . \tag{5.8}$$

The first boundary condition on the $\bar{A}_i$ in (5.12) expresses the assumption that the global-mode amplitude is zero at the upstream flow boundary X=0, while the second boundary condition requires the amplitude to vanish far downstream as before. Equation (5.7) is recognized as Airy's equation with the solution

$$\bar{A}_0 = \mathrm{Ai}\{(2\omega_X^t/\omega_{kk}^t)^{1/3}\;[\bar{X} - (\tilde{\omega}_2/\omega_X^t)]\} \quad . \tag{5.9}$$

The boundary condition at X=0 then leads to the relation between $\tilde{\omega}_2$ and X^t

$$-(2\omega_X^t/\omega_{kk}^t)^{1/3}\;[\epsilon^{-2/3}X^t + (\tilde{\omega}_2/\omega_X^t)] = -a_n \quad , \tag{5.10}$$

where the $-a_n$ are the zeros of the Airy function Ai (a_0=2.338, a_1=4.088, etc.). With the location of the turning point given, to leading order, by (3.14), i.e. coinciding with the boundary, we obtain

$$X^t = 0 \quad , \tag{5.11a}$$

$$\tilde{\omega}_{2n} = \omega_X^t\,(2\omega_X^t/\omega_{kk}^t)^{-1/3}\,a_n \quad . \tag{5.11b}$$

The quantization of the global frequency is therefore of order $\epsilon^{2/3}$, larger than the $O(\epsilon)$ quantization (4.15a) in the doubly-infinite case. For the matching to the WKBJ solution, it is more convenient to have $\tilde{\omega}_2$=0. This

can be achieved by moving the turning point, around which all quantities are expanded, slightly away from the boundary. Setting $\tilde{\omega}_2$=0 in (5.10) yields

$$\tilde{\omega}_2 = 0 \quad , \tag{5.12a}$$

$$X_n^t = \epsilon^{2/3} \, (2\omega_X^t/\omega_{kk}^t)^{-1/3} \, a_n \quad . \tag{5.12b}$$

With the assumptions of a large-wave-number cutoff [i.e. $Im(\omega_{kk}^t)<0$] and maximum absolute growth rate at the boundary [i.e. $Im(\omega_X^t)<0$] equation (5.12b) places the "dominant oscillator" close to the origin into the first quadrant of the complex X-plane. This displacement reflects the fact, that a finite region of absolute instability is required on the real X-axis near the origin before one can have global instability, as discussed in detail by Chomaz et al. (1988) (see also figure 1c).

In the Fourier-domain we again obtain the Taylor expansion of the dispersion relation around X_o^t

$$\begin{aligned} \epsilon \, \tilde{\omega}_3 = \omega - \omega_o^t - \epsilon \, \delta\omega^t + (\omega_{kk}^t/2)(k-k_o^t)^2 + \omega_X^t(X-X_n^t) \\ + (\omega_{kkk}^t/6)(k-k_o^t)^3 + \omega_{kX}^t(k-k_o^t)(X-X_n^t) \quad , \end{aligned} \tag{5.13}$$

where it is understood that, for the n-th global mode, all constants are evaluated at $X^t=X_n^t$, and where

$$\omega_{kkk}^t = [3L_k^t(\phi_{1kk}^t) + 3L_{kk}^t(\phi_{1k}^t) - 6L_k^t(\phi_{2k}^t) - L_{kkk}^t(\phi_0^t)][L_\omega^t(\phi_0^t)]^{-1} \, . \tag{5.14}$$

In these expressions the results up to $O(\epsilon)$ have been incorporated which is carried out in the preprint listed in section 1.1.

In the two generic cases analyzed in this paper, in which the global instability is dominated either by a saddle point of the absolute frequency $\omega_o(X)$ within the flow or by one streamwise boundary of the flow domain, we have developed approximate expressions for the global-mode frequency ω_{Gr}, its growth rate ω_{Gi} and its streamwise amplitude distribution in terms of local stability properties alone. The complex frequency ω_G in particular can be estimated very easily from the knowledge of the local absolute frequency ω_o and absolute wave number k_o on the <u>real</u> x-axis, except for the nonparallel frequency shift $\delta\omega$ (equs. 4.15a and 5.13) of order $O(\epsilon)$. All that is required is the analytic continuation of $\omega_o(X)$, $k_o(X)$ and $\omega_{kk}(X;k_o)$ from the real x-axis, on which the mean-flow data are generally defined, to the respective turning points X^t (equs. 3.13 and 5.12b). Moreover we can conclude that, in the context of the present analysis, global modes only become amplified if the streamwise extent of absolute instability is sufficiently large: in the doubly-infinite case the interval ΔX of absolute instability has to be at least of order $O(\epsilon^{1/2})$ when X^t is within $\epsilon^{1/2}$ of the real axis, and larger for X^t far from the real axis (see Hunt & Crighton, 1991). In the semi-infinite case, on the other hand, global instability results whenever the interval of absolute instability at the end grows to $\Delta X=O(\epsilon^{2/3})$ (see equ. 5.12b).

The question naturally arises of how relevant our two generic cases are to practical applications. It can be answered quite convincingly for the wake behind a rectangular plate. Hannemann & Oertel (1989) provide in their figure 16 a comparison between the linear ω_G from their fully nonparallel numerical

simulation and the local absolute frequency $\omega_0(X)$, which clearly displays a saddle at x≈1 on or very close to the real x-axis. Despite the proximity of the trailing edge, it appears from this comparison that the linear global mode, here the nascent Kármán vortex street, is dominated by a "wave maker" at x≈1 ! Hence the doubly-infinite model of section 1.4. will be used in section 4 to interpret the wake control experiments.

1.6. Appendices

A. The Rayleigh operator and its derivatives

In the following the Rayleigh operator $\mathcal{L}[\bullet;k,\omega,X]$ and its formal derivatives with respect to the parameters k, ω and X are compiled. In addition, the operator $\mathcal{L}_\epsilon$ which contains the nonparallel terms of the disturbance equation (2.6) is listed as (A.8). In all the argument lists the relevant parameters are given after a semi-colon. For the operators they include the eigenvalue pair k and ω associated with a parallel flow U(y;X) that coincides with the local velocity profile U(X,y) at X.

$$\mathcal{L}(\bullet;k,\omega,X) = [kU(y;X) - \omega][\partial_y^2 - k^2]\bullet - k[\partial_y^2 U(y;X)]\bullet \qquad (A.1)$$

$$\mathcal{L}_k(\bullet;k,\omega,X) = 2k\omega\,\bullet + U(y;X)[\partial_y^2 - 3k^2]\bullet - [\partial_y^2 U(y;X)]\bullet \qquad (A.2)$$

$$\mathcal{L}_\omega(\bullet;k,\omega,X) = -[\partial_y^2 - k^2]\bullet \qquad (A.3)$$

$$\mathcal{L}_X(\bullet;k,\omega,X) = k[\partial_X U(y;X)][\partial_y^2 - k^2]\bullet - k[\partial_X \partial_y^2 U(y;X)]\bullet \qquad (A.4)$$

$$\mathcal{L}_{kk}(\bullet;k,\omega,X) = 2\omega\,\bullet - 6kU(y;X)\bullet \qquad (A.5)$$

$$\mathcal{L}_{kX}(\bullet;k,\omega,X) = [\partial_X U(y;X)][\partial_y^2 - 3k^2]\bullet - [\partial_X \partial_y^2 U(y;X)]\bullet \qquad (A.6)$$

$$\mathcal{L}_{XX}(\bullet;k,\omega,X) = k[\partial_X^2 U(y;X)][\partial_y^2 - k^2]\bullet - k[\partial_X^2 \partial_y^2 U(y;X)]\bullet \qquad (A.7)$$

$$\mathcal{L}_{kkk}(\bullet;k,\omega,X) = -6U(y;X)\bullet \qquad (A.8)$$

$$\mathcal{L}_\epsilon(\bullet;k,\omega,X) = V(y;X)[\partial_y^3 - k^2\partial_y]\bullet + [\partial_X \partial_y U(y;X)]\partial_y\bullet - R^{-1}[\partial_y^2 - k^2]^2\bullet \qquad (A.9)$$

B. The k-derivative of the Rayleigh eigenfunction

The derivative of the Rayleigh equation (B.1) with respect to the wavenumber k, where $\mathcal{L}$ is given by (A.1), leads to the inhomogeneous Rayleigh equation (B.2).

$$\mathcal{L}(\phi_0;k,\omega,X) = 0 \;;\quad |\phi_0(|y|\to\infty;X)| = 0 \qquad (B.1)$$

$$\mathcal{L}(\partial_k\phi_0;k,\omega,X) = -\mathcal{L}_k(\phi_0;k,\omega,X) - \partial_k\omega\,\mathcal{L}_\omega(\phi_0;k,\omega,X) \qquad (B.2)$$

The solvability of (B.2) requires that the right-hand side be orthogonal to the homogeneous solution of the adjoint Rayleigh equation, i.e. to $\phi_0(y;X)\,[kU(y;X)-\omega]^{-1}$. With the notation (B.3) for the inner product

$$L_f(\cdot;k,\omega,X) = \int_{y_1}^{y_2} \mathcal{L}_f(\cdot;k,\omega,X)\,\frac{\phi_0(y;X)}{kU(y;X)-\omega}\,dy\ , \tag{B.3}$$

one obtains a convenient expression (B.4) for the complex group velocity $\partial_k\omega$ in terms of the Rayleigh eigenfunction ϕ_0.

$$\partial_k\omega + L_k(\phi_0;k,\omega,X)\,[L_\omega(\phi_0;k,\omega,X)]^{-1} = 0 \tag{B.4}$$

C. The X-derivative of the Rayleigh eigenfunction

In an analogous manner an expression for the X-derivative of ϕ_0 can be obtained. Differentiation of (B.1) with respect to X leads to the inhomogeneous Rayleigh equation (C.1).

$$\mathcal{L}(\partial_X\phi_0;k,\omega,X) = -\partial_X k\,\mathcal{L}_k(\phi_0;k,\omega,X) - \partial_X\omega\,\mathcal{L}_\omega(\phi_0;k,\omega,X) - \mathcal{L}_X(\phi_0;k,\omega,X) \tag{C.1}$$

With the notation (B.3), the solvability condition reads

$$\partial_X k\,L_k(\phi_0;k,\omega,X) + \partial_X\omega\,L_\omega(\phi_0;k,\omega,X) + L_X(\phi_0;k,\omega,X) = 0\ . \tag{C.2}$$

Using the result (B.4), this can be recast in the form

$$-\partial_X k\,\partial_k\omega + \partial_X\omega + L_X(\phi_0;k,\omega,X)\,[L_\omega(\phi_0;k,\omega,X)]^{-1} = 0\ . \tag{C.3}$$

For use in §3 we also list a particular solution of (C.1)

$$\partial_X\phi_0 = -\partial_X k\,\phi_{1k} - \partial_X\omega\,\phi_{1\omega} - \phi_{1X}\ , \tag{C.4}$$

in which the functions $\phi_{1k}(y;X)$, etc. are particular solutions of the inhomogeneous Rayleigh equations (C.5) which satisfy the same boundary conditions as ϕ_0

$$\mathcal{L}(\phi_{1f};k,\omega,X) = \mathcal{L}_f(\phi_0;k,\omega,X)\ ;\quad |\phi_{1f}(|y|\to\infty;X)| = 0\ . \tag{C.5}$$

In addition we will also need the following "second-generation" forced solution

$$\mathcal{L}(\phi_{2k};k,\omega,X) = \mathcal{L}_k(\phi_{1k};k,\omega,X)\ ;\quad |\phi_{2k}(|y|\to\infty;X)| = 0\ , \tag{C.6}$$

where ϕ_{1k} is given by (C.5).

1.7. References Pertaining to Section 1

ABRAMOWITZ, M. & STEGUN, I.A. 1965 *Handbook of mathematical functions*. Dover, New York.

BENDER, C.M. & ORSZAG, S.A. 1978 *Advanced mathematical methods for scientists and engineers*. McGraw Hill, New York.

BERS, A. 1983 Space-time evolution of plasma instabilities - absolute and convective. *Handbook of Plasma Physics* (M.N. Rosenbluth & R.Z. Sagdeev, Eds.), *Vol. 1*, 451-517.

BOUTHIER, M. 1972 Stabilité linéaire des écoulements presque paralleles. J. Mech. 4, 599-621.

BRIGGS, R.J. 1964 *Electron-stream interaction with plasmas*. MIT Press, Cambridge, Mass.

BURRIDGE, R. & WEINBERG, H. 1977 Horizontal rays and vertical modes. *Wave propagation and underwater acoustics* (J.B. Keller & J.S. Papadakis, Eds.), 86-150, Lecture Notes in Physics Vol. 70, Springer, Berlin.

CHOMAZ, J.-M., HUERRE, P. & REDEKOPP, L.G. 1988 Bifurcation to local and global modes in spatially developing flows. Phys. Rev. Lett. 60, 25-28.

CHOMAZ, J.-M., HUERRE, P. & REDEKOPP, L.G. 1991 A frequency selection criterion in spatially developing flows. Studies in Appl. Math. 84, 119-144.

CRIGHTON, D.G. & GASTER, M. 1976 Stability of slowly diverging jet flow. J. Fluid Mech. 77, 397-413.

GASTER M. 1968 Growth of disturbances in both space and time. Phys. Fluids 11, 723-727.

HANNEMANN, K. & OERTEL, H. Jr. 1989 Numerical simulation of the absolutely and convectively unstable wake. J. Fluid Mech. 199, 55-88.

HUERRE, P. & MONKEWITZ, P.A. 1985 Absolute and convective instabilities in free shear layers. J. Fluid Mech. 159, 151-168.

HUERRE, P. & MONKEWITZ, P.A. 1990 Local and global instabilities in spatially developing flows. Ann. Rev. Fluid Mech. 22, 473-537.

HUNT, R.E. & CRIGHTON, D.G. 1991 Instability of flows in spatially developing media. Proc. R. Soc. Lond. A 435, 109-129.

MONKEWITZ, P.A. 1988 The absolute and convective nature of instability in two-dimensional wakes at low Reynolds numbers. Phys. Fluids 31, 999-1006.

MONKEWITZ, P.A. 1990 The role of absolute and convective instability in predicting the behavior of fluid systems. Eur. J. Mech. B/Fluids 9, 395-413.

PIERREHUMBERT, R.T. 1984 Local and global baroclinic instability of zonally varying flow. J. Atmos. Sci. 41, 2141-2162.

SOWARD, A.M. & JONES, C.A. 1983 The linear stability of the flow in the narrow gap between two concentric rotating spheres. Quart. J. Appl. Math. 36, 19-42.

TRIANTAFYLLOU, G.S. & KARNIADAKIS, G.E. 1990 Computational reducibility of unsteady viscous flows. Phys. Fluids A 2, 653-656.

ZEBIB, A. 1987 Stability of viscous flow past a circular cylinder. J. Engr. Math. 21, 155-165.

2. SINGLE-INPUT SINGLE-OUTPUT CONTROL OF GLOBAL MODES: REDUCTION OF THE PLANT MODEL TO A STUART-LANDAU (SL) EQUATION, THE CONTROLLER DESIGN AND ITS IMPLEMENTATION IN A HEATED 2-D JET

2.1. Related Publications and Presentations

HENRICH, EDWARD A., Control of limit cycle oscillations with applications in fluid mechanics. Ph.D. Thesis, University of California, Los Angeles, 1991.

HENRICH, EDWARD A., MINGORI, TINO D.L. & MONKEWITZ, PETER A., Control of Hopf bifurcations. Proc. of NATO ASI on Chaotic Dynamics: Theory and Practice, Patras, Greece, July 1991.

GAMET, LIONEL, Control of a two-dimensional hot jet. DEA Thesis (ENSICA, Toulouse) carried out at the University of California, Los Angeles, 1991.

MONKEWITZ, PETER A., GAMET, LIONEL, HENRICH, EDWARD A. & MINGORI, TINO D.L., Feedback control of a self-excited heated two-dimensional jet. Bull Am. Phys. Soc. Vol. 36, p. 2629, 1991.

MONKEWITZ, PETER A., MINGORI, TINO D.L., HENRICH, EDWARD A. & YU, MING-HUEI, Adaptive and nonadaptive feedback control of global instabilities. Proc. AFOSR Contractors Meeting on Turbulence - Structure and Control, Columbus Ohio, pp. 103-106, April 1991.

HENRICH, EDWARD A., MINGORI, TINO D.L. & MONKEWITZ, PETER A., Control of Pitchfork and Hopf bifurcations. Submitted to 1992 ACC.

HENRICH, EDWARD A., MINGORI, TINO D.L. & MONKEWITZ, PETER A., Control of limit cycle oscillations with applications in fluid mechanics. To be submitted to Int. J. Control, 1992.

2.2. Introduction and the Analysis of a Hopf Bifurcation by Multiple Scales

Many systems in nature develop self-excited or limit cycle behavior when the most amplified global mode becomes temporally unstable. In fluid mechanics, two examples are a wake behind a cylinder and a heated jet [1,2]. The goal of this research is to control the self-excited oscillations exhibited by such systems or to induce them in globally stable systems.

For the control of flow oscillations, the primary task is the development of simplified model as the underlying partial differential equations are too unwieldy. In Section 1 we have derived linearized GL equations describing global modes in doubly- and semi-infinite systems which can be extended to the weakly nonlinear regime. When considering only a single gobla mode, the GL equation can be reduced to a Stuart-Landau equation for its characteristic amplitude, which is an ordinary differential equation in time. The latter can be viewed as describing the output of the probe at some fixed space location. The following development is carried out in this spirit and the resulting mathematical model for control, not being specific to the wake or the hot jet, should be able to control limit cycles in a variety of physical systems.

A common bifurcation in fluid mechanics is the Hopf bifurcation of a steady state to a limit cycle. In many cases, one bifurcates from the zero state to a non-zero steady-state to a limit cycle as a parameter is increased These bifurcations are generally the first steps in the transition to chaos or turbulence [3, 4] For a given physical system there are often design constraints which specify a fixed

region of parameter space in which one would like to operate. If this particular choice of parameters exhibits some undesirable dynamic behavior (e.g. limit cycles or chaos) then the goal of the control engineer is to suppress this behavior while still operating in the same parameter range. A distinction is made between a 'control parameter' or 'bifurcation parameter' which is the parameter one uses to study successive bifurcations and a 'control force' which is a prescribed function of time and possibly space used to modify the system's output. As an example, consider that one might desire to suppress the Von Kármán vortex street in the wake behind a cylinder. The control parameter is the Reynolds number which may be fixed at some supercritical value, where the wake is no longer steady. The control force could be an induced acoustic field designed to eliminate flow oscillations. This method uses the control force to stabilize the system in contrast to methods which modify the bifurcation parameter until the state behaves as desired [5].

In an attempt to understand the underlying properties of control, the research reported here concentrates on the development of control laws for finite dimensional nonlinear systems which undergo a Hopf bifurcation to a limit cycle. The relevance to fluid oscillations is that the finite dimensional nonlinear system can be thought of as a finite difference or Galerkin approximation to the Navier-Stokes equations. The Stuart-Landau equation is valid when the eigenvalues of these approximations are well separated.

Using a multiple scale perturbation technique we derive a Stuart-Landau equation which governs the effect of a linear regulator on a system undergoing a bifurcation. Often one does not know the differential equations governing the system, but one does know that the system exhibits behavior indicative of a Hopf bifurcation. In this case one still knows that asymptotically the dynamics are governed by a Stuart-Landau equation, so that this simplified equation can be used as a generic model. One can then estimate the parameters of the Stuart-Landau equation using experimental data and then determine an appropriate control strategy based on this information.

The Hopf bifurcation is a branching of time-periodic solutions from an equilibrium solution branch. When the bifurcation is supercritical, as one increases a parameter μ the equilibrium solution becomes unstable and a limit cycle is born. As one increases the control parameter further one sees more and more complicated behavior. These successive bifurcations comprise the basis for several theories for the transition to turbulence including period doubling, intermittency and quasi-periodicity [3, 4]. We now derive an amplitude equation for the Hopf bifurcation, the development follows that of [6].

For a physical system with a finite number of degrees of freedom, the dynamics may be described by a set of first order ordinary differential equations in vector fo

$$\frac{d\mathbf{X}(t)}{dt} = \mathbf{F}(\mathbf{X}(t);\mu) \tag{2.1}$$

where $\mathbf{X} \in R^n$ is the system state, $\mathbf{F}$ is a vector field and $\mu \in R$ is a control parameter in the problem. Equation (2.1) is presumed to have an equilibrium solution $\mathbf{X}_0(\mu)$ which satisfies $\mathbf{F}(\mathbf{X}_0(\mu);\mu) = 0$. We can then express (2.1) as a Taylor series about the equilibrium point $\mathbf{X}_0(\mu)$ so that

$$\frac{d\mathbf{x}}{dt} = L\mathbf{x} + M\mathbf{xx} + N\mathbf{xxx} + \cdots \tag{2.2}$$

where the expansion is in terms of $\mathbf{x} = \mathbf{X} - \mathbf{X}_0$. For the Taylor series to be valid we need $\mathbf{x}$ to be small, so that the nonlinear terms in (2.2) are small compared to the linear terms, i.e. the system is "weakly nonlinear". The matrix L is the Jacobian whose elements are given by

$$L_{jk} = \frac{\partial}{\partial X_k}(F_j)\,|_{x=x_0} \tag{2.3}$$

The abbreviations $M\mathbf{xx}$ and $N\mathbf{xxx}$ denote vectors containing the quadratic and cubic terms in the expansion. The jth component of these vectors is given by

$$(M\mathbf{xx})_j = \frac{1}{2!}\sum_k \frac{\partial}{\partial X_k}[\sum_l \frac{\partial}{\partial X_l}(F_j)\mathbf{x}_l]\mathbf{x}_k\,|_{x=x_0} \tag{2.4}$$

$$(N\mathbf{xxx})_j = \frac{1}{3!}\sum_k \frac{\partial}{\partial X_k}[\sum_l \frac{\partial}{\partial X_l}[\sum_m \frac{\partial}{\partial X_m}(F_j)\mathbf{x}_m]\mathbf{x}_l]\mathbf{x}_k\,|_{x=x_0} \tag{2.5}$$

We are interested in Hopf bifurcations, so we introduce some restrictions on the linear operator L. The stability of the equilibrium solution $\mathbf{X}_0$ is determined by the eigenvalues of L. We assume that L is stable for $\mu < 0$ and unstable for $\mu > 0$. By L unstable, we mean that at least one of the eigenvalues, λ, found by solving $Lr = \lambda r$ has a real part greater than zero. We also assume that these eigenvalues have nonzero transversal "velocity" when crossing the imaginary axis. That is

$$\frac{dRe(\lambda(\mu))}{d\mu}\,|_{\mu=0} > 0 \tag{2.6}$$

which we will shortly see fixes the scaling for the slow time scale to be $|\mu|\,t$.

We expand the linear operator in powers of μ

$$L = L^{(0)} + \mu L^{(1)} + \mu^2 L^{(2)} + \cdots \tag{2.7}$$

similar expressions may be developed for M and N. The eigenvalues of L are expressed as

$$\lambda_j(\mu) = \lambda_j^{(0)} + \mu\lambda_j^{(1)} + \mu^2\lambda_j^{(2)} + \cdots \tag{2.8}$$

The convention that a superscript in parentheses denotes a perturbation and a subscript refers to an index will be used throughout. The eigenvalues are complex in general and can be written as $\lambda_j^{(k)} = \sigma_j^{(k)} + i\omega_j^{(k)}$. Let $\mathbf{r}_j$ and $\mathbf{l}_j$ denote the right and left eigenvectors of $L^{(0)}$ so that

$$L^{(0)}\mathbf{r}_j = \lambda_j^{(0)}\mathbf{r}_j \tag{2.9}$$

$$\mathbf{l}_j L^{(0)} = \lambda_j^{(0)}\mathbf{l}_j \tag{2.10}$$

For simple eigenvalues, the eigenvectors are orthogonal ($\mathbf{l}_j\mathbf{r}_k = 0$ for $j \neq k$) and we can choose to normalize such that $\mathbf{l}_j\mathbf{r}_j = 1$. We now define a small positive parameter ϵ such that $\mu = \epsilon^2\mathcal{X}$ where $\mathcal{X} = \mathrm{sgn}(\mu)$. We can expand the state in powers of ϵ as

$$\mathbf{x} = \epsilon\mathbf{x}^{(1)} + \epsilon^2\mathbf{x}^{(2)} + \cdots \tag{2.11}$$

Note that the expansion starts with terms of order ϵ. This follows from the assumption that the system (2.1) is weakly nonlinear. For systems where this is not the case the equations (2.15) are not generally solvable since the $O(1)$ equation is also nonlinear. Also note that defining $\epsilon = \sqrt{|\mu|}$ represents a balance of the relevant nonlinear terms and the linear damping or dedamping of the critical modes.

Since the real part of the critical eigenvalue is $O(\epsilon^2)$ it is natural to introduce a second time scale $\tau = |\mu|\,t = \epsilon^2 t$. We treat the two time scales as independent variables so that the $\mathbf{x}^{(k)}$'s are functions of two variables [7]. The rule for calculating derivatives becomes

$$\frac{d}{dt} \to \frac{\partial}{\partial t} + \epsilon^2\frac{\partial}{\partial\tau} \tag{2.12}$$

Inserting these expansions in μ and ϵ into the Taylor expansion (2.2) and equating like powers of ϵ results in an infinite set of linear inhomogeneous partial differential equations of the form

$$(\frac{\partial}{\partial t} - L^{(0)})\mathbf{x}^{(k)} = \mathcal{F}^{(k)} \tag{2.13}$$

The first few $\mathcal{F}^{(k)}$ are

$$O(\epsilon): \quad \mathcal{F}^{(1)} = 0 \tag{2.14}$$

$$O(\epsilon^2): \quad \mathcal{F}^{(2)} = M^{(0)}\mathbf{x}^{(1)}\mathbf{x}^{(1)} \tag{2.15}$$

$$O(\epsilon^3): \quad \mathcal{F}^{(3)} = 2M^{(0)}\mathbf{x}^{(1)}\mathbf{x}^{(2)} + N^{(0)}\mathbf{x}^{(1)}\mathbf{x}^{(1)}\mathbf{x}^{(1)} - (\frac{\partial}{\partial\tau} - \mathcal{X}L^{(1)})\mathbf{x}^{(1)} \tag{2.16}$$

Note that the $\mathcal{F}^{(k)}$'s are functions of $\mathbf{x}^{(j)}$ with $j < k$ so that they are known functions if we solve the set of equations in order.

The lowest order problem, $O(\epsilon)$, is linear and homogeneous, and the higher order problems are linear and inhomogeneous. The $O(\epsilon)$ equation is

$$\frac{\partial}{\partial t}\mathbf{x}^{(1)} = L^{(0)}\mathbf{x}^{(1)} \tag{2.17}$$

which has the solution in terms of the eigenvectors

$$\mathbf{x}^{(1)}(t,\tau) = \sum_{j=1}^{n} c_j(\tau) e^{\lambda_j^{(0)} t}\mathbf{r}_j \tag{2.18}$$

Since (2.17) is a partial differential equation, the solution is found in terms of an arbitrary function of the slow time scale τ. For this reason, the coefficients, c_j, are allowed to depend on the slow time scale $\tau = \epsilon^2 t$ in standard multiple scale fashion. The higher order problems determine conditions on these arbitrary functions in order to make the solution $\mathbf{x}^{(1)}(t,\tau)$ uniformly valid for times of $O(1/\epsilon)$. One must impose "solvability" conditions so that the solution $\mathbf{x}^{(1)}(t,\tau)$ does not involve any "secular" terms (i.e. terms which become unbounded). Since the operator on the left hand side of (2.13) is the same for each order, the solvability condition is that we must eliminate terms on the right hand side of (2.13) which are marginally stable solutions of the homogeneous equation.

We number the two critical eigenvalues first so that $\lambda_1^{(0)} = \bar{\lambda}_2^{(0)} = i\omega^{(0)}$ and rewrite (2.18) as

$$\mathbf{x}^{(1)}(t,\tau) = A(\tau)e^{i\omega^{(0)}t}\mathbf{r}_1 + \bar{A}(\tau)e^{-i\omega^{(0)}t}\bar{\mathbf{r}}_1 + \sum_{j=3}^{n} c_j(\tau)e^{\lambda_j^{(0)}t}\mathbf{r}_j \tag{2.19}$$

where $A(\tau) = c_1(\tau) = \bar{c}_2(\tau)$ will be the dependent variable in a complex amplitude equation. Since the real part of the critical eigenvalues is $O(\epsilon^2)$ the slow temporal growth or decay is absorbed in the slowly varying amplitude $A(\tau)$.

The second equation, $O(\epsilon^2)$, is

$$\frac{\partial}{\partial t}\mathbf{x}^{(2)} = L^{(0)}\mathbf{x}^{(2)} + M^{(0)}\mathbf{x}^{(1)}\mathbf{x}^{(1)} \tag{2.20}$$

To solve the $O(\epsilon^2)$ equation we note that since $\mathcal{F}^{(2)}$ is quadratic it acts like an input forcing at $2\omega^{(0)}$ and D.C. as well as other nonsecular inputs. The solution is

$$\mathbf{x}^{(2)} = \mathbf{V}_+ A^2 e^{2i\omega^{(0)}t} + \mathbf{V}_- \bar{A}^2 e^{-2i\omega^{(0)}t} + \mathbf{V}_0 |A|^2 + \cdots \tag{2.21}$$

where $+\cdots$ are terms which will not cause a secularity at $O(\epsilon^3)$. Substitution of (2.19) and (2.21) into (2.20) and equating coefficients of A^2, $\bar{A}^2$ and $|A|^2$ and solving for $\mathbf{V}_+$, $\mathbf{V}_-$ and $\mathbf{V}_0$ we obtain

$$\mathbf{V}_+ = \bar{\mathbf{V}}_- = -[L^{(0)} - 2i\omega^{(0)}]^{-1} M^{(0)}\mathbf{r}_1\mathbf{r}_1 \tag{2.22}$$

$$\mathbf{V}_0 = -2[L^{(0)}]^{-1} M^{(0)}\mathbf{r}_1\bar{\mathbf{r}}_1 \tag{2.23}$$

Now we concentrate on eliminating the secular terms at order ϵ^3. To do this form $\mathbf{l}_1\mathcal{F}^{(3)}(t,\tau)$ and then set the coefficients of $e^{i\omega^{(0)}t}$ equal to zero, which gives the solvability condition at order ϵ^3

$$\begin{aligned}&\mathbf{l}_1[2\bar{A}A^2 M^{(0)}\bar{\mathbf{r}}_1\mathbf{V}_+ + 2|A|^2 A M^{(0)}\mathbf{r}_1\mathbf{V}_0\\ &+3N^{(0)}\mathbf{r}_1\mathbf{r}_1\bar{\mathbf{r}}_1 A^2\bar{A} - \frac{\partial}{\partial\tau}A\mathbf{r}_1 + \mathcal{X}L^{(1)}A\mathbf{r}_1] = 0\end{aligned} \tag{2.24}$$

This can be rewritten as an amplitude equation

$$\frac{dA}{d\tau} = \mathcal{X}\lambda_1^{(1)}A - g|A|^2 A \tag{2.25}$$

where

$$\lambda_1^{(1)} = \mathbf{l}_1 L^{(1)} \mathbf{r}_1 \tag{2.26}$$

$$g = -2\mathbf{l}_1 M^{(0)} \bar{\mathbf{r}}_1 \mathbf{V}_+ - 2\mathbf{l}_1 M^{(0)} \mathbf{r}_1 \mathbf{V}_0 - 3\mathbf{l}_1 N^{(0)} \mathbf{r}_1 \mathbf{r}_1 \bar{\mathbf{r}}_1 \tag{2.27}$$

Equation (2.25) is known as the Stuart-Landau equation.

Example: *Van der Pol Oscillator*

To illustrate the method, we consider the Van der Pol equation in dimensionless form

$$\ddot{y} + (y^2 - \mu)\dot{y} + y = 0 \tag{2.28}$$

If we take the state to be $\mathbf{X} = [y\ \dot{y}]^T$ then the vector field is

$$\mathbf{F}(\mathbf{X};\mu) = \begin{bmatrix} 0 & 1 \\ -1 & \mu \end{bmatrix} \mathbf{X} + \begin{bmatrix} 0 \\ -X_1^2 X_2 \end{bmatrix} \tag{2.29}$$

The equilibrium state is $\mathbf{X}_0 = [0\ 0]^T$, so that the Jacobian is

$$L = \begin{bmatrix} 0 & 1 \\ -1 & 0 \end{bmatrix} + \mu \begin{bmatrix} 0 & 0 \\ 0 & 1 \end{bmatrix} = L^{(0)} + \mu L^{(1)} \tag{2.30}$$

and the cubic term in the Taylor expansion is

$$(N\mathbf{xyz})_2 = -\frac{1}{3}(x_2 y_1 z_1 + x_1 y_2 z_1 + x_1 y_1 z_2) \tag{2.31}$$

The left and right eigenvectors for the critical eigenvalue $\lambda_1^{(0)} = i$ are $\mathbf{l}_1 = \frac{1}{2}[1\ -i]$ and $\mathbf{r}_1 = [1\ i]^T$. The perturbation in the eigenvalue is $\lambda_1^{(1)} = \mathbf{l}_1 L^{(1)} \mathbf{r}_1 = \frac{1}{2}$. The coefficient of the nonlinear term in the Stuart-Landau equation is $g = -3\mathbf{l}_1 N^{(0)} \mathbf{r}_1 \mathbf{r}_1 \bar{\mathbf{r}}_1 = \frac{1}{2}$. The Stuart-Landau equation for this example is

$$\frac{dA}{d\tau} = \frac{1}{2}\mathcal{X} A - \frac{1}{2} A\,|A|^2 \tag{2.32}$$

The initial condition for the Stuart-Landau equation is $A(0) = \frac{1}{2\epsilon}(y(0) - i\dot{y}(0))$. Figure 1 compares the exact solution of the Van der Pol equation (by numerical integration) to the asymptotic solution found by solving the Stuart-Landau equation. In this figure our small parameter is $\epsilon = .5$. The important thing to note is that the short term prediction using this model is very good, and short term prediction is all that is needed for control. □

2.3. The Linear Regulator and the Nonlinear Plant

This paper addresses the problem of controlling a system by external forcing when the control parameter is fixed by some other design constraint. We assume that the plant (subscript p) is a single-input single-output system with nonlinear dynamic equations which undergo a Hopf bifurcation at $\mu = 0$

$$\frac{d\mathbf{X}_p}{dt} = \mathbf{F}(\mathbf{X}_p;\mu) + B_p u \tag{3.1}$$

$$y = C_p \mathbf{X}_p + D_p \tag{3.2}$$

$$\mathbf{X}_p \in R^{N_p} \text{ and } \mu, u \in R \tag{3.3}$$

The goal of the control system is to return the system to its equilibrium state which has become open loop unstable for $\mu > 0$. A natural choice for a control system is the linear regulator as depicted in Figure 2. The differential equations governing the control system are such that the Laplace transform of the impulse response of the linear compensator (subscript c) is $KG(s)$.

The equations governing the regulator are

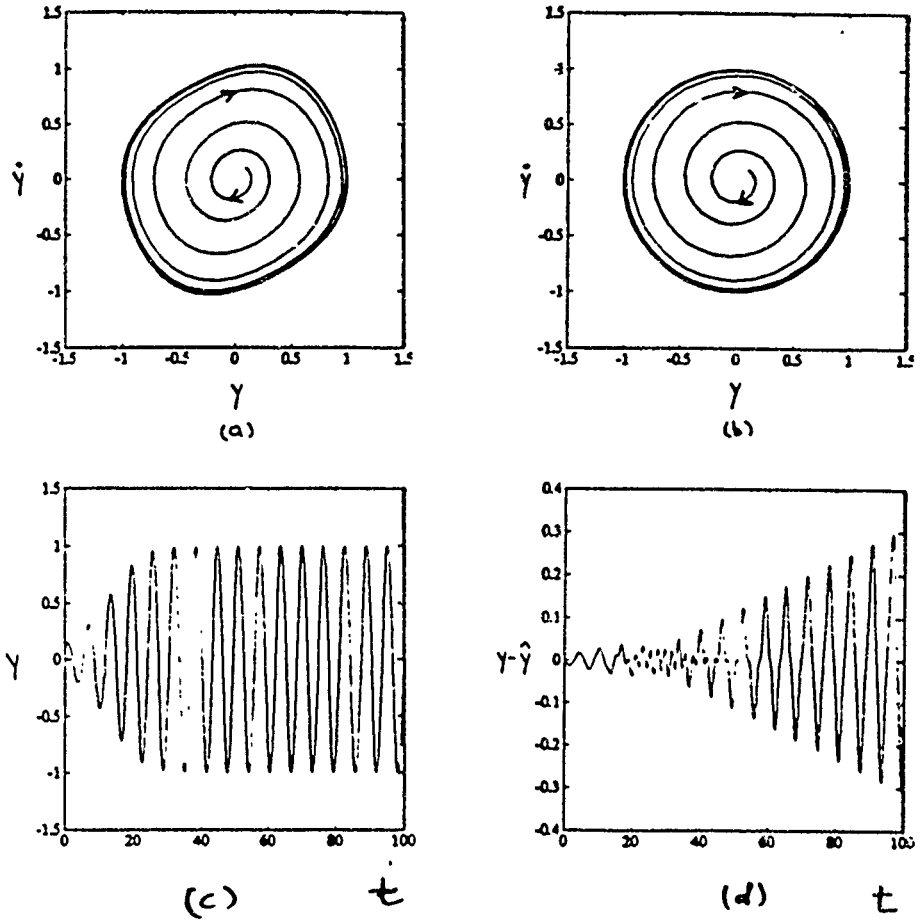

Figure 1: Comparison of Exact and Asymptotic solutions of the Van der Pol equation for $\epsilon = .5$ a) Phase plane for exact solution b) Phase plane for asymptotic solution c) Exact solution d) Difference between exact and asymptotic solutions

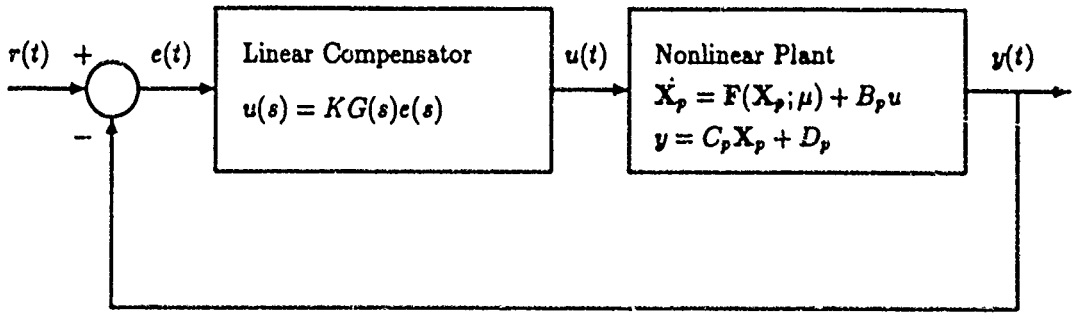

Figure 2: Block diagram of the control system

$$\dot{\mathbf{x}}_c = A_c\mathbf{x}_c + KB_c e \tag{3.4}$$

$$u = C_c\mathbf{x}_c + KD_c e \tag{3.5}$$

$$\mathbf{x}_c \in R^{N_c} \text{ and } e, \mu \in R \tag{3.6}$$

Where $e = r - y$ is the error signal, and the reference signal is the output which corresponds to the equilibrium solution $r = y_0 = C_p\mathbf{X}_{p0} + D_p$. The compensator is asymptotically stable, that is, the eigenvalues of A_c lie in the open left half plane.

We may expand (3.1) in a Taylor series about its equilibrium point $\mathbf{X}_{p0}$ so that

$$\frac{d\mathbf{x}_p}{dt} = L_p\mathbf{x}_p + M_p\mathbf{x}_p\mathbf{x}_p + N_p\mathbf{x}_p\mathbf{x}_p\mathbf{x}_p + \cdots + B_p u \tag{3.7}$$

where $\mathbf{F}(\mathbf{X}_{p0}; \mu) = 0$ defines the equilibrium point and $\mathbf{x}_p = \mathbf{X}_p - \mathbf{X}_{p0}$ is the expansion variable. The output equation becomes $y = C_p\mathbf{x}_p + C_p\mathbf{X}_{p0} + D_p$. Combining these two vector equations into a composite equation we obtain

$$\frac{d}{dt}\begin{bmatrix} \mathbf{x}_p \\ \mathbf{x}_c \end{bmatrix} = \begin{bmatrix} L_p - KB_pD_cC_p & B_pC_c \\ -KB_cC_p & A_c \end{bmatrix}\begin{bmatrix} \mathbf{x}_p \\ \mathbf{x}_c \end{bmatrix} + \begin{bmatrix} M_p\mathbf{x}_p\mathbf{x}_p + N_p\mathbf{x}_p\mathbf{x}_p\mathbf{x}_p + \cdots \\ 0 \end{bmatrix} \tag{3.8}$$

which is in the standard form (2.2). We assume that the plant undergoes a Hopf bifurcation at $\mu = 0$ and that we can expand

$$L_p = L_p^{(0)} + \mu L_p^{(1)} + \cdots \tag{3.9}$$

in the usual way. We assume that we choose a small gain such that $KC_p \sim O(\mu)$ and so we rewrite $K = |\mu|\,\kappa$. The expansion for the composite system's linear operator is

$$L = L^{(0)} + \mu L^{(1)} + \cdots \tag{3.10}$$

where

$$L^{(0)} = \begin{bmatrix} L_p^{(0)} & B_pC_c \\ 0 & A_c \end{bmatrix} \tag{3.11}$$

and

$$L^{(1)} = \begin{bmatrix} L_p^{(1)} - \mathrm{sgn}(\mu)\kappa B_pD_cC_p & 0 \\ -\mathrm{sgn}(\mu)\kappa B_cC_p & 0 \end{bmatrix} \tag{3.12}$$

Order the plant's eigenvalues such that the marginal eigenvalues are first and denote the plant's left and right eigenvectors by $\mathbf{l}_{1p}L_p^{(0)} = i\omega^{(0)}\mathbf{l}_{1p}$ and $L_p^{(0)}\mathbf{r}_{1p} = i\omega^{(0)}\mathbf{r}_{1p}$. The right eigenvector for the composite matrix $L^{(0)}$ is $\mathbf{r}_1 = \begin{bmatrix} \mathbf{r}_{1p}^T & 0_{N_c} \end{bmatrix}^T$ and the left eigenvector is

$$\mathbf{l}_1 = \begin{bmatrix} \mathbf{l}_{1p} & \mathbf{l}_{1p}B_pC_c[i\omega^{(0)} - A_c]^{-1} \end{bmatrix} \tag{3.13}$$

We compute the perturbation in the critical eigenvalue as

$$\lambda_1^{(1)} = \mathbf{l}_1L^{(1)}\mathbf{r}_1 = \mathbf{l}_{1p}L_p^{(1)}\mathbf{r}_{1p} - \mathrm{sgn}(\mu)\mathbf{l}_{1p}BC\mathbf{r}_{1p}\kappa[C_c(i\omega^{(0)} - A_c)^{-1}B_c + D_c] \tag{3.14}$$

We can rewrite (3.14) as

$$\lambda_1^{(1)} = \lambda_{1p}^{(1)} - \mathcal{X}\kappa J_{1p}G(i\omega^{(0)}) \tag{3.15}$$

where $\lambda_{1p}^{(1)}$ is the uncontrolled perturbation in the critical eigenvalue, $J_{1p} = \mathbf{l}_{1p}BC\mathbf{r}_{1p}$ is the receptivity of the critical mode and

$$KG(s) = K[C_c(sI - A_c)^{-1}B_c + D_c] \tag{3.16}$$

is the transfer function of the linear compensator. We see that, in the context of multiple scales, all compensators with the same gain and phase at the critical frequency have the same effect on the plant. Note that J_{1p} is what is known as a "modal influence coefficient" in structural mechanics or the "receptivity" in fluid mechanics corresponding to the critical mode. This complex constant determines how the control input couples to the output. The goal of the control system is to force "in phase" to enhance oscillation and "out of phase" to reduce oscillation. The coefficient J_{1p} tells us which phase is "in" and which phase is "out".

The nonlinear term in the Stuart-Landau equation is unchanged by the addition of this linear compensator. The Landau constant remains $g = g_p$. To see this, first compute $\mathbf{V}_+^T = [\ \mathbf{V}_{+p}^T \quad 0_{Nc}\ ]^T$ and $\mathbf{V}_0^T = [\ \mathbf{V}_{0p}^T \quad 0_{Nc}\ ]^T$. Then

$$g = -2l_{1p}M_p^{(0)}\bar{\mathbf{r}}_{1p}\mathbf{V}_{+p} - 2l_{1p}M_p^{(0)}\mathbf{r}_{1p}\mathbf{V}_{0p} - 3l_{1p}N_p^{(0)}\mathbf{r}_{1p}\mathbf{r}_{1p}\bar{\mathbf{r}}_{1p} = g_p \tag{3.17}$$

Hence, the Stuart-Landau equation for the regulated system is

$$\frac{dA}{d\tau} = (\mathcal{X}\lambda_{1p}^{(1)} - J_{1p}\kappa G(i\omega^{(0)}))A - g_p\,|A|^2\,A \tag{3.18}$$

The preservation of the nonlinear term is a consequence of choosing the compensator gain to be $O(\mu)$.

Example: *Van der Pol Oscillator with a Linear Regulator*

The equation for the Van der Pol oscillator with a control force is

$$\ddot{y} + (y^2 - \mu)\dot{y} + y = u \tag{3.19}$$

The Stuart-Landau equation for the regulated system is

$$\frac{dA}{d\tau} = \frac{1}{2}(\mathcal{X} + iKG(i))\,A - \frac{1}{2}\,|A|^2\,A \tag{3.20}$$

The method of multiple scales predicts the closed loop system will be stable for $Im(KG(i)) > 1$. If we consider derivative feedback so that

$$u(s) = KG(s)y(s) = Ksy(s) \tag{3.21}$$

then we expect stability for $K > \mu$. It is easy to check that this is in fact the exact result. If we consider a lead compensator so that

$$G(s) = \frac{(s+a)}{(s+b)} \tag{3.22}$$

then the multiple scales method predicts closed loop stability for

$$\frac{\kappa(b-a)}{b^2+1} > 1 \tag{3.23}$$

For $\mu > 0$ the closed loop system is stable for

$$\frac{\kappa(b-a)}{b^2+1} > 1 + \mu\frac{\kappa - b}{b^2+1} \tag{3.24}$$

So the multiple scales stability result is correct to $O(1)$.

For comparison, we consider the same plant and control and determine the center manifold reduction and normal form [8]. The dynamics are

$$\dot{\mu} = 0 \tag{3.25}$$

$$\dot{y} = v \tag{3.26}$$

$$\dot{v} = -y + \mu v - y^2 v + u \tag{3.27}$$

$$\dot{u} = -bu - \kappa\mathcal{X}\mu v - \kappa\mathcal{X}a\mu y \tag{3.28}$$

where terms involving μ are nonlinear since μ is also a state variable. We have a three dimensional center manifold. The center manifold is

$$u = u(\mu, y, v) = -\kappa\mathcal{X}\frac{1+ab}{b^2+1}\mu y - \kappa\mathcal{X}\frac{b-a}{b^2+1}\mu v + \cdots \tag{3.29}$$

The dynamics on the center manifold are governed by the equation

$$\ddot{y} + y = -\mu\left[\frac{\kappa\mathcal{X}(b-a)}{b^2+1} - 1\right]\dot{y} - \left[\mu\frac{\kappa\mathcal{X}(1+ab)}{b^2+1}\right]y - \dot{y}y^2 + \cdots \tag{3.30}$$

Reducing this equation to normal form gives

$$\frac{dr}{dt} = \frac{\mu}{2}\left[1 - \frac{\kappa\mathcal{X}(b-a)}{b^2+1}\right] - \frac{1}{8}r^3 \tag{3.31}$$

which is identical to the multiple scales result ($A = re^{i\theta}/(2\epsilon), \tau = \epsilon^2 t$). □

By specifying the gain of the compensator to be $O(\mu)$ we have derived an amplitude equation which explicitly shows the effect of any linear compensator on a nonlinear system near a Hopf bifurcation. The importance of this result goes beyond analyzing the effect of a control system on the plant. Since any plant which exhibits the features of a Hopf bifurcation is asymptotic to the solution of some Stuart-Landau equation, we can use the Stuart-Landau equation as a generic model for a Hopf bifurcation even when the plant equations are unknown. We can assume the plant is the Stuart-Landau equation and then try to estimate its coefficients. We may select several compensators in order to estimate the coefficients $\lambda_{1p}^{(1)}$ and J_{1p} through control induced transients. Once we have accurate estimates for these parameters we may specify the correct phase of the compensator at the critical frequency. That is we can determine the best $G(i\omega^{(0)})$.

Using the same type of analysis we find that equation (3.18) holds for pitchfork bifurcations as well if we set $\omega^{(0)} = 0$ [9, 10].

2.4. An Amplitude Equation for Parameter Estimation

To control a given physical system, we intend to use a feedback control based on a set of measurements which depend on the system state. A general nonlinear measurement equation $y = H(\mathbf{X})$ can be written as a Taylor series

$$y = H^{(0)} + H^{(1)}\mathbf{x} + H^{(2)}\mathbf{xx} + H^{(3)}\mathbf{xxx} + \cdots \tag{4.1}$$

Since $\mathbf{x}$ is $O(\epsilon)$, the leading order contribution is the affine equation

$$y = C\mathbf{X} + D \tag{4.2}$$

The leading order effect of the measurement equation is to scale the system state and provide a D.C. bias. If the system we are interested in contains a small parameter $\mu = \mathcal{X}\epsilon^2$ and exhibits limit cycles when $\mu > 0$, we detect ϵ not by the size of the output, but by the slow time scale and by how far the phase plane diagram of the limit cycle is "out-of-round". In the limit as $\epsilon \to 0$ the output is a sinusoid. So that in terms of the physical observation, the term "weakly nonlinear" implies the system has "almost sinusoidal" oscillations. The leading order asymptotic expression for $\mathbf{x}$ is

$$\mathbf{x} \sim \epsilon[A(\tau)e^{i\omega^{(0)}t}\mathbf{r}_1 + \text{c.c.}] \tag{4.3}$$

We define $Y(\tau)$ as the output "amplitude"

$$Y(\tau) \equiv 2\epsilon A(\tau)C\mathbf{r}_1 \tag{4.4}$$

From equations (4.2), (4.3) and (4.4) the leading order asymptotic expression for the output is

$$y(t) \sim 2\epsilon Re[A(\tau)C\mathbf{r}_1 e^{i\omega^{(0)}t}] + C\mathbf{X}_0 + D = Re[Y(\tau)e^{i\omega^{(0)}t}] + C\mathbf{X}_0 + D \tag{4.5}$$

Equation (4.4) relates the physical amplitude $Y(\tau)$ to the amplitude in the normalized Stuart-Landau equation $A(\tau)$. We are interested in real-time estimation, so we also return to the physical time scale $t = \tau/\epsilon^2$. Making the appropriate substitutions in the Stuart-Landau equation (3.18) leads to an amplitude equation for $Y(t)$

$$\frac{dY}{dt} = \Lambda^{OL}Y - g\,|Y|^2\,Y + JU(t) \tag{4.6}$$

where

$$\Lambda^{OL} = \mu\lambda_1^{(1)} \tag{4.7}$$

$$g = \frac{-2\mathbf{l}_1 M^{(0)}\bar{\mathbf{r}}_1\mathbf{V}_+ - 2\mathbf{l}_1 M^{(0)}\mathbf{r}_1\mathbf{V}_0 - 3\mathbf{l}_1 N^{(0)}\mathbf{r}_1\mathbf{r}_1\bar{\mathbf{r}}_1}{4\,|C\mathbf{r}_1|^2} \tag{4.8}$$

$$J = (C_p\mathbf{r}_1)(\mathbf{l}_1 B_p) \tag{4.9}$$

and $U(t) = KG(i\omega^{(0)})Y(t)$ for the linear regulator. Note that this is an input-output description. The coefficient J combines the effects of control and observation like a "modal influence coefficient" used in model reduction.

The dimensional output $y(t)$ is recovered from (4.5). The dimensional value of the control is given by

$$u(t) = Re[U(t)e^{i\omega^{(0)}t}] \tag{4.10}$$

Notice that we have eliminated the unknown parameter ϵ.

The complex amplitude equation which models Hopf bifurcations is

$$\dot{Y} = \Lambda Y - g\,|Y|^2\,Y \tag{4.11}$$

where $\Lambda = \Lambda^{OL}$ without control and $\Lambda = \Lambda^{CL} = \Lambda^{OL} - JKG(i\omega^{(0)})$ with feedback control. One can demodulate the measured output $y(t)$ using a Hilbert transform to get $Y(t)$ [9, 11]. We consider parameter estimation for the Stuart-Landau equation with transient data. We use a Lyapunov function $E = |Y|^2$ to develop a procedure for estimating the real parts of Λ^{OL} and g. From (4.11) we have

$$\dot{E} = 2\Lambda_r E - 2g_r E^2 \tag{4.12}$$

If $\Lambda_r > 0$ and $g_r > 0$ a stable limit cycle exists. If $\Lambda_r < 0$ and $g_r > 0$ then the Stuart-Landau equation is globally asymptotically stable. We expect that a feedback which makes $\Lambda_r < 0$ in the closed loop should stabilize the system, that is it should eliminate limit cycle oscillations.

Since we are primarily interested in controlling the amplitude of the limit cycle, it is sufficient for our purposes to estimate the coefficients Λ_r and g_r. The coefficients Λ_i and g_i can also be determined (see [11]).

To estimate the parameters of (4.12), we can approximate the derivative in order to estimate the parameters of the Stuart-Landau equation. Using an Euler approximation to the time derivative equation (4.12) becomes

$$E(k+1) = (1 + 2\Lambda_r\Delta)E(k) - (2g_r\Delta)E(k)^2 \tag{4.13}$$

The equilibrium solutions of equation (4.13) are $E(\infty) = 0$ and $E(\infty) = \Lambda_r/g_r$ which is the same as the equilibrium solutions of equation (4.12), independent of the sample time, Δ.

So we should be able to replace the continuous time Stuart-Landau equation (4.11) by an approximate sampled data equation in the form

$$E(k+1) = \theta_1 E(k) + \theta_2 E(k)^2 \tag{4.14}$$

Since this equation is linear in the parameters we can derive a least squares estimator for the parameter vector Θ. As a cautionary note, we observe that we have replaced the well behaved continuous time logistic equation (4.12) with a discrete logistic equation or quadratic map (4.14), which is known to exhibit chaos for a range of its parameters. For $0 < \Lambda_r < f_s$ that the dynamics will asymptote to the fixed point $E(\infty) = \Lambda_r / g_r$. That is, as long as the sampling rate, $f_s = 1/\Delta$, is larger than the slow exponential growth rate, Λ_r, there will be no periodic or chaotic solutions to equation (4.13) [9].

From the batch form of the least squares problem

$$\begin{bmatrix} E_2 \\ \vdots \\ E_{N+1} \end{bmatrix} = \begin{bmatrix} E_1 & E_1^2 \\ \vdots & \vdots \\ E_N & E_N^2 \end{bmatrix} \begin{bmatrix} \theta_1 \\ \theta_2 \end{bmatrix} \tag{4.15}$$

we could also derive a formula for the least squares parameter estimate.

$E = |Y|^2$ is known since we can find Y by using the Hilbert transform. The estimation procedure works best when the initial conditions are small so that we have some data in the linear growth range. In practice this might require several parameter excursions below the critical value of μ to obtain a steady state which is a fixed point. Then we could increase μ above critical and get a transient with some data in the linear range. In principle the system could be identified by using parameter excursions, but for the hot jet this is impractical since we cannot instantaneously change the density of the hot fluid. A more practical parameter estimation scheme is to use a feedback control system to induce transients.

If we consider a closed loop control with a fixed gain the closed loop Stuart-Landau equation is

$$\dot{Y} = (\Lambda^{OL} - JKG(i\omega^{(0)}))Y - g\,|Y|^2\,Y \tag{4.16}$$

We can use the same procedure on the closed loop system as the uncontrolled system to find

$$\Lambda_r^{CL} = \Lambda_r^{OL} - J_r K \cos\phi + J_i K \sin\phi \tag{4.17}$$

and g_r. Using "control induced transients" is a more practical approach to estimation. By selecting several different gains and phases, we can use the data from each of these control induced transients to determine the parameters Λ_r, J_r and J_i by least squares.

$$\begin{bmatrix} 1 & -K_1\cos\phi_1 & K_1\sin\phi_1 \\ \vdots & \vdots & \vdots \\ 1 & -K_N\cos\phi_N & K_N\sin\phi_N \end{bmatrix} \begin{bmatrix} \Lambda_r^{OL} \\ J_r \\ J_i \end{bmatrix} = \begin{bmatrix} \Lambda_{r,1}^{CL} \\ \vdots \\ \Lambda_{r,N}^{CL} \end{bmatrix} \tag{4.18}$$

Once we have estimated J the optimum choice for the gain is $K = \gamma \bar{J}$ where γ is a real scalar and the overbar denotes complex conjugate. This control will use the least amount of control energy for a fixed amount of stabilization.

2.5. Simulation Results

We consider a nonlinear plant which undergoes a Hopf bifurcation to a limit cycle under the action of a linear regulator. We study the effect of controller gain (for a fixed phase) on the amplitude of the limit cycle oscillations. We also perform a computational experiment for fixed gain and vary the phase of the controller.

First we consider the "steady-state" solutions of equation (4.6). The term steady-state in this context refers to a steady Fourier amplitude or constant "energy" $E = |Y|^2$ of the system For a pitchfork bifurcation this is a steady-state in time. For a Hopf bifurcation this corresponds to a

time-periodic state or limit cycle. We write $KG(i\omega^{(0)}) = Ke^{i\phi}$ so that the gain of the compensator is unity at the critical frequency ($|G(i\omega^{(0)})| = 1$). When the system is in a limit cycle, the steady state solution of equation (4.16) yields

$$|Y| = \sqrt{\frac{\Lambda_r^{OL} - J_r K\cos\phi + J_i K\sin\phi}{g_r}} \tag{5.1}$$

We cannot uniquely determine the parameters Λ_r^{OL}, J_r, J_i and g_r using steady-state data. If one normalizes by the amplitude without control, $|Y|_{NC} = \sqrt{\Lambda_r^{OL}/g_r}$, the normalized amplitude, $|\mathcal{Y}| = |Y| / |Y|_{NC}$, satisfies

$$|\mathcal{Y}| = \sqrt{1 - \frac{J_r}{\Lambda_r^{OL}} K\cos\phi + \frac{J_i}{\Lambda_r^{OL}} K\sin\phi} \tag{5.2}$$

That is, we normalize the coefficients by the growth rate, Λ_r^{OL}, which cannot be determined by steady-state measurements. The normalized amplitude exhibits the following dependence on the controller gain and phase:

$$|\mathcal{Y}| = \sqrt{1 - K(\alpha\cos\phi - \beta\sin\phi)} \tag{5.3}$$

where α and β depend on the plant parameters via equation (4.6). A qualitative prediction from (5.3) is that for a fixed small gain, it is easier to reduce limit cycle oscillations than it is to enhance them using harmonic forcing. This is verified by simulations in this section and by fluid experiments in the next section. For large gains, on the other hand, one generally destabilizes another mode and this relation no longer holds.

Example: *Van der Pol Oscillator with a Linear Regulator Simulations*

We now describe the nonlinear plant model, the Van der Pol oscillator, in state space form.

$$\begin{aligned} \dot{X}_{p1} &= X_{p2} + B_{p1}u \\ \dot{X}_{p2} &= -X_{p1} + \mu X_{p2} - X_{p1}^2 X_{p2} + B_{p2}u \\ y &= C_{p1}X_{p1} + C_{p2}X_{p2} \end{aligned} \tag{5.4}$$

The linear regulator consist of a gain, a band pass filter and a lead compensator in series used as a linear regulator, that is $G(s) = B(s)L(s)$. The band pass filter has the transfer function

$$B(s) = \frac{cs}{s^2 + cs + 1} \tag{5.5}$$

where the parameter c determines the bandwidth of the filter. The lead compensator has the transfer function

$$L(s) = \frac{T^2(s + 1/T)^2}{(s+T)^2} \tag{5.6}$$

The maximum lead occurs at 1 rad/sec and its value is $\angle L(i) = 2\tan^{-1}(\frac{1}{2}(T - 1/T))$. By changing the sign of the gain we can obtain phase changes from -180 deg to $+180$ deg by varying T. Note that $|G| = K$ and $\phi = \angle G = \angle L$.

The values used in the simulation are $B_{p1} = C_{p2} = 0$, $B_{p2} = C_{p1} = 1$, $c = .5$ and $\mu = .1$. Changing the values of B_p and C_p will only change J_{1p} so that the gain and phase of the compensator would have to be adjusted accordingly. The results are the same, scaled in gain and shifted in phase. For these particular values suppression of limit cycle oscillation occurs at 90 deg phase and gain $K = \mu$. According to the asymptotic theory, the normalized amplitude should be given by

$$|\mathcal{Y}| = \sqrt{1 - \frac{K}{\mu}\sin\phi} \tag{5.7}$$

The data from the simulations are depicted as circles in Figure 3 and the solid curve is the value predicted by the Stuart-Landau equation for $K = .1 = \mu$. If one increases the gain K above μ then the limit cycle amplitude will be suppressed for a range of phases symmetric about 90 deg. As one varies the gain of the compensator with a phase of ± 90 deg the normalized amplitude behaves as expected, see Figure 4.

An important result for the practitioner to be aware of is that using a band pass filter which is too narrow, will violate the assumptions used in deriving the Stuart-Landau equation. Note that $G(i)$ is independent of the value of c. A narrow band pass filter results when c becomes smaller. As one decreases c the filter poles move toward the imaginary axis. When $c \sim O(\mu)$, then the filter poles are of the same order as the critical poles of the plant, so that they would need to be accounted for in the multiple scale analysis, leading to an additional amplitude equation. In practice, this is realized as a degradation in performance. This is shown for the Van der Pol oscillator in Figure 5. As the band pass filter becomes more narrow, the limit cycle amplitude is not suppressed as well, and is no longer well predicted by the multiple scales theory (5.7).

We now consider control induced transients to estimate the growth rate Λ_r. To simulate the estimation of the parameters in the Stuart-Landau equation for an unknown plant, we pretend that we do not know the form of the governing equation (5.4). We pick an arbitrary small gain and four arbitrary phases for the compensator $G(i)$. Here we use $K = \mu = 0.1$ and $\phi = 60$, 120, 240 and 300

		60°	120°	240°	300°
Least Squares	$\hat{\Lambda}_r^{CL}$	.0063	.0055	.0567	.0563
Estimate	$\hat{g}_r$	.1003	.0839	.0741	.0733
Multiple Scales	Λ_r^{CL}	.0067	.0067	.0933	.0933
Computation	g_r	.1250	.1250	.1250	.1250

Table 1: Parameter estimates for closed loop Stuart-Landau equation

degrees. The uncontrolled system exhibits limit cycle oscillations of magnitude 0.6 for $\mu = 0.1$. At time $t = 0$ the control is turned on. The results are shown in Figure 6. Using equation (4.15) we determine the estimates of the coefficients for the closed loop Stuart-Landau equation, $\hat{\Lambda}_r^{CL}$ and $\hat{g}_r$, given in Table 1.

We list the true values, Λ_r^{CL} and g_r, computed from the governing equation (5.4) for comparison. As a general rule, the ratio of $\hat{\Lambda}_r^{CL}/\hat{g}_r$ is quite close to the true value Λ_r^{CL}/g_r since the estimates for the limit cycle amplitude are good. The growth rates are more difficult to obtain.

Using the values in Table 1 we can use equation (4.18) to find the estimates of the coefficients for the open loop Stuart-Landau equation, $\hat{\Lambda}_r$ and $\hat{J}$, as

$$\begin{aligned} \hat{\Lambda}_r &= .0312 \\ \hat{J} &= -.0021 - i.2921 \end{aligned} \tag{5.8}$$

The values computed from the governing equation are

$$\begin{aligned} \Lambda_r &= .05 \\ J &= 0.0 - i0.5 \end{aligned} \tag{5.9}$$

From the estimated values of the parameters (5.8) the compensator that should give marginal stability has

$$KG(i) = \frac{\hat{\Lambda}_r \hat{J}}{|\hat{J}|^2} = -.0008 + i.1067 \tag{5.10}$$

that is $K = .1067$ and $\phi = 90.409$ deg as opposed to the exact values of $K = .1$ and $\phi = 90$ deg Using this value for the compensator we obtain the first time series in Figure 7 The second time series is for the same phase but with a gain $K = .12$.

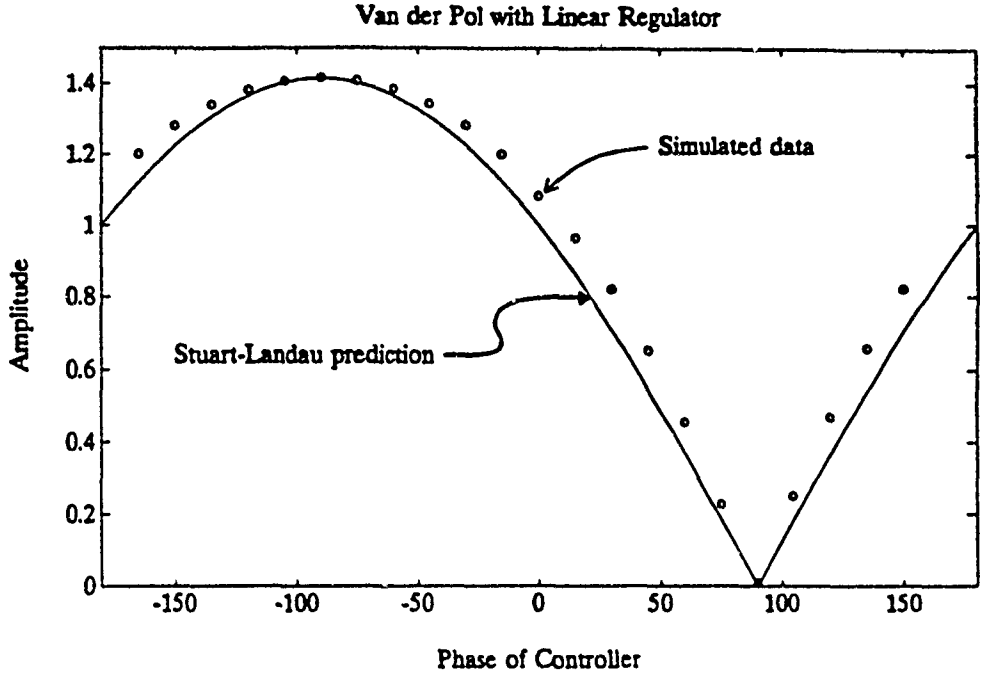

Figure 3: The effect of controller phase on the Van der Pol oscillator.

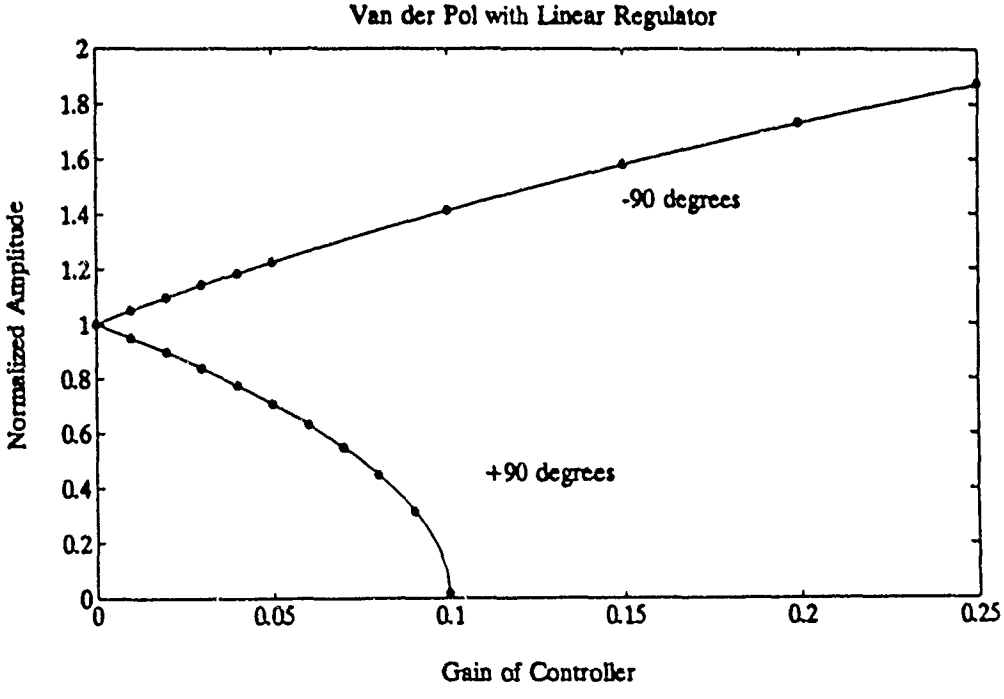

Figure 4: The effect of controller gain on the Van der Pol oscillator.
o simulated data and - Stuart-Landau prediction

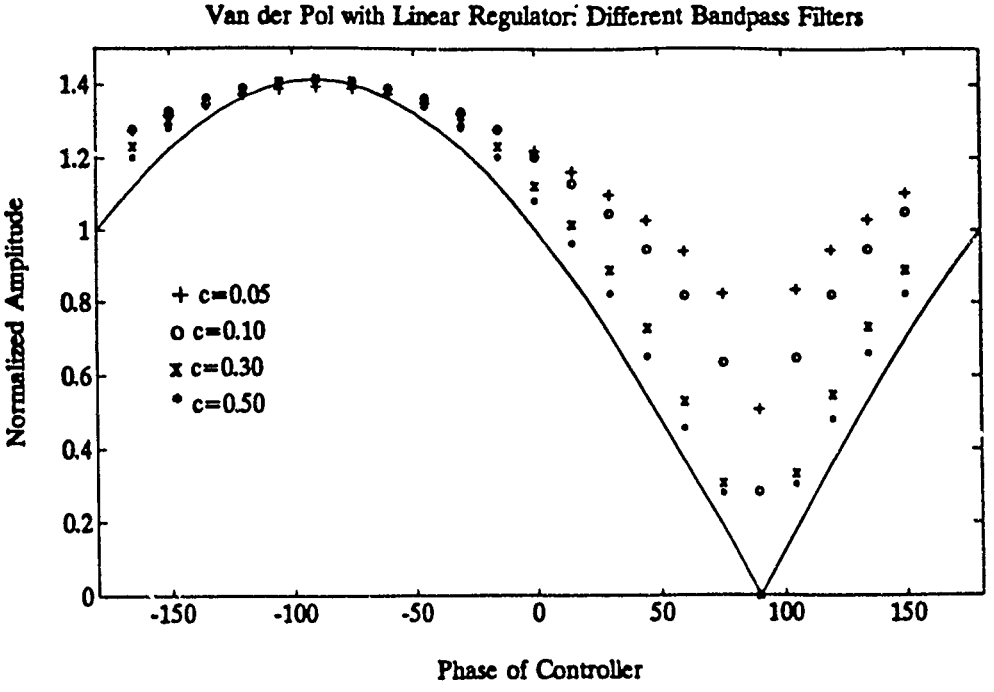

Figure 5: The effect of bandpass filter pole location on suppression.

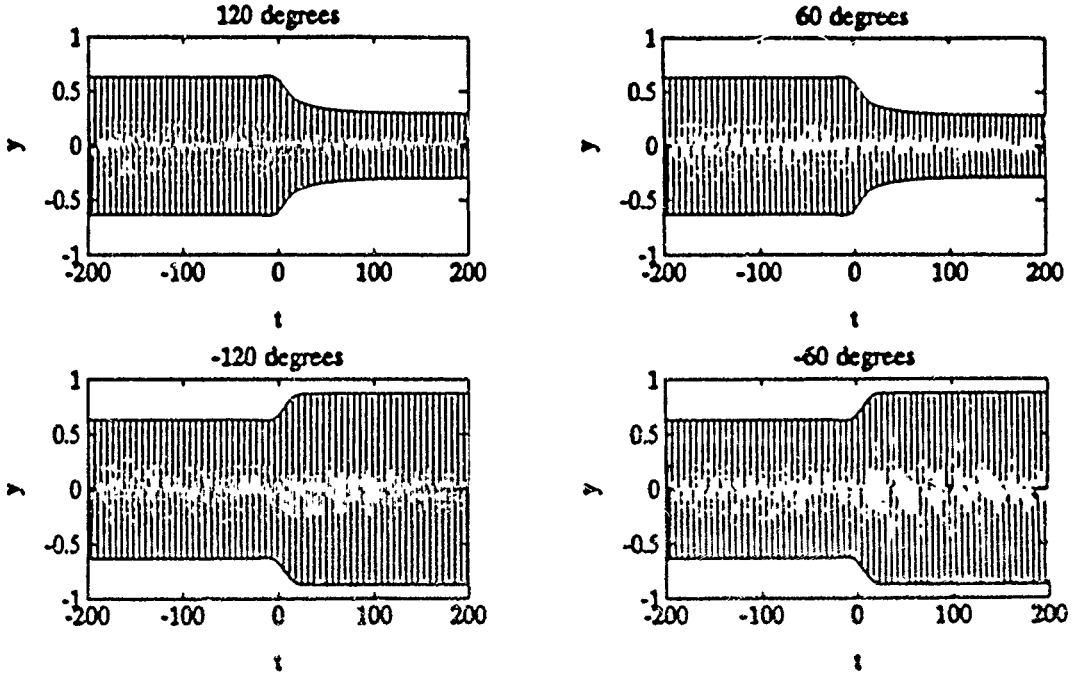

Figure 6: The effect of four different phases on the limit cycle amplitude

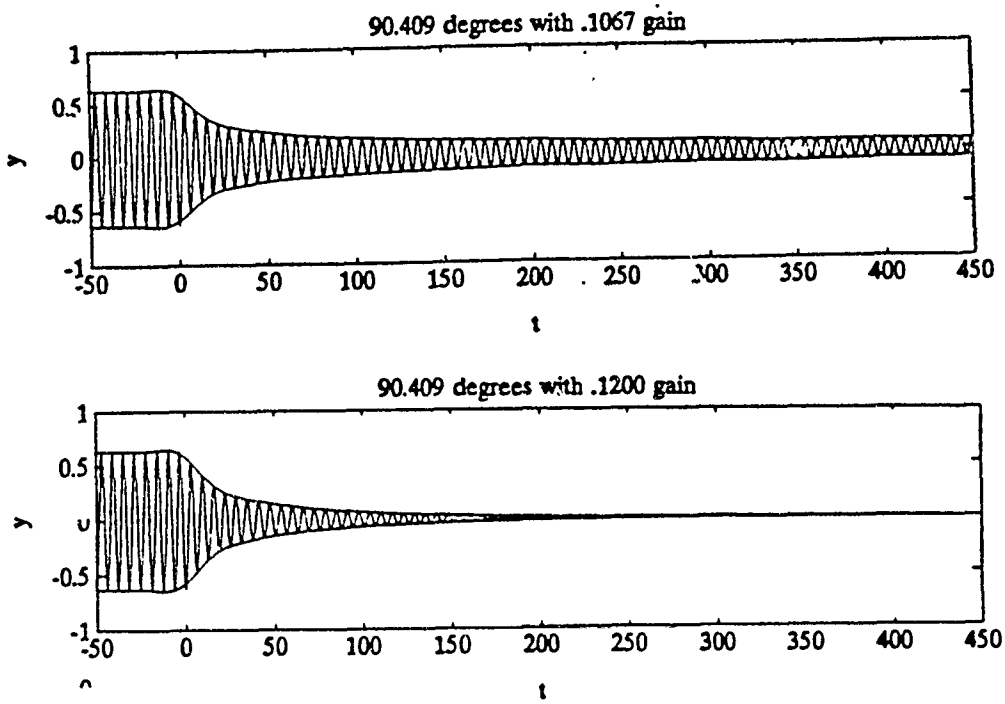

Figure 7: After parameter estimation we may select a gain and phase which stabilizes the plant.

2.6. Experimental Results

To test the relevance of the control scheme to fluid flow oscillations an experimental apparatus has been studied. The plant we desire to control is a heated two dimensional jet. The details of the hot jet facility and some of its uncontrolled characteristics are discussed in [12]. It has been demonstrated that the hot jet exhibits self-excited oscillations when the ratio, S, of the jet density to the ambient fluid density is below a critical value $S_c \approx .95$. A linear stability analysis of this flow is given in [12] and [2]. Above this ratio the flow is laminar when there is no noise present. As the density ratio is decreased the steady laminar flow undergoes a Hopf bifurcation to a limit cycle. The self-excited nature of the hot jet is similar to that of the von Kármán vortex street in the wake behind a cylinder.

To verify that the hot jet exhibits limit cycle oscillations which are consistent with our assumptions, we measured the spectral peak for several different temperatures. The data presented in

Figure 8 shows experimental data acquired on three different days (o, x, and +) and the least squares fit of the data to the equation for an imperfect bifurcation

$$\left(\frac{S_c - S}{S_c}\right) |Y| - p_1 |Y|^3 - p_2 = 0 \tag{6.11}$$

To implement the control we choose acoustic forcing which acts like a point actuator at the lip of the jet according to Bechert [13, 14] and Crighton [15] who have shown that long acoustic waves can be converted to short vorticity waves where the flow has a strong spatial inhomogeneity. The control actuators consist of two 100 Watt woofers, one on each side of the jet approximately 1 meter downstream of the jet exit. For commercial applications, one would likely use some form of vibrating plate at the nozzle exit (for an example of such an actuator see [16]). In order to demonstrate the feasibility of the control systems considered here, the acoustic actuators are however effective and much less expensive.

The single, point sensor is a hot wire probe. The anemometer is operated in constant current mode such that the output of the measurement conditioning circuit is proportional to the fluctuating component of the temperature, $T'(\mathbf{x}_s, t)$. The controller consists of analog filters and an Intel 486 based personal computer. Rather than separately estimate the dynamics of the speakers, the time delay associated with the speed of sound and the transfer functions of various filters, all the dynamics are lumped together and considered as part of the (unknown) plant. The problem is then reduced to estimating the plant (i.e. the coefficients of the Stuart-Landau equation) and specifying the control system gain and phase at the critical frequency.

The sensor was located at $x/H = 1.4$, $y/H \approx 0.5$ and $z = 0$ which is upstream of the initial roll up of the vortices. A probe placed in the shear layer at this location has a distinct spectral peak at about $100Hz$. As the probe is moved downstream inside the shear layer one enters a region of mode switching in which the Fourier amplitudes at $50Hz$ and $100Hz$ exchange energy in time. This is believed to be a result of vortex pairing which is not completely fixed in space. Further downstream the vortex has paired and the primary feature of the flow is a large peak in the spectrum at $50Hz$, and a smaller peak at $100Hz$.

We now consider the results of experiments on the hot jet with a feedback controller. We specify the gain and phase of the controller at the critical frequency of the uncontrolled jet. The data in this section are steady-state in the sense that the Fourier amplitudes of the critical frequency (approximately $100Hz$) are steady, that is the measured output $y(t)$ is time periodic.

Recall that the model for the flow's oscillations is the Stuart-Landau equation with a control term added

$$\frac{dY}{dt} = \Lambda^{OL} Y - g |Y|^2 Y + JU \tag{6.12}$$

where $U = Ke^{i\phi}Y = KG(i\omega^{(0)})Y$ for feedback control. Since the flow is spatially dependent, the coefficients J and g will depend on the sensor location $\mathbf{x}_s$. Since Λ^{OL} results from the real part of the critical eigenvalue, it must be independent of the sensor location.

As discussed in Section 2.5, we can study the validity of the Stuart-Landau equation as a model for the plant by examining steady-state data. The Fourier amplitudes are computed from the hot wire output in constant current mode using a spectrum analyzer. A distinct spectral peak is present for a density ratio of $S < S_c \approx .95$. At a density ratio of $S = .88$ the effect of controller phase has been tested and compared to the predictions of the Stuart-Landau model in Figure 9. The probe is located inside the shear layer and the amplitude in the figure is normalized by the open loop amplitude. The solid curve is a least squares fit of the data to the Stuart-Landau model

$$|Y|^2 = p_1 + p_2 \cos\phi + p_3 \sin\phi \tag{6.13}$$

The model is successful at predicting the response of the hot jet to different linear regulators.

The effect of controller gain is shown in Figure 10 for the same plant parameters as were used to study the effect of controller phase The data is curve fit to the equation (6.11) for an imperfect

bifurcation with S replaced by K and p_1 and p_2 consistent with the normalization of Y to $\mathcal{Y}$. The effect of random disturbances and unmodeled dynamics prevent the oscillations from being completely suppressed for any value of the controller gain. The dashed line is the least-squares fit to the imperfect bifurcation and the solid line is the perfect bifurcation (i.e. $p_2 = 0$).

Another prediction of the multiple scales theory for small gain controllers is that the eigenfunction for the least stable eigenvalue is the same with control as for the uncontrolled case. That is, the spatial structure is the same with or without control. This is verified in Figure 11. The figure depicts a Schlieren image with and without control.

In order to estimate the growth rate Λ_r in the Stuart-Landau equation we must perform transient experiments comparable to Section2.5.To obtain time series suitable for estimation of the coefficients in the Stuart-Landau equation we start with the controller turned on at phase which causes the maximum amplification in Figure 9. At time $t = 0$ a digital switch switches the phase by 180 deg (i.e. multiplies the control signal by -1). The resulting transient is shown in Figure 12. The first time trace is raw data and the second time series is bandpass filtered and displays the amplitude obtained using the Hilbert transform.

Fifty of these transients were obtained and averaged to obtain an average for the amplitude $|Y(t)|$ and the instantaneous frequency $\frac{d}{dt}\angle Y(t)$. The result is displayed in Figure 13. Note that the frequency shifts and becomes somewhat erratic when the controller switches to the phase for reduced oscillation. This inhibits our ability to completely suppress the flow oscillations. If we increase the gain further we find that a different mode is destabilized: While the mode at $100Hz$ is suppressed, a mode at $150Hz$ appears. This result is generic and has also been demonstrated for the wake in [1].

In summary, a procedure for determining the effect of a linear regulator on bifurcating solutions of weakly nonlinear ordinary differential equations has been developed. Using this model one can specify the gain and phase of a linear controller to stabilize the system. One may also specify a controller to modify the size of the limit cycle.

Often one does not know the differential equations governing the system, but one does know that the system exhibits behavior similar to a Hopf bifurcation. The Stuart-Landau equation can then be used as a generic model for the system. One can then estimate the parameters of the Stuart-Landau equation using experimental data. Different controllers can be used to provide transient data for estimation without the need to change the plant parameters for their generation. [9, 17, 18].

Simulations of the Van der Pol oscillator and experiments on a heated two dimensional jet demonstrate the usefulness of the Stuart-Landau equation for control and estimation. Work is still underway to develop a fully adaptive control scheme using the Stuart-Landau equation as a reference model.

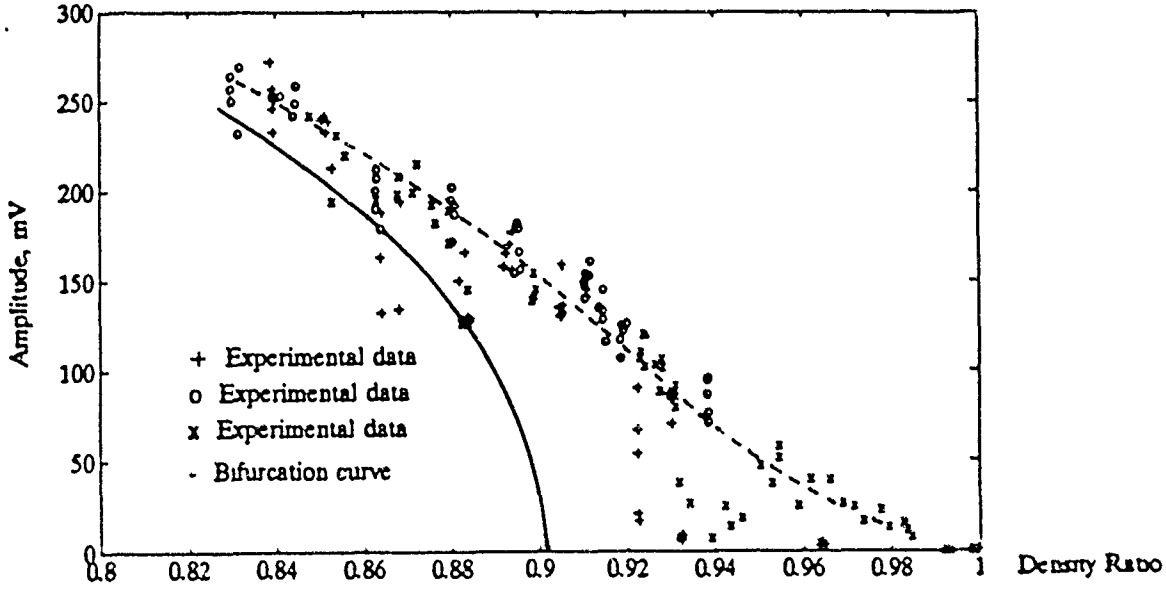

Figure 8: Hopf bifurcation for the heated two dimensional jet

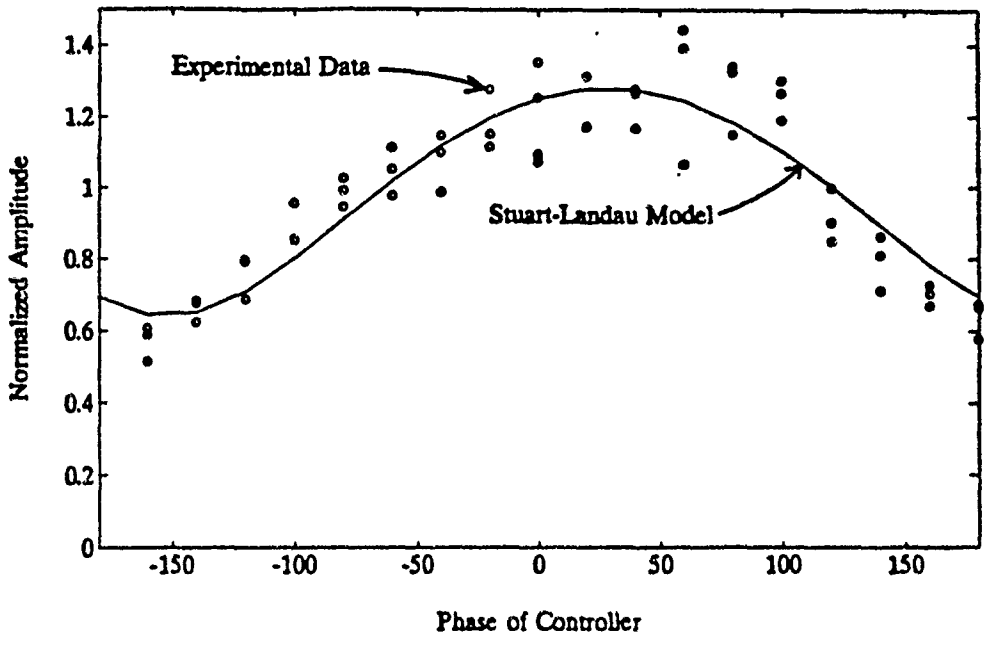

Figure 9: Effect of controller phase on the hot jet.

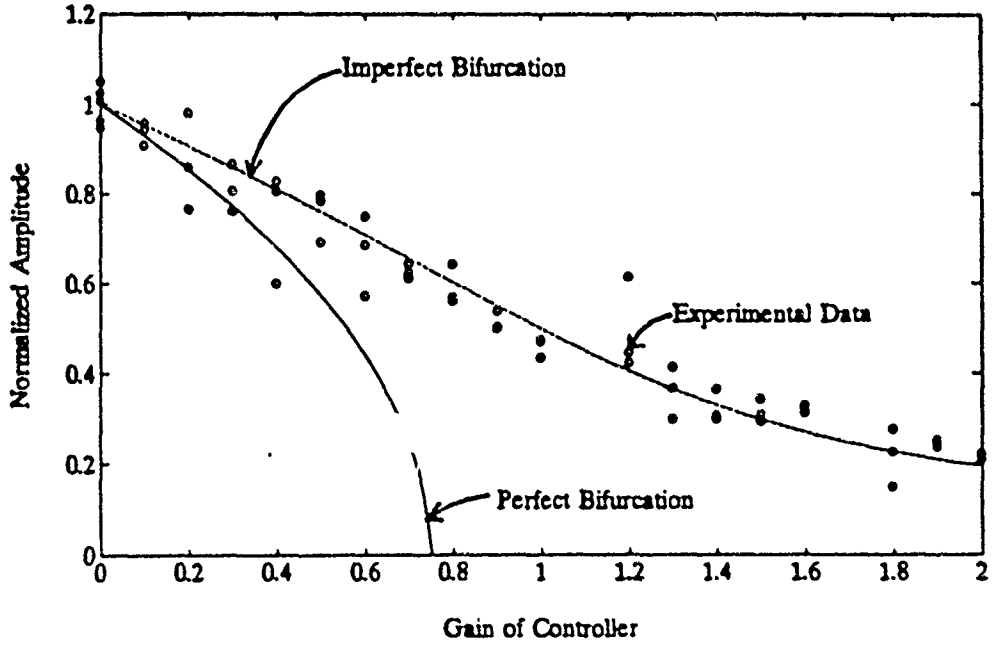

Figure 10: Effect of controller gain on the hot jet.

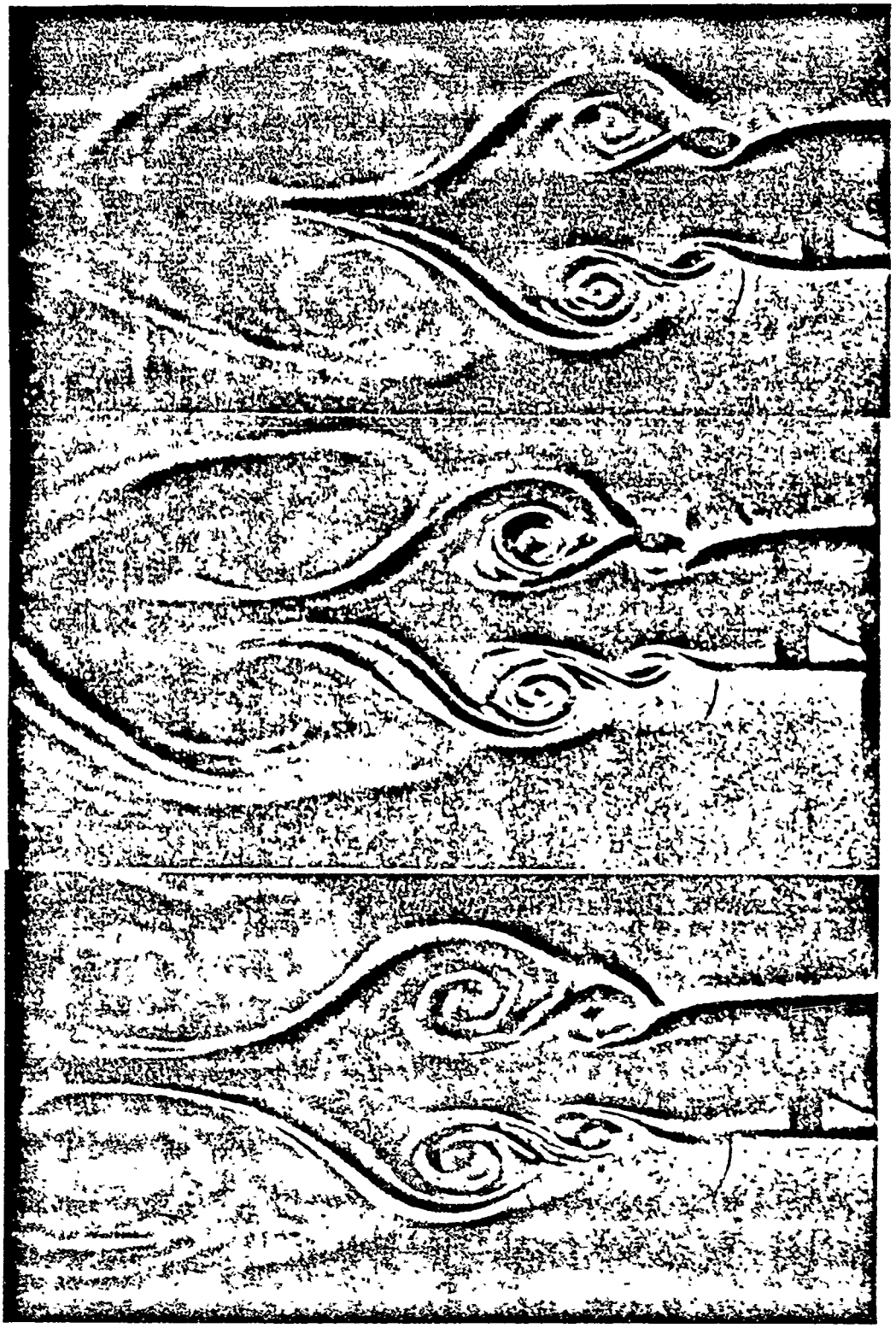

Figure 11 Schlieren photographs showing the invariance of the spatial structure

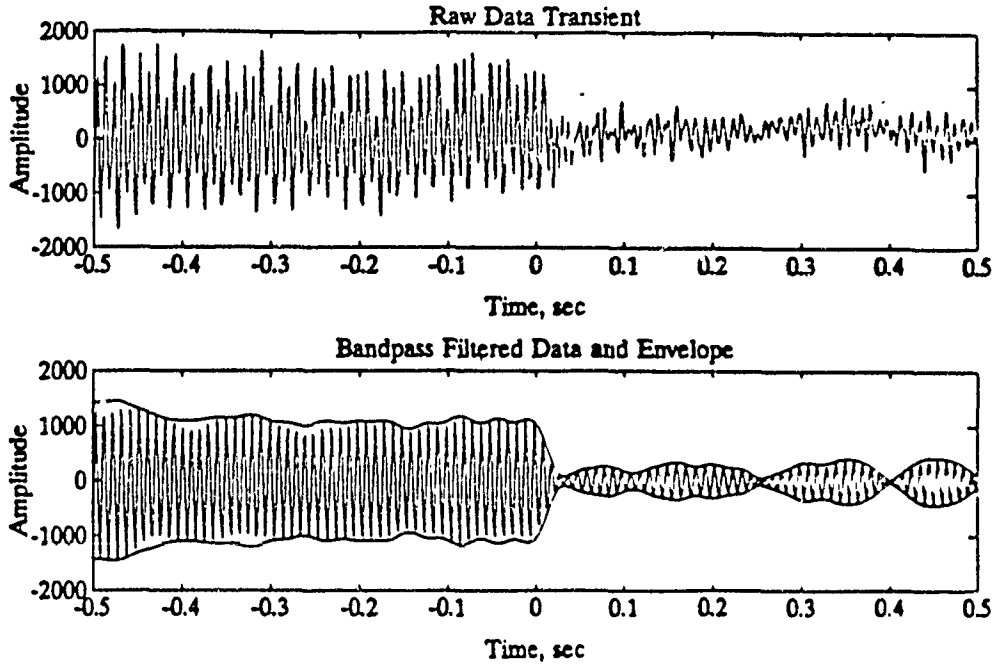

Figure 12: Raw transient and bandpass filtered transient.

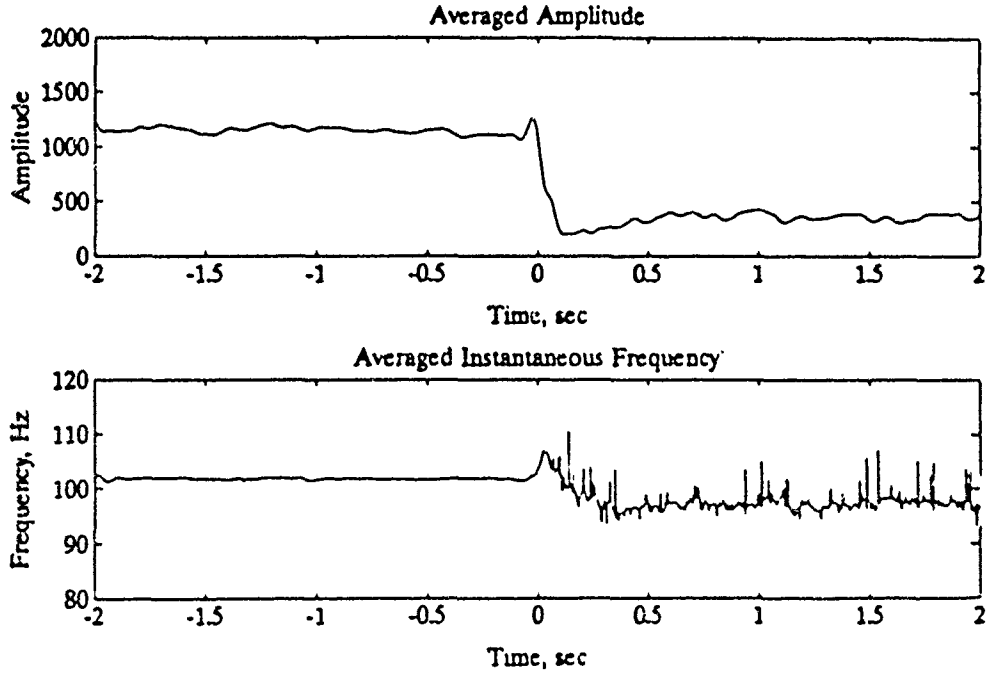

Figure 13: Averaged value of amplitude and instantaneous frequency

2.7. References Pertaining to Section 2

[1] P. A. Monkewitz, E. Berger, and M. Schumm, "The nonlinear stability of spatially inhomogeneous shear flows including the effect of feedback," *European Journal of Mechanics B/Fluids supplement*, vol. 10, no. 2, pp. 295–300, 1991.

[2] M. Yu and P. A. Monkewitz, "The effect of nonuniform density on the absolute instability of two-dimensional inertial jets and wakes," *Physics of Fluids A*, vol. 2, no. 7, pp. 1175–1181, 1990.

[3] P. Manneville, *Dissipative Structures and Weak Turbulence*. Academic Press, 1990.

[4] M. G. Velarde, "Steady States, Limit Cycles and the Onset of Turbulence. A few model calculations and exercises," *Nonlinear Phenomena at Phase Transitions and Instabilities*. T. Riste, Editor. 1982.

[5] S. Sinha, R. Ramaswamy, and J. S. Rao, "Adaptive control in nonlinear dynamics," *Physica D*, vol. 43, pp. 118–128, 1990.

[6] Y. Kuramoto, *Chemical Oscillations, Waves and Turbulence*. Springer-Verlag, 1984.

[7] J. Kevorkian and J. D. Cole, *Perturbation Methods in Applied Mathematics*. Springer-Verlag, 1981.

[8] J. Guckenheimer and P. Holmes, *Nonlinear Oscillations, Dynamical Systems, and Bifurcations of Vector Fields*. Springer-Verlag, 1983.

[9] E. A. Henrich, *Control of limit cycle oscillations with applications in fluid mechanics*. PhD thesis, University of California, Los Angeles, 1991.

[10] E. A. Henrich, D. L. Mingori, and P. A. Monkewitz, "Control of pitchfork and hopf bifurcations," in *American Control Conference*, 1992.

[11] S. Raghu and P. A. Monkewitz, "The bifurcation of a hot round jet to limit-cycle oscillations," *Physics of Fluids A*, vol. 3, pp. 501–503, April 1991.

[12] M. Yu, *Local and global instability of heated 2-D jets and wakes*. PhD thesis, University of California, Los Angeles, 1990.

[13] D. W. Bechert, "Excitation of instability waves in free shear layers, Part 1. Theory," *Journal of Fluid Mechanics*, vol. 186, pp. 47–62, 1988.

[14] D. W. Bechert and L. Stahl, "Excitation of instability waves in free shear layers, Part 2 Experiments," *Journal of Fluid Mechanics*, vol. 186, pp. 63–84, 1988.

[15] D. G. Crighton, "The Kutta condition in unsteady flows," *Annual Review of Fluid Mechanics*, vol. 17, pp. 411–445, 1985.

[16] A. Glezer, "Manipulation of a square jet using piezoelectric actuators," in *Turbulence Structure and Control*, Air Force Office of Scientific Research, 1991.

[17] P. A. Monkewitz, D. L. Mingori, E. A. Henrich, and M. Yu, "Adaptive and nonadaptive feedback control of global instabilities," in *Turbulence: Structure and control*, (Columbus, Ohio), Air Force Office of Scientific Research Meeting, April 1991.

[18] E. A Henrich, D L. Mingori, and P. A Monkewitz, "Control of Hopf bifurcations," in *Chaotic Dynamics. Theory and Practice*, (Patras, Greece), NATO Advanced Study Institute, July 1991

3. IMPLEMENTATION OF THE CONTROL IN THE WAKE OF A CYLINDER AT LOW REYNOLDS NUMBER - THE SWITCHING BETWEEN DIFFERENT GLOBAL MODES

3.1. Related Publications and Presentations

MONKEWITZ, PETER A., BERGER, EBERHARD & SCHUMM, MICHAEL, The nonlinear stability of spatially inhomogeneous shear flows, including the effect of feedback. Eur. J. Mech. B/Fluids Vol. 10 No. 2 - Suppl., pp. 295-300, 1991.

HENRICH, EDWARD A., MONKEWITZ, PETER A., SCHUMM, MICHAEL & BERGER, EBERHARD, The effect of proportional feedback control on the wake behind a cylinder. Bull Am. Phys. Soc. Vol. 35, p. 2326, 1990.

LEE, CHRIS, Feedback control of global oscillations in a bluff-body wake. M.S. Thesis in preparation, University of California, Los Angeles, 1992.

MONKEWITZ, PETER A., SCHUMM, MICHAEL & BERGER, EBERHARD, The effect of proportional feedback control on the wake behind a cylinder. Paper in preparation.

3.2. The Doubly-Infinite GL Model with Control

In the following we implement the controller, developed in Section 2, in the doubly-infinite Ginzburg-Landau (GL) model of Section 1.4. which we are using for a cylinder wake at low Reynolds number. Since the GL model retains the streamwise structure of global modes, the locations x_s and x_a of the single sensor and of the single actuator, respectively, have to be specified. Furthermore, as it has been shown in Section 2, the controller gain and phase are only relevant at the frequency of the critical (most amplified) mode. Therefore it is possible to use a simple proportional feedback on equation (4.9) of Section 1.

Reverting to unscaled physical coordinates, the GL equation for the amplitude A of any physical quantity is rewritten as

$$\partial_t A - L_2\,\partial_x^2 A - L_1\,\partial_x A - L_0\,A + N_0\,|A|^2 A = F(x,t)\ , \tag{2.1}$$

where, using the notation (4.10) of Section 1, the coefficients are defined as

$$L_0(x) = -i[\omega_0(x) + \delta\omega^t + (\omega^t_{kk}/2)k_0^2(x)]\quad , \quad \text{with}$$

$$\omega_0(x) = \omega_0^t + (1/2)[\omega^t_{xx} - (\omega^{t\,2}_{kx}/\omega^t_{kk})]\,(x-x^t)^2 \quad \text{and}$$

$$k_0(x) = k_0^t - (\omega^t_{kx}/\omega^t_{kk})\,(x-x^t)\quad ;$$

$$L_1(x) = \omega^t_{kk}\,k_0(x)\quad ;$$

$$L_2(x) = (\omega^t_{kk}/2)\quad ;$$

$$N_0(x) = n_r + n_i = \text{complex constant with } n_r>0\ . \tag{2.2}$$

In equation (2.1) we have, in addition, introduced the standard nonlinear term, which can be obtained from a weakly nonlinear extension of the analysis

of Section 1 (work in progress by LeDizes and Monkewitz), and a forcing term F(x,t). To represent the controller designed in Section 2, the forcing term is specified as

$$F(x,t) = g \exp(i\gamma)\, \delta(x-x_a)\, A(x_s,t) \ , \qquad (2.3)$$

where g is the controller gain and γ the controller phase. We note that the forcing term (2.3) preserves the eigenvalue character of the problem. At this point we consider specifically the wake of a oblong bimorph (piezoceramic) cylinder. By applying a voltage across electrodes at top and bottom of the cylinder, it can be moved in the direction normal to the oncoming flow and is used directly as an actuator in our setup. Hence x_a=0 and (2.3) expresses the fact that the sensor signal is amplified, phase-shifted and then fed directly to the actuator after "mild" bandpass filtering. The latter had typical cutoffs at 0.5 and 1.5 times the dominant Karman frequency, which was sufficient to implement the control of Section 2 because the dominant spectral peak in the low-Reynolds number wake is at least 20dB above all other spectral features. The oblong cylinder of thickness D=0.69mm , a chord of T=1.68mm and a length of approximately 100D is shown schematically on Figure 1a, together with the position of the hot wire sensor at x/D=10 and y/D=1. The cylinder was mounted across the nozzle of a high quality jet facility as shown on the photograph of Figure 1b.

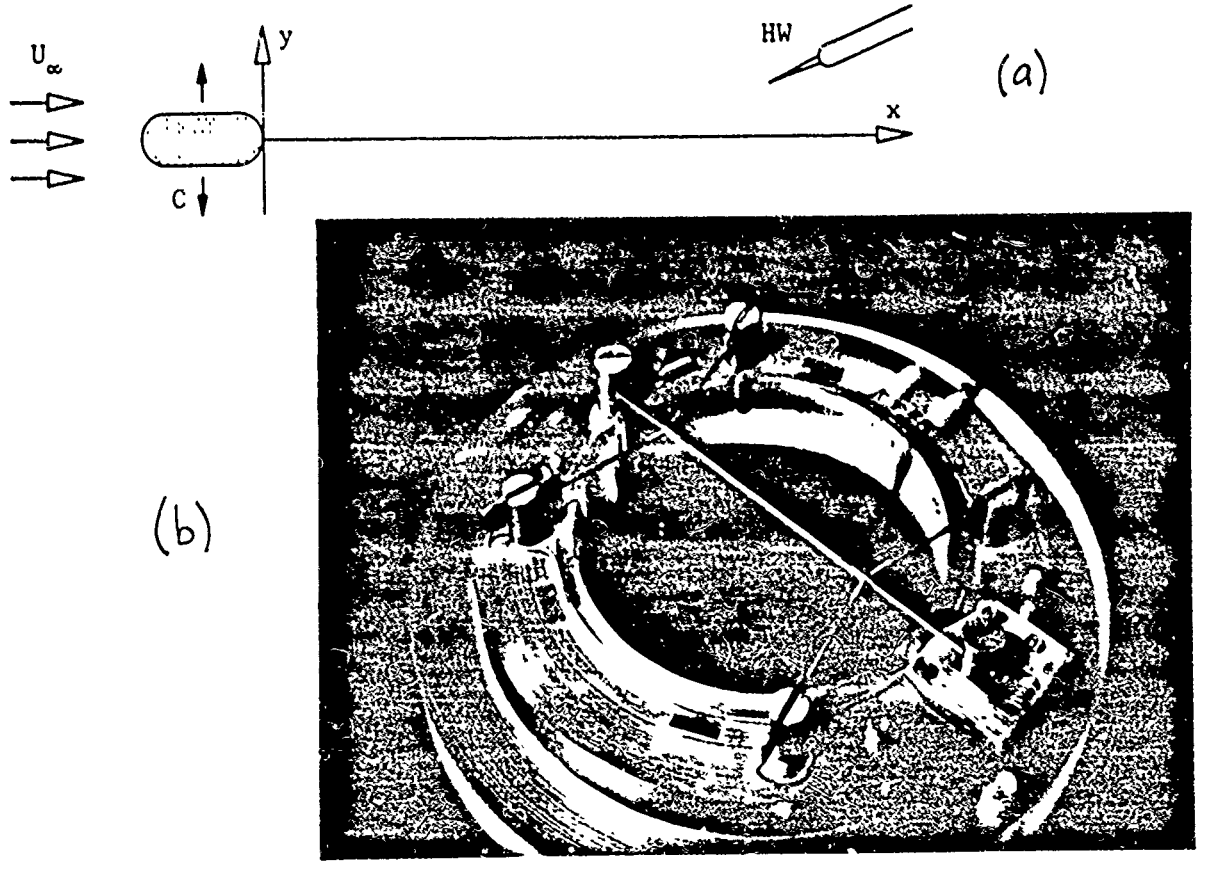

Figure 1. a) Schematic of the experimental arrangement with: C, oblong cylinder; HW, hot wire. b) View of the bimorph cylinder mounted on the nozzle of the jet facility.

Next, the global stability characteristics of the uncontrolled oblong cylinder wake was determined by transient measurements analogous to the ones of Raghu & Monkewitz (1991) in a hot jet (see also Schumm, 1991). The results are shown on Figure 2 and the correlations for the global linear growth rate, the linear frequency and the saturation (limit cycle) frequency are given in the caption.

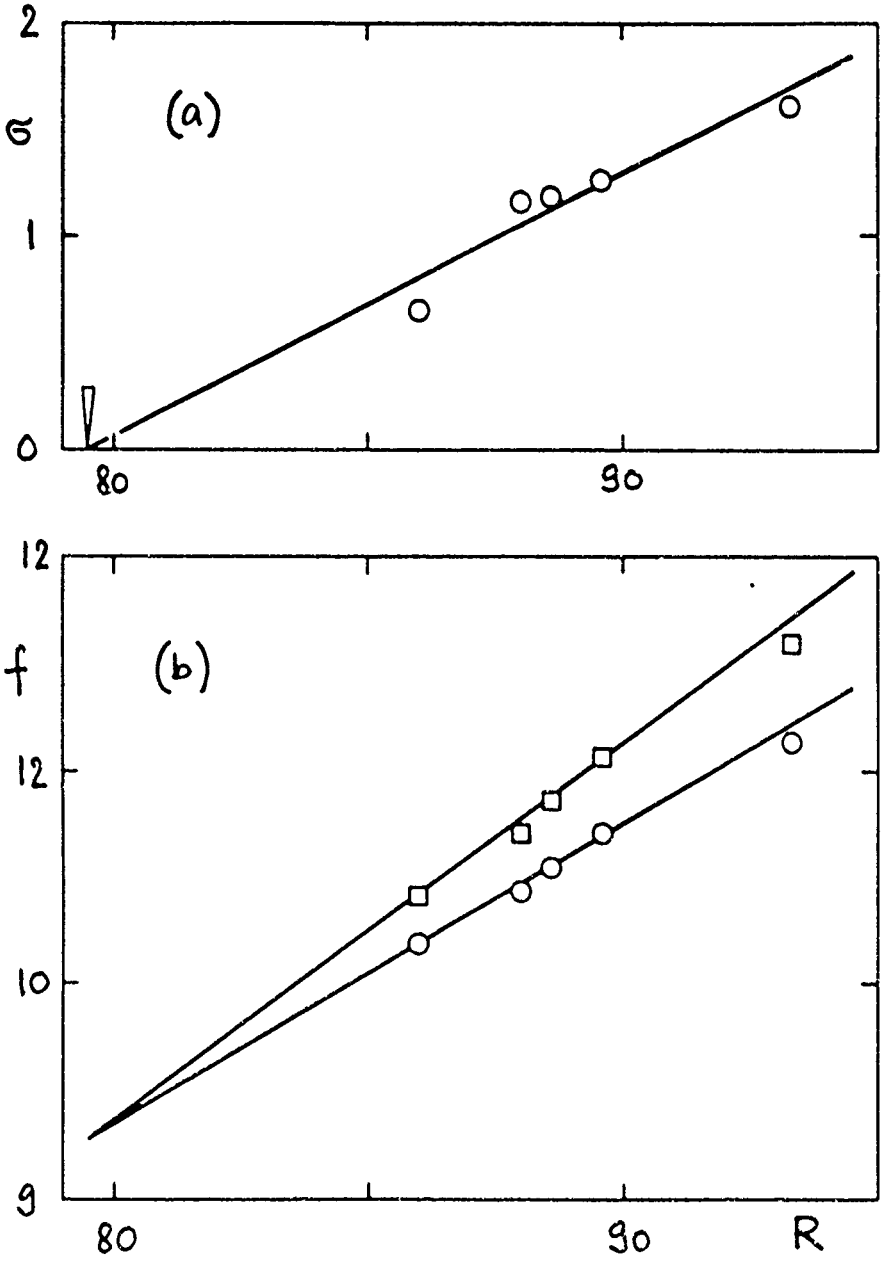

Figure 2. Experimentally determined global stability characteristics of the bimorph cylinder wake. a) Linear growth rate $\sigma=\sigma^*D^2/\nu$ with curve fit $\sigma=0.123(R-R_c)$. b) O, linear frequency $f_{lin}=f^*_{lin}D^2/\nu$ with fit $f_{lin}=9.27+0.142(R-R_c)$; □, saturation frequency $f_{sat}=f^*_{sat}D^2/\nu$ with fit $f_{sat}=9.27+0.177(R-R_c)$.

From the results of Figure 2 and an estimate of the length of the recirculation region in the near-wake coupled with local stability calculations, the parameters (2.2) have been estimated as follows:

$$
\begin{aligned}
R_c &= 79.5 \\
x^t &= (1.183 - 0.031i) \\
\omega_0^t + \delta\omega^t &= (0.708 + 0.081i) + (0.0015 + 0.011i)\times(R-R_c) \\
k_0^t &= (1.452 - 0.844i) + (0.018 + 0.019i)\times(R-R_c) \\
\omega_{kx}^t &= (0.00175 + 0.0479i) \\
\omega_{xx}^t &= (0.107 - 0.065i) \\
n_i/n_r &= -1.8
\end{aligned}
\qquad (2.4)
$$

The ratio n_i/n_r is a universal constant for a given system and is directly related to the nonlinear frequency shift. The value of n_r, on the other hand, can be chosen arbitrarily and is related to the normalization of the amplitude. It is noted that the above parameters have not yet been obtained from the solvability conditions developed in Section 1 due to a lack of precise mean flow information, but represent an a priori estimate which has not been adjusted to fit the experiments.

With (2.4) the linear stability of time-harmonic solutions of equation (2.1) with homogeneous boundary conditions at $|x|\to\infty$ and the control (2.3) can be investigated. As long as all free (uncontrolled) global modes are damped the control can only be used to destabilize the system for some phase and a gain beyond a critical gain. The situation becomes more interesting, when the first global mode (n=0 in equ. 4.15 of Section 1) becomes unstable. In this case the controller with nonzero gain is needed to stabilize the fundamental Karman mode in the wake. The linear stability boundaries for the wake parameters (2.4) and supercritical Reynolds numbers are shown on Figure 3.

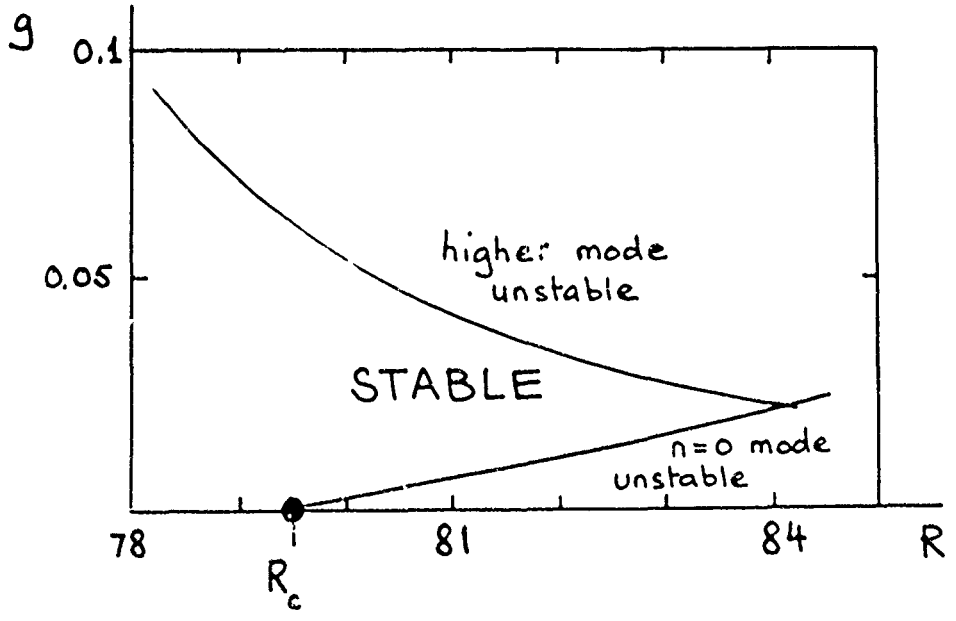

Figure 3. Stability boundaries predicted from the GL model with the parameters given by (2.4).

The lower stability boundary on Figure 3 represents the MINIMUM gain g required to stabilize the Karman mode at the OPTIMUM controller phase. The upper boundary, on the other hand, represents the MAXIMUM gain below which the system can be stabilized for at least one controller phase. In other words, beyond the upper boundary at least one (controlled) global mode is unstable at ANY controller phase. A typical situation on the upper boundary is shown on Figure 4: Although the n=0 (Karman) mode can be stabilized for a small interval of controller phases around π, the range of phases for which a "higher mode" is destabilized completely overlaps the stabilization interval of the Karman mode. What becomes clear from the result of Figure 3 is that the range of Reynolds numbers for which our controller is able to stabilize the system is rather limited. The reason for this is that the controller is designed to suppress only a single mode, namely the Karman mode, under the assumption that all other modes are well damped (see Section 2), which is clearly no longer the case in the GL system. The fact that the controller still "works" close to the bifurcation is explained by the very small gain required to stabilize the weakly amplified Karman mode.

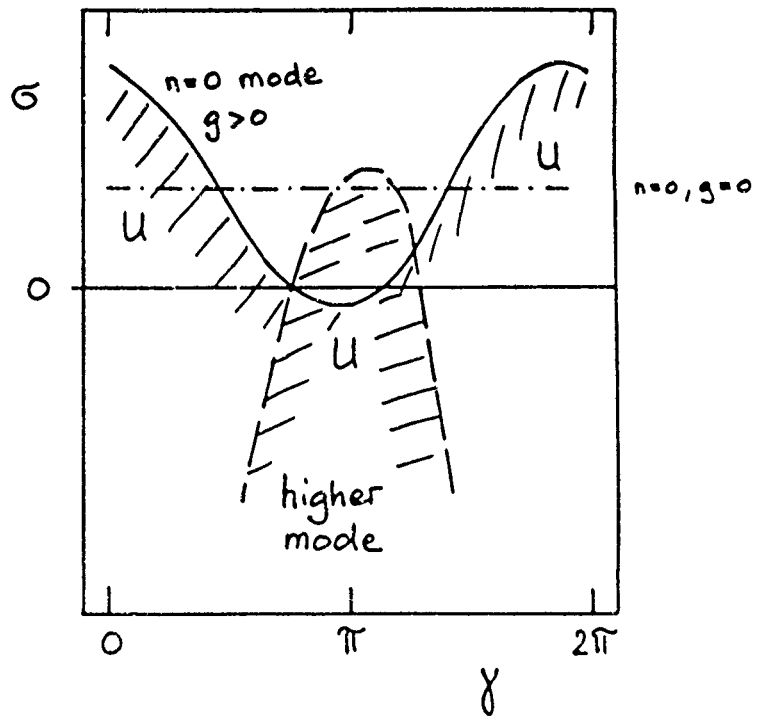

Figure 4. Typical situation for the temporal amplification rate σ versus phase on the upper stability boundary of Figure 3. -·-, amplification rate of uncontrolled Karman mode. U, regions of instability.

The situation becomes even clearer if equation (2.1) with the nonlinear term and the controller (2.3) is integrated numerically to yield the limit cycle amplitude as a function of controller gain and phase. The resulting amplitudes for a supercritical Reynolds number of 81 are shown on Figure 5a on which the triangular region of stabilization in the gain-phase plane is clearly visible Figure 5b shows the corresponding limit cycle frequency which illustrates the mode switching on the stability boundary.

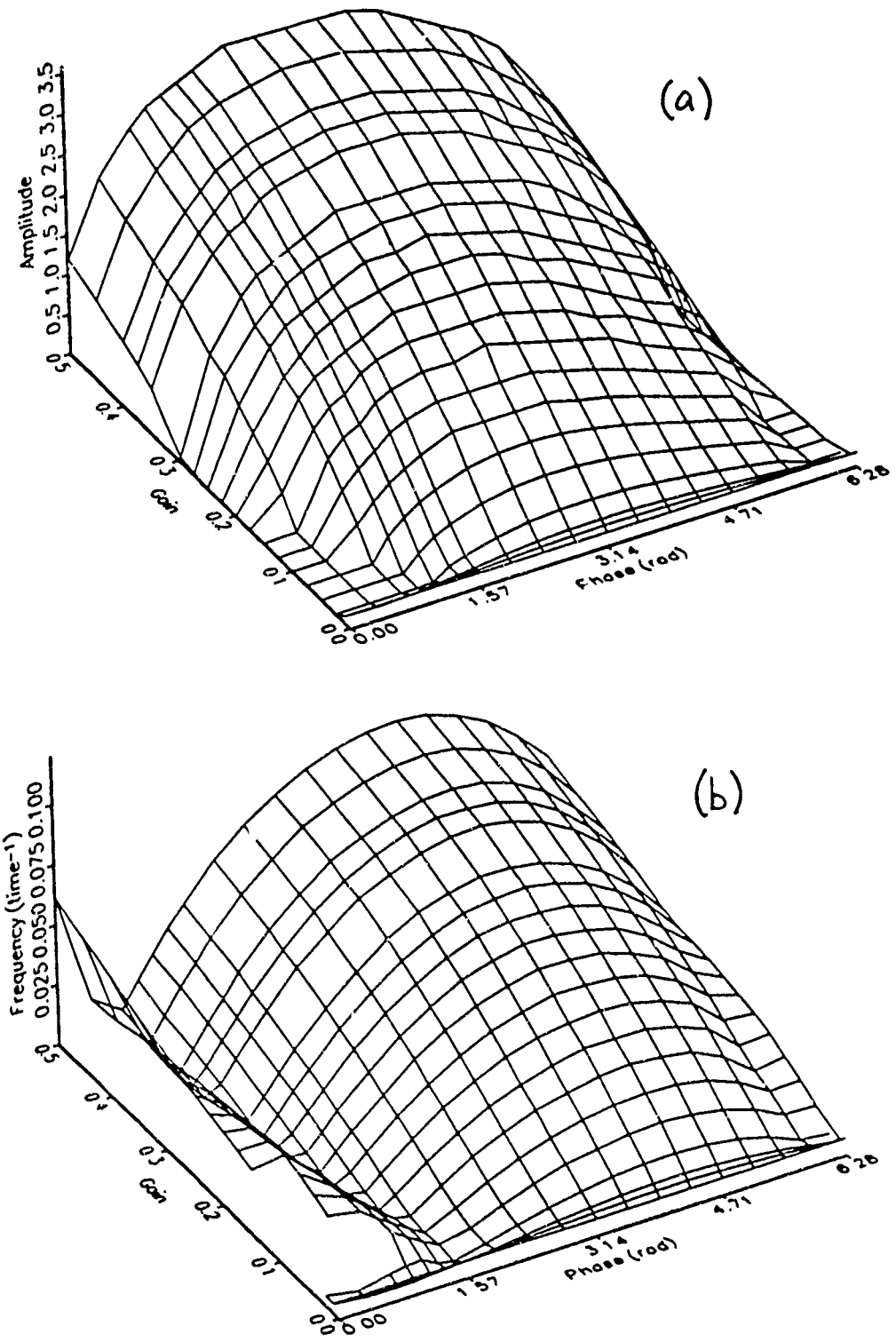

Figure 5. a) Perspective view of the controlled limit cycle amplitude versus controller gain and phase. b) Perspective view of the difference between controlled limit cycle frequency and uncontrolled linear frequency versus controller gain and phase. R=81, x_f=0, x_s=2 .

3.3. The Experimental Verification of the Model Predictions

The model predictions of Section 3.2. have been tested in the cylinder wake of Figure 1. First it was confirmed that the subcritical system could be destabilized by the controller. This is illustrated in Figure 6 by the transient of the sensor signal after closing the feedback loop. The processing of the transient shown on Figure 6 b&c is described in detail in Raghu and Monkewitz (1991) (see also Schumm, 1991) and yields the global linear growth rate as well as the linear and the saturation frequencies. In an analogous manner it is shown on Figure 7 that the unstable Karman vortex street can be stabilized by our controller. In this latter case it is noted that the problem of extraneous noise has become much more severe and starts to push the data reduction scheme to its limits. It appears that this problem with the signal-to-noise ratio is pervasive in all self-excited OPEN flows.

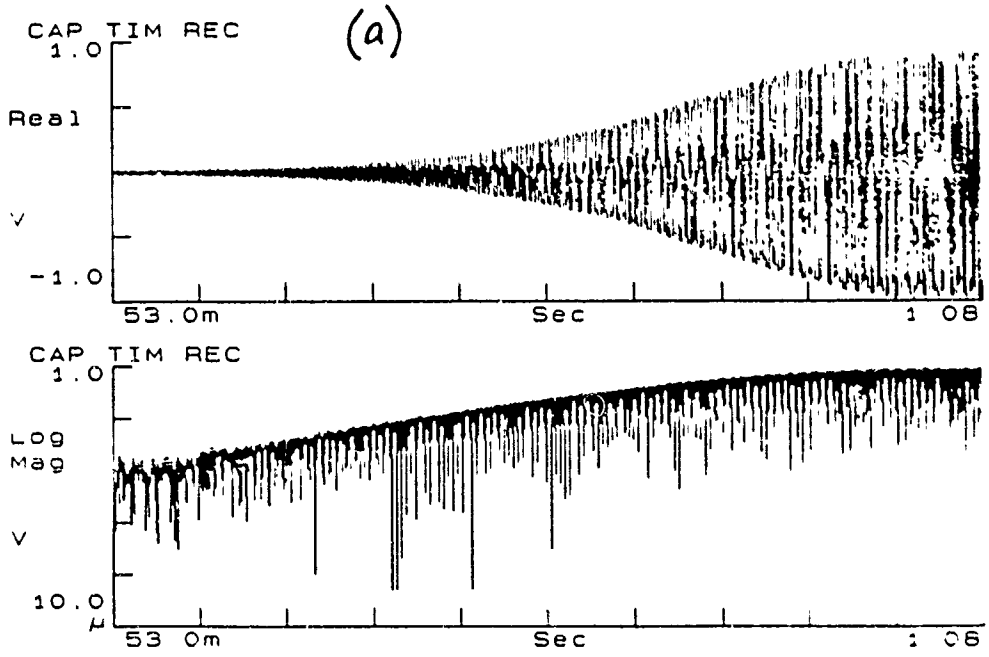

Figure 6. For caption see next page.

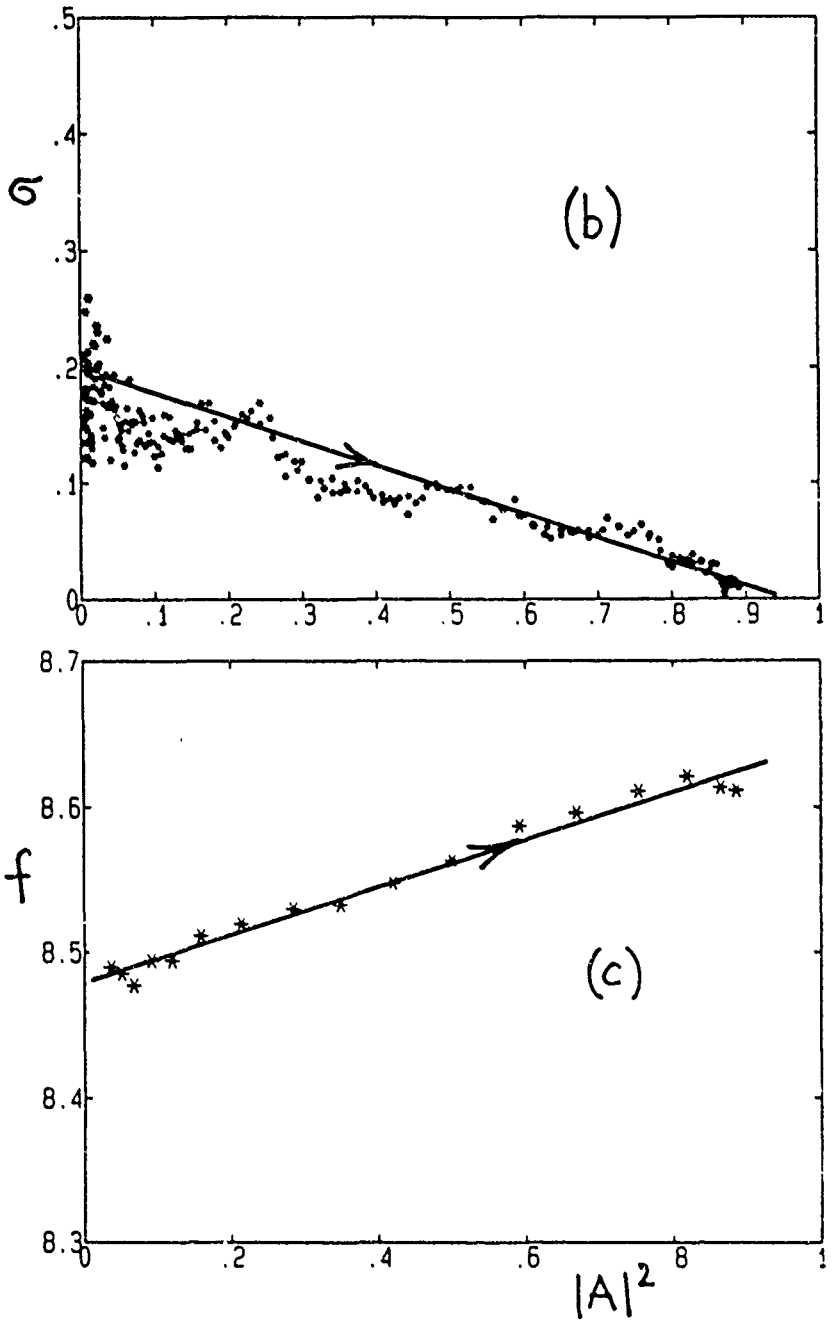

Figure 6. a) Transient from subcritical (stable) state to a limit cycle after closing the feedback loop (linear scale on top and logarithmic scale on bottom). R=79.2, gain g=0.01 . b) Instantaneous growth rate of transient 6a versus amplitude squared A^2, yielding σ=0.2 . c) Instantaneous frequency of transient 6a versus A^2, yielding f_{lin}=8.48 and f_{sat}=8.62 .

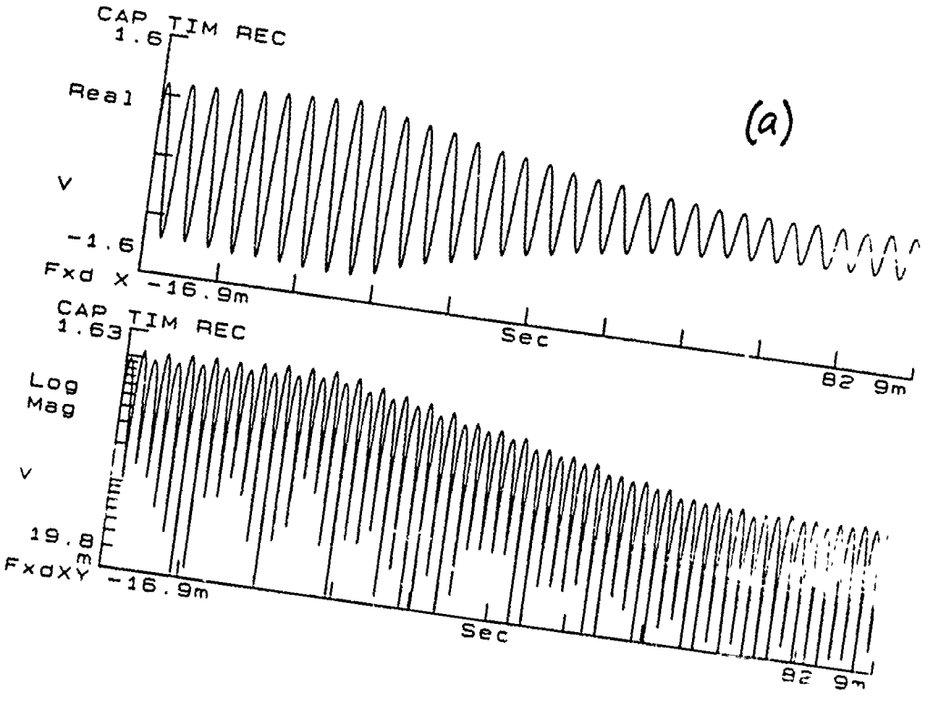

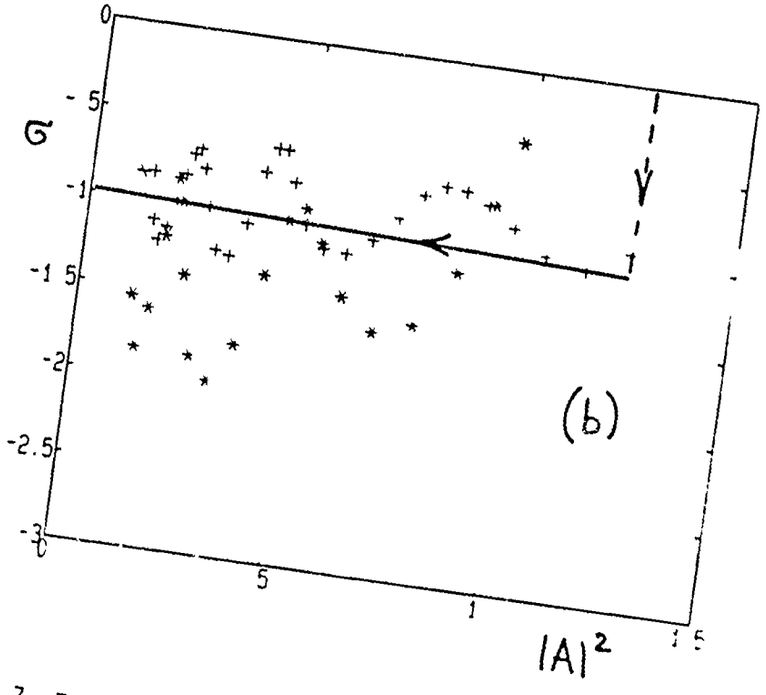

Figure 7. For caption see next page.

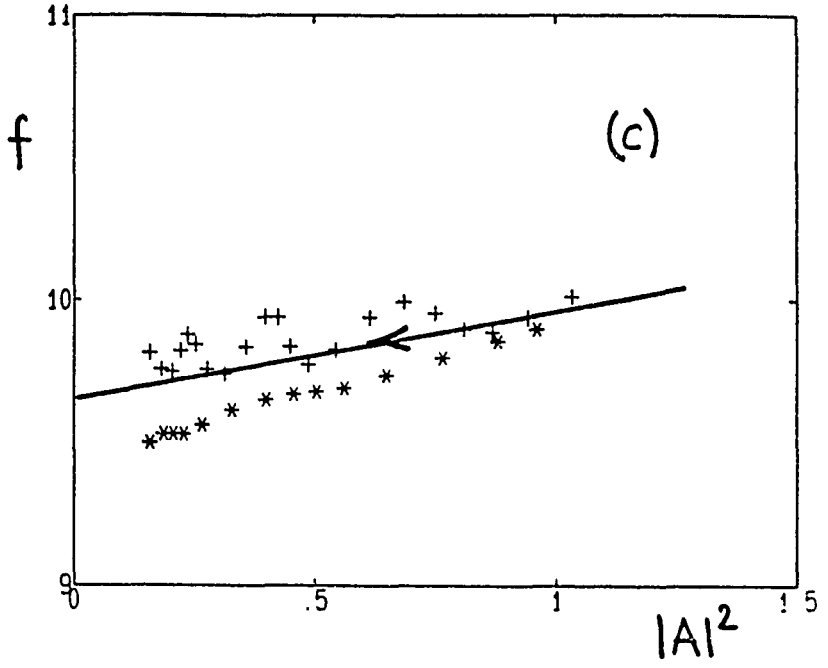

Figure 7. a) Transient from supercritical (unstable) state to a noisy stable state after closing the feedback loop (linear scale on top and logarithmic scale on bottom). R=83.8, gain g=0.003 . b) Instantaneous growth rate of transient 7a versus amplitude squared A^2, yielding σ=-1 . c) Instantaneous frequency of transient 7a versus A^2, yielding f_{lin}=9.6 and f_{sat}=10 .

The stability properties of the wake have been systematically explored at several supercritical Reynolds numbers. The procedure was first to find the optimal phase for suppression of the Karman mode, and then to increase the gain at that fixed optimal phase, while recording the spectrum of the sensor signal on an HP spectrum analyzer. An example of the results for R=83.8 is shown on Figure 8. The bottom part of the figure shows the magnitude of the dominant spectral peak u'_{rms} of the sensor signal. To provide a direct physical interpretation of gain, it is defined as $g=v'_{rms}(cylinder)/u'_{rms}(sensor)$, where v'_{rms} is the transverse velocity amplitude of the bimorph cylinder which was estimated optically. The bifurcation values g_c of the gain were determined by fitting the experimental data with the steady-state limit cycle amplitude of a NOISY system. Denoting the amplitude of the sensor signal by $|A|_s$, the latter is given by

$$\sigma|A|_s - \nu|A|_s^3 + \alpha = 0 \quad \text{with} \quad \sigma = \mu(g-g_c) \ , \tag{3.1}$$

where a represents the external noise. Hence we determine at each Reynolds number the parameters μ, ν, g_c and α by least-square fitting to the experimental results. The location of the first bifurcation at g_{1c}=1.3 10^{-3} has been verified by transient measurements like the ones shown on Figures 6 and 7, which allowed to measure the linear growth rate σ directly as shown in the top part of Figure 8. This figure clearly demonstrates the existence of a gain window from g_{1c} to g_{2c}=8.1 10^{-3} where another global mode is destabilized by the controller, and qualitatively confirms the GL model predictions.

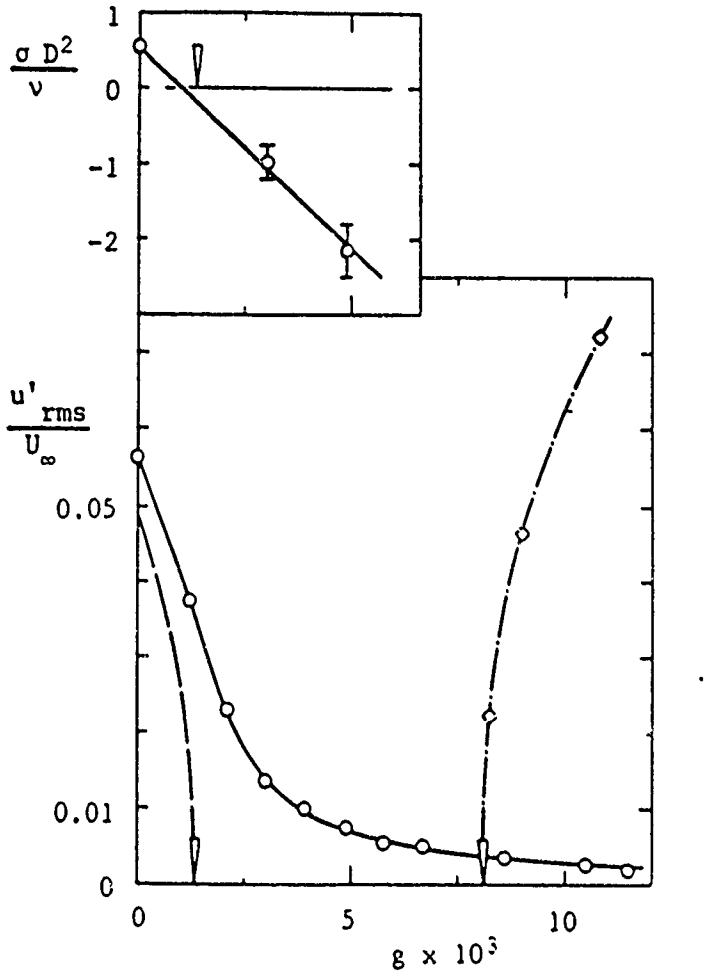

Figure 8. Spectral peak of streamwise velocity fluctuations at x/D=10, y/D=1 versus gain $g=v'_{rms}$(cylinder)/u'_{rms}(sensor). O, Karman mode at 320 Hz; ——, equation (3.1); – –, equ. (3.1) with $\alpha=0$; ◊, "higher mode" at 298 Hz. –·–, equ. (3.1).

Furthermore, the triangular shape of the region of stability in the gain-phase plane (see Figure 5) has been verified near the critical Reynolds number. The result is plotted on Figure 9 where the stability boundaries represent the destabilization of "higher" modes since the Karman mode is marginally stable for the experimental conditions shown.

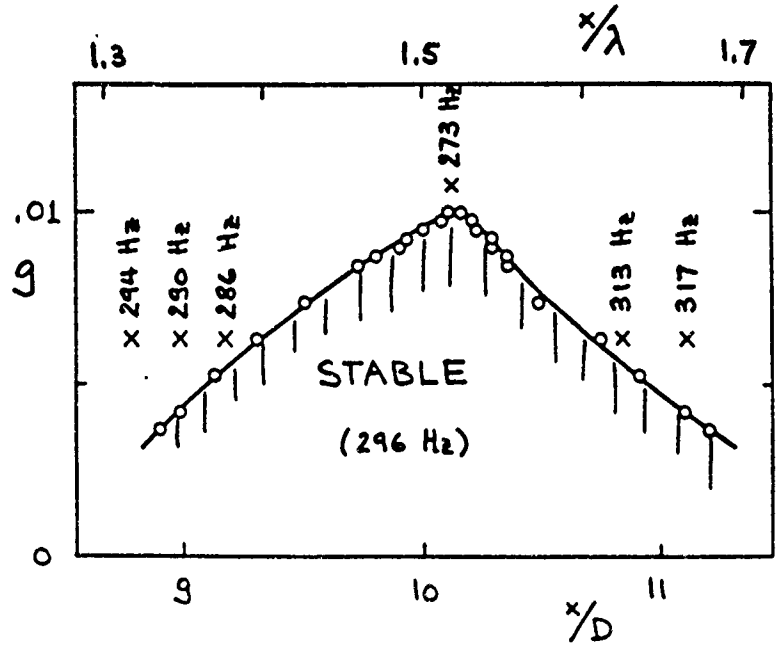

Figure 9. Experimental stability boundary as a function of controller gain for different sensor locations (phases). λ is the Karman wave length. R=79.3 $\approx R_c$.

Finally, all the experimental results for the stability boundaries are compiled in the last figure 10 which has to be compared to Figure 3 obtained from the GL model. Although the qualitative agreement is excellent, we note that the experimental Reynolds number range from 79.5 to about 90, over which wake oscillations can be suppressed, is approximately twice as large as the theoretically predicted range on Figure 3. This is due to the fact that the parameters (2.4) have been estimated in a rather crude manner and that no attempt has been made to fine-tune them for a quantitative match.

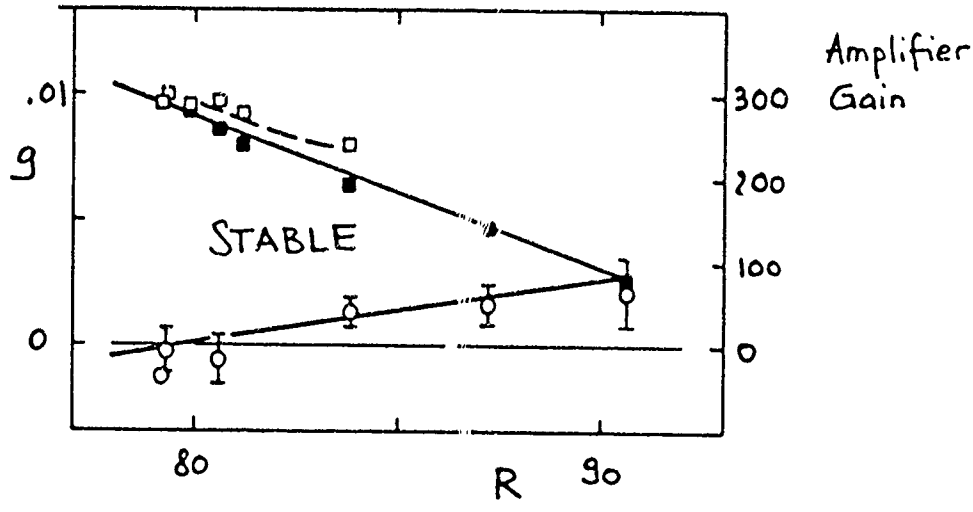

Figure 10. Experimental stability boundary of the controlled wake in the gain-Reynolds number plane. O, gain g=v'(cylinder)/u'(sensor) (left gain scale) at which Karman mode is suppressed; □, gain g at which "higher mode" is destabilized; ■, amplifier gain (right gain scale) at which "higher mode" is destabilized.

3.4. References Pertaining to Section 3

MONKEWITZ, P.A. 1989 Feedback control of global oscillations in fluid systems. AIAA Paper # 89-0991.

MONKEWITZ, P.A., BERGER, E. & SCHUMM, M. 1991 The nonlinear stability of spatially inhomogeneous shear flows, including the effect of feedback. Eur. J. Mech. B/Fluids 10, no. 2 - Suppl., 295-300.

RAGHU, S. & MONKEWITZ, P.A. 1991 The bifurcation of a hot round jet to limit cycle oscillations. Phys. Fluids A 3, 501-503.

SCHUMM, M. 1991 Experimentelle Untersuchungen zum Problem der absoluten und konvektiven Instabilitaet im Nachlauf zweidimensionaler stumpfer Koerper. Ph.D. Thesis, Technical University Berlin. In preparation: SCHUMM, M., BERGER, E. & MONKEWITZ, P.A. Self-excited oscillations and their control in the wake of two-dimensional bluff bodies.

4. APPENDIX: REPRINTS OF PAPERS PUBLISHED AS OF APRIL 92

Eur. J. Mech., B/Fluids, 10, n° 2 - Suppl., 295-300, 1991

The nonlinear stability of spatially inhomogeneous shear flows, including the effect of feedback

P. A. MONKEWITZ

Department of Mechanical, Aerospace and Nuclear Engineering
University of California, Los Angeles, CA 90024-1597, U.S.A.

E. BERGER and M. SCHUMM

Hermann-Foettinger Institut
Technical University Berlin, 1000 Berlin 12, Germany

Abstract. The stability of spatially-developing free shear flows is studied, which are taken to be weakly diverging We seek two-dimensional time-periodic perturbations of such flows, which vanish at infinity in all space directions and are termed global modes. Of particular interest are flow conditions at which the first of these global modes becomes linearly unstable, i.e. self-excited Assuming that the Hopf bifurcation at this point is supercritical and that the weak nonparallel and nonlinear effects are of equal importance, the spatio-temporal evolution of the global-mode amplitude is found to be governed by a Ginzburg-Landau equation with variable coefficients The usefulness of the model is demonstrated by comparison with experiments in which the vortex shedding behind a cylinder is modified by fixed-gain feedback control, which is easily incorporated into the Ginzburg-Landau equation

1. Introduction

The stability of spatially developing free shear flows, such as jets and wakes, is studied under the assumption that the basic flow is two-dimensional and incompressible, and that its streamwise development, characterized for instance by its width $\delta(x)$, is "slow" on the scale of a typical instability wavelength λ, that is $\epsilon = (\lambda/\delta)\times(d\delta/dx) \ll 1$. This means that the basic flow depends only on the transverse coordinate y and the rescaled "slow" streamwise coordinate

$$X = \epsilon x \ . \qquad (1)$$

Furthermore, the non-parallelism of the flow is assumed to be mainly due to pressure or body forces such that, in the case of viscous flows, the Reynolds number is not directly related to ϵ. Under the additional assumptions of an infinite flow domain without internal boundaries and locally stable flow far up- and downstream, the linear global modes have been studied by Chomaz, Huerre & Redekopp [1990a], Huerre & Monkewitz [1990]

EUROPEAN JOURNAL OF MECHANICS. B FLUIDS VOL 10 N° 2-SUPPL., 1991
0997-7546 91 295 6 $ 2 60 © Gauthier-Villars

and Monkewitz [1990], where global modes are understood to be time-periodic perturbations of the basic flow which vanish at infinity in all space directions. The above authors have shown formally that in flows without solid boundaries the global modes are "driven" by a "wave-maker" centered around X_s, which is in general complex and defined by

$$\frac{\partial \omega}{\partial k}(k_s, X_s) = 0 \ , \quad \frac{\partial \omega}{\partial X}(k_s, X_s) = 0 \ ; \quad \omega_s = \omega(k_s) \ . \tag{2}$$

In words, X_s is a saddle point of the local absolute frequency $\omega_0(X)$ (the frequency of the mode with zero group velocity) obtained from linear parallel stability analyses of the local velocity profile at each X. In physical terms the global response is driven by the "local oscillator" at X_s with frequency ω_s which has the "most compatible neighbors" oscillating at the same frequency (to linear order in $X-X_s$). The linear analysis (a paper on the full derivation from the governing equations by Monkewitz, Huerre & Chomaz is in preparation) shows that, far from X_s, global mode shapes can be described by WKB approximations [see for instance Crighton & Gaster, 1976]. The connection of the WKB solutions across X_s, which is a second order turning point of the problem, is shown to be described by a linearized complex Ginzburg-Landau (LCGL) equation, valid in an $O(\epsilon^{1/2})$ neighborhood of X_s. The resulting eigen-frequencies of the low-order global modes are found to be within $O(\epsilon)$ of ω_s, which means that the flow must contain an interval of absolute instability on the real X-axis in order to become self-excited, i.e. to support time-amplified global modes.

In this paper, we extend the linear global-mode analysis to the weakly nonlinear regime. Since marginal instability of a global mode, which is a prerequisite for a weakly nonlinear approach, is generally reached far from the traditional parallel-flow stability boundary, this represents a nontrivial extension of Stuart's parallel theory [see e.g. Stuart, 1971]. So far, nonlinear effects on global modes have been studied by adding a cubic nonlinearity to the LCGL equation in an ad hoc fashion [Chomaz, Huerre & Redekopp, 1990b]. More recently, in an effort parallel to ours, LeDizes and Huerre [LeDizes, 1990] have formally analyzed several situations with different relative importance of nonparallel and nonlinear effects. In the following, we concentrate on the case in which the spatio-temporal evolution of global modes is equally affected by nonlinear and nonparallel effects in the neighborhood of the "wave maker" at X_s.

2. The Ginzburg-Landau Equation Governing the Evolution of Global Modes

In this section we sketch the derivation of the nonlinear CGL equation in the region around X_s. As in the linear analysis [see e.g. H & M, 1990], the x-coordinate and time are rescaled according to

$$\xi = \epsilon^{1/2}(x-x_{0,r}) = \epsilon^{-1/2}(X-X_{0,r}) \ , \tag{3a}$$

$$T = \epsilon t \ . \tag{3b}$$

For the present nonlinear analysis the reference location x_s is conveniently replaced by its real part $x_{0,r}$ (see equation 5). The slow time T characterizes the evolution of a localized initial impulse into a linear global mode. If we wish the nonlinear saturation of a global mode to take place on the same time scale (assuming the Hopf bifurcation to be supercritical), the maximum amplitude of the disturbance must be of order $O(\epsilon^{1/2})$ and the stream function may be expanded in powers of $\epsilon^{1/2}$:

$$\Psi = \Psi_0(y,X) + \epsilon^{1/2}\Psi_1 + \epsilon\Psi_2 + \epsilon^{3/2}\Psi_3 + O(\epsilon^2) \ . \tag{4}$$

As usual, the degree of supercriticality, i.e. the temporal growth rate $\omega_{0,i}$, has to be of order $O(\epsilon)$. The new feature is that nonlinear effects are concentrated around the location of maximum amplitude of the linear global mode. Hence, one has to distinguish between a maximum amplitude outside an $O(\epsilon^{1/2})$ neighborhood of X_s, and a maximum within. In the first case the amplitude at X_s is exponentially small and the "wave maker" region remains linear. Focussing on the second possibility, we show that it leads to the CGL equation for the global-mode amplitude. To ensure that the maximum amplitude is reached within $O(\epsilon^{1/2})$ of X_s, one has to limit the spatial growth rate $k_{0,i}$ to $O(\epsilon^{1/2})$. Finally, for the maximum amplitude to be of the same order as $|\Psi_1|(X_s)$, X_s must be within $O(\epsilon)$ of the real X-axis. In summary, we have

$$\omega_s = \omega_{0,r} + i\epsilon\Omega_{0,i} \ , \quad k_{0,i} = \epsilon^{1/2}\kappa_{0,i} \ , \quad X_{0,i} = \epsilon x_{s,i} \ ; \quad \Omega_{0,i} \ , \ \kappa_{0,i} \ , \ x_{s,i} = O(1) \ . \tag{5}$$

For $\xi \leq O(1)$, the mean flow is expanded around $X_{s,r}$

$$\Psi_0(y,X) = \Psi_0(y,X_{0,r}) + \epsilon^{1/2}\xi \frac{\partial \Psi_0}{\partial X}(y,X_{0,r}) + \epsilon \frac{\xi^2}{2}\frac{\partial^2 \Psi_0}{\partial X^2}(y,X_{0,r}) + O(\epsilon^{3/2}) \ , \tag{6}$$

and the amplitude expansion (4) is introduced into the Euler or Navier-Stokes equations. At order $O(\epsilon^{1/2})$ the linear, parallel stability problem for the mean velocity profile at $X_{s,r}$ yields

$$\begin{aligned} &\Psi_1 = A(\xi,T)\,\Phi(y;X_{0,r})\,E(x,t)\,\exp[-\kappa_{0,i}\xi + \Omega_{0,i}T] \ + \ \text{c.c.} \ , \\ &E(x,t) = \exp[ik_{0,r}(x-x_{0,r}) - i\omega_{0,r}t] \ , \end{aligned} \tag{7}$$

where c.c. stands for complex conjugate. As there is only a slight flow divergence within $\xi \leq O(1)$, the transverse structure of Ψ_1 is frozen and given by the linear eigenfunction $\Phi(y,X_{0,r})$. At higher order, solvability conditions are enforced, noting that secular terms have to be suppressed already at $O(\epsilon)$ because of the nonparallel basic flow. This yields at $O(\epsilon^{3/2})$ the CGL equation with j-th degree polynomials $\sigma_j(\xi)$ as coefficients.

$$\frac{\partial A}{\partial T} + \sigma_0 \frac{\partial^2 A}{\partial \xi^2} + \sigma_1(\xi)\frac{\partial A}{\partial \xi} + \sigma_2(\xi)\,A + \eta\, e^{-2(\kappa_{0,i}\xi - \Omega_{0,i}T)}|A|^2 A = F(\xi,T) \tag{8}$$

The forcing function $F(\xi,T)$ has been added here for later reference. The linearized version of (8) with F=0 yields a spectrum of closely-spaced global eigen-frequencies $\omega_{0n} = \omega_{s,r} + \epsilon[i\Omega_{s,i} + \Omega' + n\Omega'']$ with quantization at $O(\epsilon)$! The associated linear global modes are products of a Gaussian and Hermite polynomials of degree n [H & M, 1990].

Before closing this discussion, a comment on the solution far away from X_s is in order. For $|X-X_s|=O(1)$ the global mode amplitude is exponentially small compared to its maximum. There, Ψ_1 takes the form of linear WKB approximations [C & G, 1976]

$$\epsilon^{1/2}\Psi_1^{\pm} = \epsilon^{1/2}\mu(\epsilon)\, A^{\pm}(X,T)\, \Phi^{\pm}(y;X)\, \exp\left[\frac{1}{\epsilon}\int k^{\pm}(X)dX - i\omega_{s,r}t\right] , \qquad (9)$$

where Ψ_1^- and Ψ_1^+ are the subdominant solutions far up- and downstream of X_s, respectively [H & M, 1990]. The amplitudes $A^{\pm}(X,T)$ are governed by first-order PDE's and have to be matched to the spatio-temporal amplitude $A(\xi,T)$ obtained from (8). This reveals the only "blemish" of the present analysis as this matching cannot be carried out analytically. It can be argued though, that the $\Psi_1^{\pm}$ only play the role of "passive tails".

3. Application to Proportional Feedback Control of Vortex Shedding Behind a Cylinder

To illustrate the predictive power of the CGL model we present a comparison with feedback experiments in the cylinder wake, which will remain qualitative in this paper. As in most practical setups, one actuator and one sensor, typically located downstream of the actuator, are specified. For simplicity we assume that both are within an $O(\epsilon^{1/2})$ of X_s, that the sensor or probe measures directly $A(\xi-\xi_p,T)$, and that the actuator acts at a point ξ_f and, in the transverse direction, just forces the eigenfunction $\Phi(y;X_{s,r})$. Such a proportional or constant-gain feedback is represented in equation (8) by the forcing term

$$F(\xi,T) = g\, \exp[i\gamma]\, \delta(\xi-\xi_f)\, A(\xi-\xi_p,T) \quad . \qquad (10)$$

The feedback gain g and the phase shift γ incorporate in practice both the (complex) electronic gain and the "receptivity" of the flow to the actuator. It is noted in passing that this model applies to physical setups with arbitrary lead- or lag compensators, as only their gain and phase shift at *the "carrier frequency"* $\omega_{s,r}$ are relevant. This model (equations 8 and 10) in its linear form has already been studied by Monkewitz [1989] and has shown interesting generic behavior: When all global modes are linearly stable at zero gain, feedback destabilizes the system beyond a critical gain, which increases as the system becomes more stable. The main point is that it is always a higher mode ω_{0n} (n>0) and not the least stable mode ω_{00} that is destabilized by feedback. Therefore, in the situation of an n=0 mode which is unstable at zero gain, one finds a "gain window" where g is sufficient to suppress the growth of the n=0 mode (at, say, the optimum phase angle γ), but is still below the critical value at which higher modes are destabilized. This

window narrows as the degree of supercriticality (e.g. the Reynolds number) is increased and control is typically lost not far beyond critical conditions.

To test these results, experiments have been conducted in the wake of a cylinder, a flow which satisfies the model assumptions quite closely [see e.g. Monkewitz, 1988]. A "Bimorph-transducer" of thickness D=0.69mm, chord T=1.68mm and a length of approximately 100D, already described by Berger [1967] [see also Berger & Schumm, 1988], served as cylinder (see figure 1). By applying a voltage between electrodes on top and bottom, the cylinder was oscillated in the transverse bending mode and served as actuator. The probe was a constant temperature hotwire located at x/D=10 and y/D=1. Its signal was linearized, passed through an amplifier/phase shifter and fed to the Bimorph-transducer.

Figure 1. Schematic of the experimental arrangement with C , oblong cylinder , HW , hot wire

For the experiments we focussed attention on the suppression of Karman vortex shedding, i.e. on the supercritical regime with Reynolds number $Re>Re_{crit}$, where Re_{crit}=79.5 for this oblong cylinder [B & S, 1988]. In the course of the study, the main qualitative predictions of the model were confirmed: First, we found at slightly supercritical Reynolds numbers a gain window in which the fundamental Karman mode could be suppressed. The result for Re=83.8 is shown on figure 2. The bottom part of the figure shows the the magnitude of the main peak u'_{rms} in the streamwise velocity spectrum, as measured by the hotwire probe, versus gain. To provide a direct physical interpretation of the gain, it is defined as $g=v'_{rms}(\text{cylinder})/u'_{rms}(\text{probe})$, where v'_{rms} is the transverse velocity amplitude of the Bimorph transducer, which was measured optically. The phase shift γ was held constant at its optimal value. The bifurcation values g_{crit} were determined by fitting the data with the steady-state limit-cycle amplitude $|A|$ at $\xi=\xi_p$ obtained from (8) and defined by

$$\sigma|A| - \nu|A|^3 + \alpha = 0 \; ; \quad \sigma = \mu(g-g_{crit}) \; . \tag{11}$$

To account for the external noise (freestream turbulence) that keeps exciting the Karman mode beyond its neutral point, a forcing term α has been added to the other fitting parameters μ, ν and g_{crit} in (11). The location of the first bifurcation at g_1=1.3 10^{-3} has in addition been verified by transient experiments in which the global linear growth or decay rate σ was determined directly. The figure clearly shows the gain window extending from g_1 to g_2=8.1 10^{-3} where another global mode is destabilized, as qualitatively predicted by the model. In addition, we also confirmed the second main

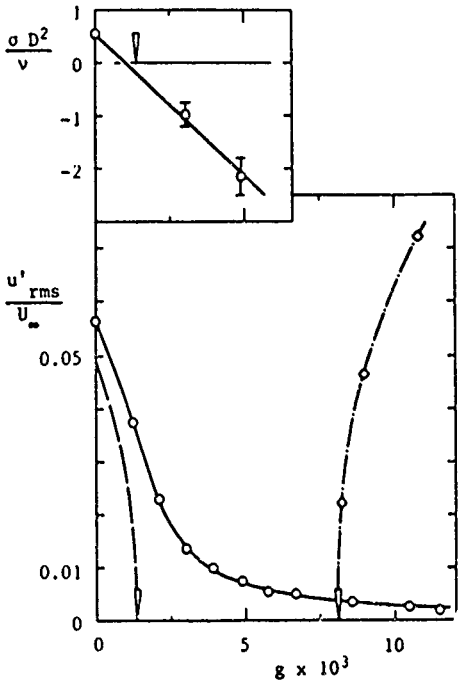

Figure 2. Spectral peak of streamwise velocity at x/D=1.0, y/D=1 versus gain g=v'(cylinder)/u'(probe) O , Karman mode at 320 Hz, —— , equ (11), – – , equ (11) with α=0 0 , "higher mode" at 298 Hz ; –·– , equ (11)

prediction that control is lost relatively close to Re_{crit} , by showing that suppression of vortex shedding in our setup is only possible between Re_{crit} and Re=90.

4. Conclusions and Acknowledgements

This study demonstrates that a relatively simple weakly nonlinear model of wake oscillations is capable of capturing the rather complex dynamics resulting from the addition of feedback. The next step will be a quantitative comparison between the model, with coefficients either determined from stability calculations or measured, and the present experiments. Further ahead, the success of Ffowcs Williams and Zhao [1989] in suppressing Karman vortex shedding at eight times Re_{crit}, where the situation is greatly complicated by turbulence, awaits explanation.

The support by AFOSR Grant 89-0421, the A. von Humboldt Foundation and ONR Grant N00014-90-J-1313 is gratefully acknowledged.

References

BERGER, E., 1967, Suppression of vortex shedding and turbulence behind oscillating cylinders, Phys. Fluids Suppl 10, S191-S193

BERGER, E., SCHUMM, M., 1988, Untersuchungen der Instabilitaetsmechanismen im Nachlauf von Zylindern, Contract Report # Be343/18-1, Technical University Berlin

CHOMAZ, J.M., HUERRE, P., REDEKOPP, L.G , 1990a, A frequency selection criterion in spatially developing flows, Stud Appl Math., in press

CHOMAZ, J.M , HUERRE, P , REDEKOPP, L.G , 1990b, The effect of nonlinearity and forcing on global modes, Proc Conf New Trends in Nonlinear Dyn and Pattern-forming Phenomena (P Coullet, P Huerre, Eds), Plenum, New York/London

CRIGHTON, D G , GASTER, M., 1976, Stability of slowly diverging jet flow, J Fluid Mech 77, 397-413

FFOWCS WILLIAMS, J.E , ZHAO, B C., 1989, The active control of vortex shedding, J Fluids and Structures 3, 115-122

HUERRE, P., MONKEWITZ, P.A , 1990, Local and global instabilities in spatially developing flows, Ann Rev Fluid Mech 22, 473-537.

LE DIZES, S., 1990, Effets non lineaires sur des ecoulements faiblement divergents, D E A de Mecanique de Paris 6

MONKEWITZ, P.A , 1988, The absolute and convective nature of instability in two-dimensional wakes at low Reynolds number, Phys. Fluids 31, 999-1006

MONKEWITZ, P.A., 1989, Feedback control of global oscillations in fluid systems, AIAA paper # 89-0991

MONKEWITZ, P.A , 1990, The role of absolute and convective instability in predicting the behavior of fluid systems, Eur J Mech B/Fluids 9, 395-413

STUART, J T , 1971, Nonlinear stability theory, Ann Rev Fluid Mech 3, 347-370

Proc. of NATO ASI on Chaotic Dynamics: Theory and Practice, Patras, Greece, July 1991.

Control of Hopf Bifurcations

Edward A. Henrich, D. L. Mingori and P. A. Monkewitz

University of California, Los Angeles

1 Introduction

Many systems in nature exhibit self-excited oscillations or limit cycle behavior. The bifurcation from a steady-state to a limit cycle is generally the first step in the transition to chaos or turbulence. For a given physical system there are often design constraints which specify a fixed region of parameter space in which one would like to operate. If this particular choice of parameters exhibits some undesirable dynamic behavior (e.g. limit cycles or chaos) then the goal of the control engineer is to suppress this behavior while still operating in the same parameter range. A distinction is made between a 'control parameter' or 'bifurcation parameter' which is the parameter one uses to study successive bifurcations and a 'control force' which is a prescribed function of time used to modify the system's output. As an example, consider that one might desire to suppress the Von Kàrmán vortex street in the wake behind a cylinder. The control parameter is the Reynolds number which may be fixed at some supercritical value, where at the desired operating speed the wake is no longer laminar. The control force could be an induced sound field designed to eliminate flow oscillations. This method uses the control force to stabilize the system in contrast to methods which modify the control parameter until the state behaves as desired [1].

2 Control System Analysis

For a physical system with a finite number of degrees of freedom, the dynamics may be described by a set of first order ordinary differential equations. Written in vector form

$$\frac{d\mathbf{X}(t)}{dt} = \mathbf{F}(\mathbf{X}(t);\mu) + Bu(t) \tag{2.1}$$

$$y = C\mathbf{X} + D \tag{2.2}$$

$$\mathbf{X} \in R^n \text{ and } \mu, u, y \in R \tag{2.3}$$

where $\mathbf{X}$ is the system state, $\mathbf{F}$ is the vector field, u is the control force, y is the measured output and μ is a control parameter in the problem. Equation (2.1) is presumed to have an equilibrium solution $\mathbf{X}_0(\mu)$ which satisfies $\mathbf{F}(\mathbf{X}_0(\mu);\mu) = 0$. For $\mu > 0$ we assume the system undergoes a Hopf bifurcation to a limit cycle. The goal of the control system is to return the system to its equilibrium state, which is unstable for $\mu > 0$.

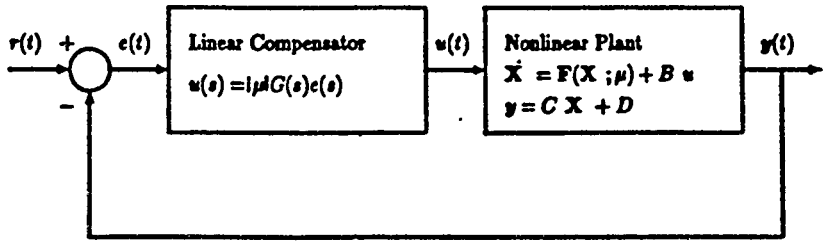

Figure 1: Block diagram of the control system

One method for controlling a set of ordinary differential equations which depend on a control parameter μ is to let the value of the control parameter be governed by a differential equation. The time derivative $\dot{\mu}$ depends on the state of the system and a gain specified by the designer. If the gain can be chosen such that μ drops below the critical value, then the $n+1$ dimensional system will be stable. This procedure is described in [1].

The goal of this research is to control the system by external forcing when the control parameter is fixed by some other design constraint. The control system which is studied is the linear regulator as depicted in Figure 1. The differential equations governing the control system are such that the Laplace transform of the impulse response of the linear compensator is $\mu G(s)$.

The action of the control system is studied by using a multiple scale perturbation technique [2, 3]. We consider the case where the real part of the critical eigenvalue is $O(\epsilon^2)$. In this case it is natural to introduce a second time scale $\tau = \epsilon^2 t$, where $\mu = \epsilon^2 \mathrm{sgn}(\mu)$. We treat the two time scales as independent variables so by the chain rule the derivative becomes

$$\frac{d}{dt} \to \frac{\partial}{\partial t} + \epsilon^2 \frac{\partial}{\partial \tau} \tag{2.4}$$

We use this formula and expand (2.1) in a Taylor series in $\mathbf{X} - \mathbf{X}_0$ and μ. Upon equating terms multiplied by like powers of ϵ we obtain a sequence of inhomogeneous partial differential equations. The elimination of secular terms leads to a solvability condition which governs the slow time evolution of the amplitude of the limit cycle oscillations. The solution on the center manifold is

$$X(t) \sim X_0 + \epsilon A(\tau) e^{i\omega_c t}\mathbf{r} + \epsilon \bar{A}(\tau) e^{-i\omega_c t}\bar{\mathbf{r}} \tag{2.5}$$

where ω_c is the imaginary part of the critical eigenvalue and $\mathbf{r}$ is the corresponding right eigenvector. The solvability condition can be written as an amplitude equation

$$\frac{dA}{d\tau} = (\mathrm{sgn}(\mu)\lambda - \mathbf{l}BC\mathbf{r}\, G(i\omega_c))A - \tilde{g}\,|A|^2 A \tag{2.6}$$

where λ is determined by the real part of the eigenvalue of the Jacobian of $\mathbf{F}$, $\tilde{g}$ is determined by the nonlinearities, and the receptivity lBCr is determined by the manner in which the control force couples to the measured output (l is the left eigenvector of the marginal mode). In fluid mechanics this type of equation is known as the Stuart-Landau equation.

An important thing to note in equation (2.6) is that the stability of the fixed point X_0 is governed by the control system only near the critical frequency ω_c. In particular, the entire class of control systems with the same gain and phase at the critical frequency are equivalent. The particular gain and phase required of the control system at the critical frequency is determined by the stability of the uncontrolled plant (i.e. λ) and its receptivity from measured output to control force (i.e. $lBC\mathbf{r}$).

3 Estimation and Control

The results of the previous section demonstrate the effect of a linear regulator on a nonlinear plant which undergoes a Hopf bifurcation to a limit cycle. In deriving the result, we assumed that the system equations (2.1) were known. If the system equations were known, we would likely use one of the standard control design methods for nonlinear plants (e.g., describing functions or Lyapunov's direct method). The more interesting situation is when the model for the system dynamics is unknown, but what is known is that the system exhibits limit cycle behavior. In this case, it is useful to think of the Stuart-Landau equation (2.6) as a generic model for the dynamics which are asymptotic to the center manifold. In many physical applications the measurement consists of a time history of a single variable. In these cases, the state $\mathbf{X}(t)$, $A(\tau)$ and the eigenvector $\mathbf{r}$ may all be unknown. This difficulty is easily overcome. Defining $Y(t) \equiv 2\epsilon A(\tau) C\mathbf{r}$, the leading order asymptotic expression for the output is

$$y(t) = Re[Y(t)e^{i\omega_c t}] + C\mathbf{X}_0 + D \tag{3.1}$$

(see (2.2) and (2.5)). Returning to the physical variables, one obtains an amplitude equation which is useful for describing the measured output of an experiment in terms of a dynamical system on the center manifold

$$\frac{dY}{dt} = \mu(\mathrm{sgn}(\mu)\lambda - lBC\mathbf{r}\, G(i\omega_c))Y - g\,|Y|^2\,Y \tag{3.2}$$

or

$$\frac{dY}{dt} = (\Lambda - J\, G(i\omega_c))Y - g\,|Y|^2\,Y \tag{3.3}$$

where Λ, J and g are unknown complex constants.

To estimate these constants from experimental data one needs a method for obtaining $Y(t)$. One way to obtain the amplitude signal $Y(t)$ would be to create a 90 degree phase shifted version of the output $y(t)$ as $\tilde{y}$. The modulus of the complex signal $\tilde{y}(t) = y(t) + i\tilde{y}(t)$ is $|\tilde{y}(t)| = |Y(t)|$. We define an analytic signal as a complex

signal of a real variable whose real and imaginary parts are Hilbert pairs [4]. This analytic signal is just an extension of the 'rotating vector' or 'phasor' used in circuit analysis and systems engineering. The Hilbert transform is

$$\tilde{y} \equiv \mathcal{H}\{y\} = \frac{1}{\pi} P.V. \int_{-\infty}^{+\infty} \frac{y(\tau)}{t-\tau} d\tau = \frac{1}{\pi t} * y(t) \tag{3.4}$$

where $*$ denotes convolution in time. Defined this way the Hilbert transform of a real time signal is a real time signal. Taking the Fourier transform of (3.4) we have

$$\mathcal{F}\{\mathcal{H}\{y\}\} = -i\,\mathrm{sgn}(\omega)\mathcal{F}\{y\} \tag{3.5}$$

which shows that the Hilbert transform is indeed a 90 degree phase shifter. From (3.5) we find that the Fourier transform of the analytic signal is

$$\mathcal{F}\{\tilde{y}\} = \begin{cases} 2\mathcal{F}\{y\} & \omega > 0 \\ \mathcal{F}\{y\} & \omega = 0 \\ 0 & \omega < 0 \end{cases} \tag{3.6}$$

Hence we can obtain the analytic signal $\tilde{y}(t)$ by using (3.6) and an inverse Fourier transform

$$\tilde{y}(t) = \mathcal{F}^{-1}\{(1 + \mathrm{sgn}(\omega))\mathcal{F}\{y\}\} \tag{3.7}$$

We use the analytic signal to find the 'envelope' of the output and its 'instantaneous phase or frequency'. The envelope is just $|\tilde{y}|$ and the instantaneous phase is $\angle\tilde{y}$. So we can identify our complex amplitude as

$$Y(t) = |\tilde{y}|\, e^{i\phi} \tag{3.8}$$

where $\phi = \angle\tilde{y} - \omega^{(0)}t$. The Hilbert transform represents a means of obtaining the demodulated output $Y(t)$ from the output $y(t)$ off-line. Equation (3.3) is solvable for $Y(t)$ as an analytic function in terms of the coefficients Λ, J and g so there are several means to estimate the parameters of the Stuart-Landau equation once we have obtained $Y(t)$ from $y(t)$ using the Hilbert transform.

The estimation and control scheme may be demonstrated using the Van der Pol oscillator as a model plant. The plant is

$$\ddot{y} + (y^2 - \mu)\dot{y} + y = u \tag{3.9}$$

The plant equation and the differential equations for the linear regulator are integrated using a fixed step fourth order Runge-Kutta algorithm. We use several test values of $G(i\omega_c)$ to identify the system parameters Λ, J and g. Once the parameters have been estimated, we use this model of the dynamics on the center manifold to select the optimum values for the controller gain and phase. The results of the final controller are depicted in Figure 2. The solid curve is the measured output $y(t)$ and the dashed curve is the control force $u(t)$.

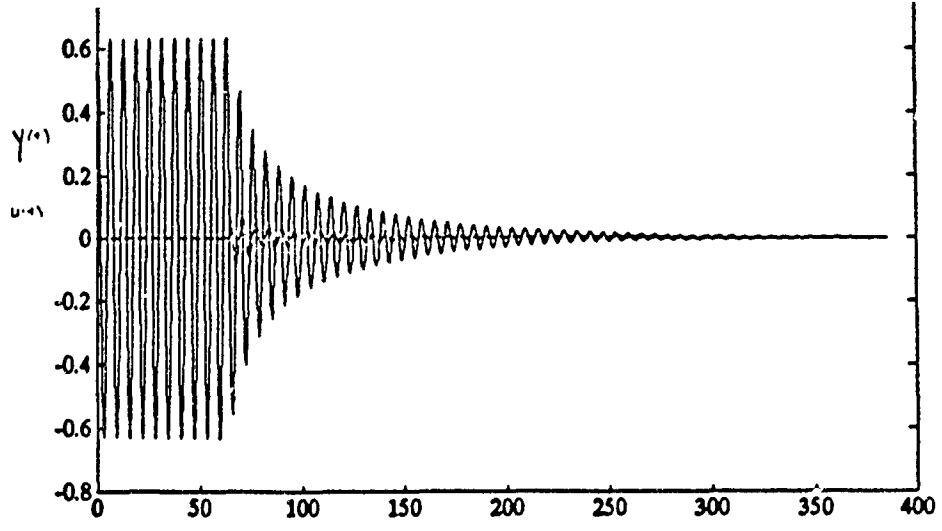

Figure 2: Stabilization of limit cycle oscillations

4 Conclusions

A procedure for finding a model for data which lies on the center manifold has been developed. Using this model one can specify the gain and phase of a linear controller to stabilize the system. One may also specify a controller to modify the size of the limit cycle.

Previous work with wakes and jets have shown the Stuart-Landau equation to be a good model for the dynamics on the center manifold [5]. We are currently investigating the results of this paper using a heated two dimensional jet experiment.

The research described in this article was performed under AFOSR contract 89-0421.

References

[1] S. Sinha, R. Ramaswamy, and J. S. Rao, "Adaptive control in nonlinear dynamics," *Physica D*, vol. 43, pp. 118–128, 1990.

[2] J. Kevorkian and J. D. Cole, *Perturbation Methods in Applied Mathematics.* Springer-Verlag, 1981.

[3] Y. Kuramoto, *Chemical Oscillations, Waves and Turbulence.* Springer-Verlag, 1984.

[4] P. Henrici, *Applied and computational complex analysis*, pp. 193–213. Vol. 3, John Wiley and Sons, 1986.

[5] S. Raghu and P. A. Monkewitz, "The bifurcation of a hot round jet to limit-cycle oscillations," *Physics of Fluids A*, vol. 3, pp. 501–503, April 1991.